Application of a Mobile Flux Lab for the Atmospheric Measurement of Emissions (FLAME)

by

Tim Orland Moore II

Dissertation submitted to the faculty of Virginia Polytechnic Institute and State University in partial fulfillment of the requirements for the degree of

DOCTOR OF PHILOSOPHY

in

Environmental Engineering

Linsey C. Marr, Ph.D, Chair
Korine N. Kolivras, Ph.D, Member
John C. Little, Ph.D, Member
Daniel L. Gallagher, Ph.D, Member
Randel L. Dymond, Ph.D, Member

September 8, 2009
Blacksburg, Virginia

Keywords: National Emission Inventory, carbon dioxide, nitrogen oxides, $PM_{2.5}$, VOC, flux, eddy covariance, relaxed-eddy accumulation, National Air Toxics Assessment

Application of a Mobile Flux Lab for the Atmospheric Measurement of Emissions (FLAME)

by

Tim Orland Moore II

Environmental Engineering

(ABSTRACT)

According to the World Health Organization, urban air pollution is a high public health priority due its linkage to cardio-pulmonary disease and association with increased mortality and morbidity *(1, 2)*. Additionally, air pollution impacts climate change, visibility, and ecosystem health. The development of effective strategies for improving air quality requires accurate estimates of air pollutant emissions. In response to the need for new approaches to measuring emissions, we have designed a mobile Flux Lab for the Atmospheric Measurement of Emissions (FLAME) that applies a proven, science-based method known as eddy covariance for the direct quantification of anthropogenic emissions to the atmosphere.

The mobile flux lab is a tool with novel, multifaceted abilities to assess air quality and improve the fidelity of emission inventories. Measurements of air pollutant concentrations in multiple locations at the neighborhood scale can provide much greater spatial resolution for population exposure assessments. The lab's mobility allows it to target specific sources, and plumes from these can be analyzed to determine emission factors. Through eddy covariance, the lab provides the new ability to directly measure emissions of a suite of air pollutants.

We have deployed the FLAME to three different settings—a rural Appalachian town where coal transport is the dominant industry; schools in the medium-sized city of Roanoke, Virginia; and the large urban areas around Norfolk, Virginia—to measure neighborhood-scale emissions of air pollution. These areas routinely experience high ozone and particulate matter concentrations and include a diverse array of residential neighborhoods and industries. The FLAME is able to capture emissions from all ground-based sources, such as motor vehicles, rail and barge traffic, refuse fires and refueling stations, for which no direct

measurement method has been available previously. Experiments focus on carbon dioxide (CO_2), the principal greenhouse gas responsible for climate change; nitrogen oxides (NO_x), a key ingredient in ground-level ozone and acid rain; volatile organic compounds (VOCs), a second key ingredient in ozone and many of which are air toxics; and fine particulate matter ($PM_{2.5}$), a cause of mortality, decreased visibility, and climate change.

This research provides some of the first measurements of neighborhood-scale anthropogenic emissions of CO_2, NO_x, VOCs and $PM_{2.5}$ and as a result, the first opportunity to validate official emission inventories directly. The results indicate that a mobile eddy covariance system can be used successfully to measure fluxes of multiple pollutants in a variety of urban settings. With certain pollutants in certain locations, flux measurements confirmed inventories, but in others, they disagreed by factors of up to five, suggesting that parts of the inventory may be severely over- or underestimated. Over the scale of a few kilometers within a city, emissions were highly heterogeneous in both space and time. FLAME-based measurements also confirmed published emission factors from coal barges and showed that idling vehicles are the dominant source of emissions of air toxics around seven schools in southwest Virginia.

Measurements from this study corroborate existing emission inventories of CO_2 and NO_x and suggest that inventories of $PM_{2.5}$ may be overestimated. Despite the tremendous spatial and temporal variability in emissions found in dense urban areas, CO_2 fluxes on average are very similar across the areas in this study and other urban areas in the developed world. Nevertheless, the high level of variability in spatial and temporal patterns of emissions presents a challenge to air quality modelers. The finding that emissions from idling vehicles at schools are likely responsible for creating hot spots of air toxics adds to the urgency of implementing no-idling and other rules to reduce the exposure of children to such pollutants. Ultimately, the results of this study can be used in combination with knowledge from existing emission inventories to improve the science and policies surrounding air pollution.

TABLE OF CONTENTS

LIST OF FIGURES

LIST OF TABLES

Chapter 1: Application of a Mobile Flux Lab for the Atmospheric Measurement of Emissions (FLAME) for the Validation of Emission Inventories

1.0 Introduction

Outdoor air pollution is responsible for approximately 1.4% of total mortality annually worldwide, 0.8% of all disability-adjusted life years (DALYs) and 2% of all cardiopulmonary disease *(1, 2)*. Additionally, air pollution impacts climate change, visibility, and ecosystem health. Considerable damages, estimated to be worth $71 – 277 billion per year *(3)*, are caused by poor air quality, and still, considerable uncertainties remain in its management and science, e.g. the ability to predict whether ozone and particulate matter concentrations will improve or worsen in response to a certain change in policy. The largest uncertainties lie in emission inventories, which are the state and federal governments' budgets of how much pollutants are being emitted by which sources. The development of effective strategies for improving air quality requires accurate accounting of air pollutant emissions.

Emission inventories are considered the foundation of air quality management. However, independent estimates suggest that the government's official emission inventories may be under or overestimated by a factor of five or more *(4-12)*. They may be inaccurate or incomplete due to limitations in the current emissions estimation processes, which relies on the use of emission factors that describe the amount of pollutant emitted per unit of activity performed, e.g. grams of particulate matter emitted per mile driven for a truck. Emission inventories contain point, nonpoint (area), mobile and biogenic sources. While air pollutant emissions from point sources such as power plants, large factories, chemical plants, and oil refineries are directly measured by Continuous Emissions Monitoring Systems (CEMS) and reported to state environmental agencies, emissions from smaller dispersed sources such as gasoline stations, refuse fires, painting, and yard tool use are only estimated via engineering calculations. Emissions from such "area" sources are typically calculated by multiplying an emission factor by the amount of activity conducted, e.g. miles driven for the example of the truck.

Emission factors are typically based on a handful of measurements that are not always representative of the population, and activity rates are often modeled. In fact, in 2001, the US General Accounting Office (GAO) called on EPA to improve its oversight of emissions reporting from area sources. The GAO study documented that only 4% of all reported emissions were based on actual monitoring or testing. The remaining 96% were based on estimates calculated using emissions factors *(13)*. Also, the National Research Council (NRC) has repeatedly called for better quantification of emission inventories and states that lack of proven measurements to test the accuracy and precision of emissions data contributes significantly to emissions uncertainty *(14-16)*.

A 1990 study summarized results of an uncertainty analysis of emissions models supported by the National Acid Precipitation Assessment Program (NAPAP). The report states that sources of emission uncertainty identified in the estimation process include variability in each of the individual components contributing to the estimate, systematic errors associated with the emission factor, variability in the accuracy and precision of data required to generate emissions estimates and the limited number of methods available to measure and treat uncertainties in emissions estimates *(17)*. Therefore, based on the information above, standard "area" and "mobile" source emission inventories have not been properly verified through direct measurements, even though the inventories serve as the basis for major decision-making when localities are attempting to improve their air quality.

The ability to measure air pollutant fluxes to the atmosphere has improved over the last two decades with the advancement of eddy covariance measurement techniques. Eddy covariance is a micrometeorological method that measures the net exchange of air pollutants across the surface-atmosphere interface. The method entails the rapid measurement of the turbulent eddies that transport trace gases such as carbon dioxide (CO_2) and nitrogen oxides (NO_x), as well as fine particulate matter ($PM_{2.5}$), into and out of the atmosphere *(18)*. The majority of eddy covariance applications have been situated on stationary towers over forest, grassland or agricultural canopies in an effort to quantify fluxes of CO_2, nitrogen, ozone and organic compounds *(19-21)*.

To a lesser extent, eddy covariance has also been used in urban areas to explore anthropogenic pollutant fluxes *(22-24)*. Grimmond et al. (2002) and Velasco et al. (2005) demonstrated via measurements from tall stationary towers (27 m and 37 m, respectively) that CO_2 fluxes in cities are typically positive, or upward under the defined coordinate system. The studies not only proved that direct measurement of emissions in urban areas were possible, but also quantified the extent to which urban areas act as net sources of CO_2 and contribute to the overall emissions budget. Martensson et al. (2006) measured particulate matter fluxes from a 105-m tower in Stockholm, Sweden and concluded that heavy-duty vehicular (HDV) traffic and construction contributed significantly to high aerosol number concentrations and fluxes.

Most of the eddy covariance systems currently used for flux measurements are stationary and therefore provide information for an area limited to the tower's footprint, defined as the area around the measurement point that contributes to the observed fluxes. Also, many of the urban eddy covariance systems described measure only one or two pollutants such as CO_2 or particulate matter. To address these limitations, we have developed a mobile eddy covariance system that is capable of measuring the most problematic contributors to violations of EPA's National Ambient Air Quality Standards: CO_2, NO_x, volatile organic compounds (VOC) and $PM_{2.5}$. Our Flux Laboratory for the Atmospheric Measurement of Emissions (FLAME) allows for the real-time neighborhood-scale measurement of pollutant fluxes. Unlike tower-based measurements that require significant physical and electrical infrastructure, the mobile FLAME has the ability to conduct measurements in many different areas and to focus on specific sources by parking downwind of them. The FLAME can advance significantly the ability to estimate emissions.

2.0 Literature Review

The regulation of anthropogenic emissions such as CO_2, NO_x, $PM_{2.5}$, carbon monoxide (CO), and VOCs has grown in recent years due to the increasing scientific and public awareness of issues such as health, climate change, reduced visibility and ecosystem fitness. The study of air pollutant emissions as it relates to this research can be divided into five major categories

of supporting literature:

1. adverse health and environmental effects due to anthropogenic emissions;
2. measurement methods for emissions;
3. emission inventories and their limitations;
4. methods of modeling anthropogenic emissions trends and their limitations, and;
5. emissions as a function of socioeconomic status.

2.1 Adverse Effects of Anthropogenic Emissions

Air pollution has wide ranging health and environmental effects. Exposure to $PM_{2.5}$ and ozone increases the risk of cardiovascular disease and lung cancer *(25)* as well as the development of acute respiratory illnesses such as asthma in children *(26, 27)*. Besides these obvious health effects, air pollutant exposure has also been linked to fetal death, birth defects, being small for gestational age (SGA), preterm birth, clinically overt cognitive, neurologic, and behavioral abnormalities and subtle neuropsychologic deficits *(26)*. The Intergovernmental Panel on Climate Change predicts that CO_2 and other greenhouse gas emissions along with some specific types of $PM_{2.5}$ will cause an increase in global surface temperature by 1 to 6 ^{o}C over the next century. Air pollution is also responsible for regional and global visibility degradation *(28-30)* as well as approximately 70% of nitrogen deposition into estuaries *(19, 20, 31)*. Mitigation of these health and global impacts requires a clear understanding of the magnitude of air pollutant emissions and how to reduce or eliminate them.

2.2 Eddy Covariance and Relaxed Eddy Accumulation Methods

Eddy covariance is a technique that allows measurement of turbulent pollutant transport, the main mechanism for dispersing pollutants after they are emitted from a source. Ground-based emissions are transported upward into the atmosphere by the random motion of eddies. Eddy covariance measurements apply micrometeorological theory, based on turbulent decomposition of the advection-diffusion equation, to capture the net exchange of pollutants across the surface-atmosphere interface. The correlation between vertical wind velocities and scalar concentration fluctuations leads to mass transfer upward or downward *(18)*.

$$F_x = \overline{w'C_x'} \qquad \text{(Eq. 1)}$$

The flux (F_x) of species x is calculated as the time averaged quantity of the covariance between the instantaneous deviation of the vertical wind velocity (w') and the instantaneous deviation of the measured concentration of x (C_x') *(18, 24)*. The deviations are calculated as the difference between the measured value and the best-fit line through the data over the averaging period, 30 min in this case. A positive flux represents species x net transfer upward into the atmosphere from the surface, whereas a negative flux represents downward net transfer from the atmosphere to the land surface. The eddy covariance method requires fast ($\geq$ 10 Hz) measurements of wind velocity and pollutant concentrations from an elevated position, typically a tower *(22, 32, 33)* and calculates fluxes according to Equation 1.

Vertical wind velocities and pollutant concentrations are correlated because pollutant concentrations are typically higher in the upward moving parcels of air (Figure 1). In other words, anthropogenic emissions are collected within the rotating eddy currents and transported during the upward motion of the current *(22, 24, 33)*. Turbulent flux can be compared to the transport of passengers on a train traveling back and forth between suburbs and the city center during morning rush hour. The train is full in the inbound direction and empty in the outbound direction. Even though the train undergoes no net motion as it travels back and forth, there is a net flow of commuters into the city *(34)*. Similarly, air undergoes no net motion in the upward direction, yet, there is a net flux of pollutants upward into the atmosphere.

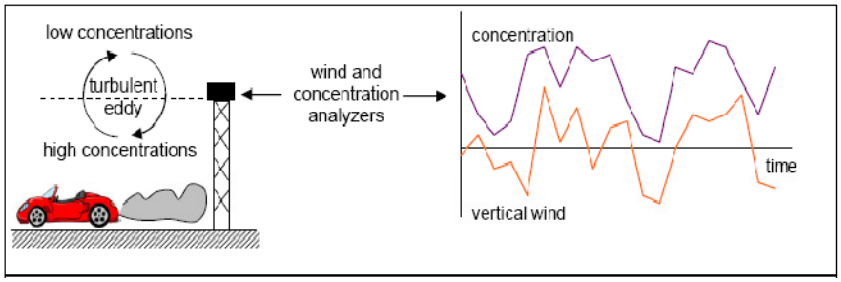

Figure 1. Turbulent eddies pick up anthropogenic emissions from the surface and transport them upward into the atmosphere; the covariance between vertical wind velocity and concentration is the pollutant's flux.

The eddy covariance technique has been used extensively in the biogeosciences to measure fluxes of CO_2, nitrogen, ozone organics and other compounds over forests, grasslands and

agricultural areas. Studies have shown that in densely vegetated areas, CO_2 flux is typically negative (downward) during the day due to photosynthetic activity and positive (upward) at night due to plant and soil respiration. The application of eddy covariance in urban areas, especially on a neighborhood scale has been limited to date. Unlike vegetated areas, fluxes of CO_2 in urban areas are generally positive, meaning that the areas are a net source rather than a net sink of CO_2 *(22, 35, 36)*.

Although eddy covariance is an ideal method for pollutant flux measurement, it also has limitations. Eddy covariance is most applicable over flat, homogeneous terrain *(18)*. Because of the requirements for homogeneity, urban measurement of pollutant fluxes by eddy covariance methods requires special considerations. Based on height of buildings and other structures in an urban environment, an elevated measuring point at least two times the height of the surface elements, e.g. –buildings and trees, must be used *(22)*. Another requirement of urban measurements is that terrain upwind of the measuring location must be relatively uniform with respect to density of buildings, trees, roads, vegetation and other surface features. However, if sited properly, urban eddy covariance measurements are possible over complex surfaces *(37)*.

Another limitation of the eddy covariance method is that many of the sensors required for fast-response (10 Hz) measurement are unavailable or very expensive for some compounds *(38)*. A technique known as relaxed eddy accumulation (REA) has been used successfully to measure fluxes of such compounds *(38-43)*; for our purposes, VOCs present the measurement challenge. Using the updraft (C_{up}) and downdraft (C_{down}) components of the vertical wind velocity, VOC fluxes are calculated as:

$$F_x = \beta\sigma_w\left(\overline{C}_{up} - \overline{C}_{down}\right) \quad \text{(Eq. 2)}$$

where β is a dimensionless empirical coefficient having a constant value of 0.56 and σ_w is the standard deviation of the vertical wind speed *(38, 40, 42)*.

One type of REA system consists of three separate sorbent tubes, each equipped with fast

response solenoid valves (Figure 2). The valves are activated based on the direction of the vertical wind velocity *w*. The third valve is for the collection of neutral, i.e. neither positive nor negative, wind velocities. Fluxes are determined from the difference of the average concentrations between the upward and downward air velocities over a relatively large timescale (30 min) *(42)*.

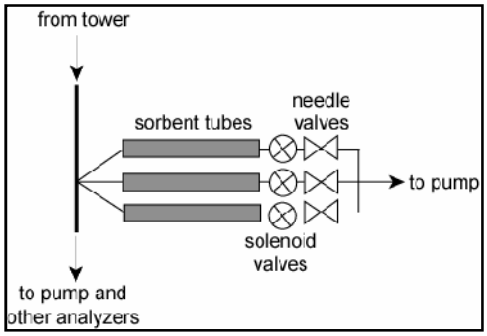

Figure 2. Relaxed eddy accumulation configuration for the conditional sampling of VOCs.

In contrast to indirect methods of emission inventory estimation using activity patterns (traffic, residential and business diurnal cycles) and emission factors, eddy covariance is a science-based method that allows direct measurement of emissions fluxes. In other words, no predictive assumptions are required about typical emission factors or activity patterns to determine what emissions levels will be; they are directly measured. A mobile system allows measurements to be made in a variety of settings. Previous efforts have demonstrated that eddy covariance measurement methods in urban areas can be successful, but a mobile system provides small-scale insight into air quality science that has not yet been realized. Then, using geographic information systems (GIS) software, we can pinpoint areas of concern based on socioeconomic factors, land use, available resources, traffic information and particular emissions sources.

2.3 Emission Inventory Inaccuracies

2.3.1 Evidence for Inaccuracies

A host of techniques has been used to validate, invalidate, or estimate emission inventories indirectly, including applying receptor models to observed concentrations *(44)*, incorporating inventories into air quality models and comparing predictions with atmospheric measurements *(45-49)* or satellite observations *(50, 51)*, comparing pollutant ratios within

the inventory to ambient ones *(52)*, conducting on-road studies for mobile sources *(53)* and applying inverse methods using three-dimensional air quality models *(54, 55)*, to highlight a handful of the most recent publications.

In many comparisons of ratios of specific pollutants in inventories with those either observed through ambient measurements or predicted by a chemical transport model (CTM), inaccuracies in the emission inventory are cited as the source of any discrepancies. CTMs require emission inventories and meteorological parameters as input and then solve fundamental physical and chemical equations to predict pollutant concentrations. An effort to validate Sao Paolo's State Environmental Agency's emission inventory suggested that on-road motor vehicle emissions of NO_x were significantly overestimated, while non-methane organic gas (NMOG) emissions were underestimated. The researchers developed a revised inventory, ran an air quality model with it and compared model output with an episodic air pollution event. The revised inventory produced air quality predictions that closely matched observed values *(56)*. Comparison of ratios of different VOCs measured during high-ozone (O_3) episodes in Hong Kong to those in an emission inventory gave mixed results. Observed alkane ratios differed significantly from those in the inventory *(57)*.

Very commonly, concentrations predicted by a CTM are compared with ground-based, aircraft or satellite observations, and any disagreement between the two is usually attributed to problems with the emission inventory. One study used aircraft observations in an effort to improve regional O_3 modeling with the regional air quality model, Sulfur Transport Eulerian Model (STEM), and found that O_3 bias came from an overestimation in reported NO_x emissions. Work conducted in eastern Texas using ground-based and aircraft measurements collected during the Texas Air Quality Study of 2000 revealed that biogenic emissions of hydrocarbons such as isoprene dominate the VOC emission inventory. When modeled predictions of isoprene were compared with measured values, differences on the order of 270% were noted. Also, the model overestimated upper air concentrations by a factor of two over rural areas and underestimated observations over urban areas. As a result, measured concentrations differed by as much as 30% from those modeled *(58)*.

2.3.2 Reasons for Inaccuracies

One of the largest sources of inaccuracy in inventories is emission factors (EFs). According to the EPA, emissions factors are the fundamental tool in developing national, regional, state, and local emission inventories for air quality management decisions. However, many emission factors are based on a limited set of data from specific types of sources under a specific set of conditions. Extending their use more broadly may result in inaccurate estimates of emissions. For example, a study of household coal burning in China discovered that different coals have very different particle emissions. The EFs calculated for four pollutants ($PM_{2.5}$, CO_2, total hydrocarbons, and NO_x) were 2 – 4 times higher for bituminous coals than for anthracites. Studies of past emission inventories and their EFs show that these two coals were not treated separately, and significant inaccuracies resulted *(59)*. Also, a comparison of ammonia (NH_3) EFs from agricultural liquid manure systems in Europe found that national differences in EFs lead to very large differences in emissions. Differences in EFs were attributed to different agricultural practices as well as different climatic factors *(60)*. A study conducted in Uppsala, Sweden closely observed the contribution of milling, smelting and refining of sulfide ores to mercury (Hg) emissions in a global context. The study concluded that Hg emitted during the processing of copper, lead and zinc ores has been severely underestimated in Hg emission inventories and that by reducing these emissions, a global impact on the reduction of Hg emissions can be accomplished *(61)*. Finally, a study involving the analysis of greenhouse gas (GHG) emissions conducted in 2007 by the Emissions Research and Development Division of Environment Canada found significant discrepancies in reported versus measured methane (CH_4) and nitrous oxide (N_2O) emissions caused by heavy-duty vehicles using diesel based fuels *(62)*. These discrepancies also have a significant effect on the EFs used to develop national inventories because EFs are used in conjunction with air quality computer models to predict and analyze air quality in various regions throughout the world.

Another specific type of inaccuracy in emission inventories is incorrect counts of pollution sources. A Belgian study in 2007 designed an air quality model using emission inventory data and compared results with measured particulate matter (PM_{10} and $PM_{2.5}$) concentrations.

Results showed a significant difference in PM_{10} values; which was found to be caused by an incomplete cataloging of PM_{10} sources in the inventory *(63)*.

Emission inventories may simply lack key categories, such as maritime sources, which in most national inventories are not even considered. Typically these emissions are omitted from the National Emission Inventory (NEI) because they occur in international waters *(64)*. A recent study asserted that emissions from ships have been overlooked for too long and that CO_2 emissions will increase by 2% – 9% and NO_x emissions will increase by 1% - 8% by 2010 due to increased shipping activity. A review of ship activity patterns from the International Comprehensive Ocean – Atmosphere Data Set (ICOADS) and the Automated Mutual-Assistance Vessel Rescue System (AMVER) data set found spatial and statistical sampling biases, which could affect the accuracy of ship emission inventories as well as atmospheric air quality modeling.

Emission inventories prepared for the same geographical area and time may use different methods and produce estimates that do not necessarily agree. For example, a comparison of global emission inventories found that differences for individual megacities were twice as large as those for the global total. The same study found that further breaking down city emissions into various sectors of the city revealed significant differences in total emissions from the city based on the differences in emissions sources. Differences stemmed from inconsistent methodologies used in emission inventory construction *(65)*.

Up to and over 10% under and overestimation of emissions due to inaccuracies in the spatial data used to assign emission sources is not uncommon. For example, a study in The Netherlands analyzed the sensitivity of nitrous oxide (N_2O) inventories in Dutch fen meadows to land cover data. The study revealed that when land cover databases were used with N_2O inventory data in those areas, propagation of random and systematic error occurred, whether using more detailed or coarse land cover databases. Errors were greater than 11% for most areas *(66)*.

Errors in mechanistic models used to predict emissions are another source of inaccuracy in

inventories. Researchers conducted measurements and modeling of atmospheric flux of ammonia from an anaerobic dairy waste lagoon in 2007. Results from these experiments revealed significant normalized mean errors in the theoretical and empirical mechanistic emission models versus the measured ammonia emissions of 120% and 21%, respectively.

2.4 The Role of GIS in Emission Inventories and Air Quality

Geographical information systems (GIS) software has been used extensively in the development of emission inventories *(67-72)*; however, minimal research has been done that compares direct measurements of non-point, i.e. area and mobile sources, emissions with GIS-based spatial characteristics (population, land use, etc.). Using GIS-based mapping software in tandem with source area modeling, it is possible to pinpoint major emissions sources and relate them to the characteristics of the surrounding areas. Emissions mapping models can be developed that account for surrounding land use, demographic and traffic characteristics of specific test areas. Spatial patterns of measured air pollutant concentrations can be used to estimate annual air pollutant exposure levels of various economically or demographically diverse areas. Measurements of fluxes combined with footprint analysis can help determine emissions source locations and regulate heavy emissions contributors. Mapping of air pollution, its effects and population exposure levels has been conducted quite often using air pollutant concentration information and GIS *(73-77)*, but relating demographics and directly measured non-point source emissions is a new concept.

Using GIS with proximity analysis has been used for investigating the distributional effects of environmental hazards, including poor air quality, on various demographic groups *(78)*. Proximity analysis uses distances between sources of pollution and receptors, i.e. humans, to provide information about exposures to pollutant concentrations. Using GIS with this method helps to account for the spatial effects of pollutant release height, meteorology and reactions or population activity patterns *(78)*. It is considered a first step towards representing exposures for complex environmental hazards such as air pollutants *(78)*. GIS spatial mapping has been used successfully with proximity analysis to examine the potential for environmental inequities between population subgroups due to ambient air pollution exposures. However, this technique is limited by the spatial sparseness of air quality

monitoring sites—usually tens of kilometers apart, at least—and makes assumptions as to the exposure levels of various groups based on proximity to emissions sites instead. The research presented here provides more direct measurement of affected areas through the use of a mobile laboratory that can probe air quality at multiple locations within a neighborhood.

Although a relatively new concept, GIS can be used as a graphical interface to relate exposure to directly measured air pollutants with various demographic spatial characteristics. Visualization of the data may facilitate discovery of relationships between population characteristics, land development, sources of emissions and exposure to pollutants.

2.5 Emissions as a Function of Socioeconomic Status

Studies on a neighborhood scale of air pollution in resource poor or economically challenged neighborhoods have focused on ambient concentrations but not emissions, the actual source of the problem. Some studies have shown that census tracts with concentrated poverty, unemployment, and dependence on public assistance displayed an adverse physical environment due to their proximity to large sources of air pollution *(2, 25, 79-81)*. Birth records from 1994 to 1996 in Los Angeles County were linked to traffic counts, census data, and ambient air pollution measures. Low birth weights occurred disproportionately often in the economically challenged neighborhoods. Further, in these poorer neighborhoods, adverse effects associated with air pollution among women and children with known risk factors were more prevalent during the winter months *(80)*. Reducing the exposure of the economically challenged to the adverse effects of air pollution warrants a concerted effort of social, economic, and environmental policies, focused on not only individual risk factors but also the reduction of localized air pollution, expansion of health-care coverage, and improvement of neighborhood resources *(80)*.

Certain aspects of air quality in economically challenged areas can be directly attributed to unequal access to resources. In Appalachia, there are many areas that are considered remote by the living standards of today. These remote areas are not afforded the same resource availability and are often forced to use alternate methods of energy generation for the purposes of warmth or electricity. For instance, some may use wood or oil as a combustion

source for fuel; these sources are dirtier than natural gas and have been well documented as causes of air pollution related illnesses *(81-86)*. Mining towns present another case where poverty and air pollution are linked. The theory behind mining is that it brings wealth to certain counties or towns, but research shows quite the contrary with a majority of mining towns and counties having higher than average poverty, disease, crime and mining/air pollution related illness *(87)*.

Demographically and racially diverse, poor neighborhoods are more likely to experience the adverse health effects and negative impacts associated with air pollution. For example, a study of adverse health effects in relation to socioeconomic factors of a specific neighborhood in Northern California suggested that higher levels of perceived neighborhood problems were associated with poorer quality of life, poorer physical functioning and increased depressive symptoms among people with asthma *(88)*. A study conducted in Detroit considered race-based residential segregation and associated concentrations of poverty and wealth to be fundamental factors influencing multiple, more proximate predictors of cardiovascular risk. Within this study, it was found that a distinct relationship exists between poverty, wealth, and race which results in high anthropomorphic and physiologic indicators of cardiovascular risk for target groups of poor minorities. The study design included efforts to collect and analyze airborne particulate matter over a three-year period to determine overall effects of air emissions among poorer areas of Detroit *(89)*.

The relationship between air pollution or environmental pollution and poverty has been documented. It is well known that developing countries as well as economically challenged neighborhoods in the US are often burdened with limited resources and limited knowledge regarding the adverse effects associated with poorly engineered water, wastewater and air treatment infrastructure. All human beings should be afforded the right to clean drinking water, adequate sanitation and the basic infrastructures necessary to sustain a community environment free of preventable disease that is associated with inadequate engineering practices.

3.0 Design of a Mobile Flux Lab for the Atmospheric Measurement of Emissions

3.1 Equipment

We designed a uniquely mobile eddy covariance system, dubbed the Flux Lab for the Atmospheric Measurement of Emissions (FLAME). It measures CO_2 and water vapor by infrared absorption (LI-COR LI-7000), NO_x by chemiluminescence (EcoPhysics CLD 88Y), $PM_{2.5}$ by aerosol photometry (DustTrak 8520), CO by infrared absorption (Teledyne 300E), temperature and three dimensional wind velocities by a sonic anemometer (Applied Technologies SATI-3K). VOCs were measured using the relaxed eddy accumulation method (Figure 3) using capture and analysis methods described in a separate section below.

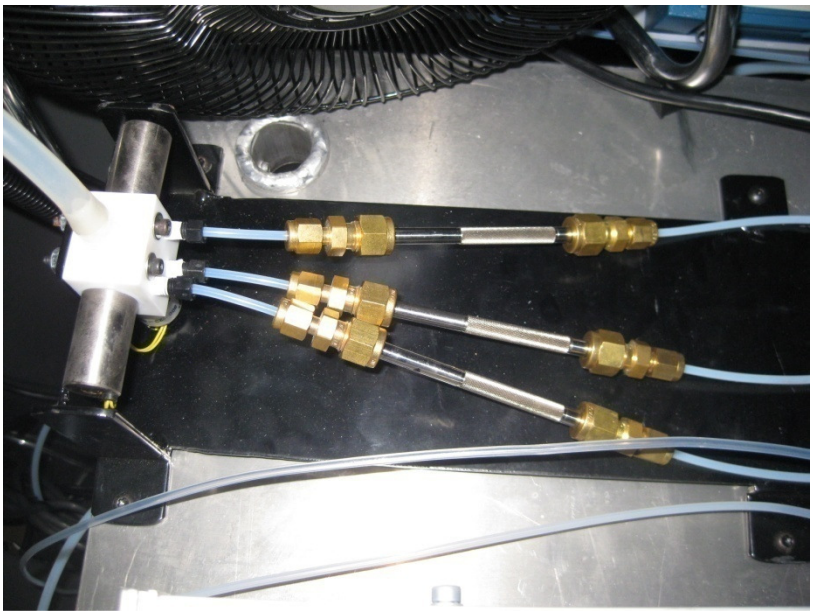

Figure 3. Relaxed eddy accumulation (REA) system used to measure VOCs in the FLAME.

The experimental platform consists of a 2.5 m tall modified television news van with an extendable 14 m mast. The sonic anemometer and sample tubing were mounted onto a pivoting/rotating base on top of the mast. The sample tubing used was 0.5 inch O.D. conductive PTFE lined polyethylene tubing (TELEFLEX T1618-08) to minimize gas and particle line losses. A pump was used to draw sample air down to ground level at 20 L min^{-1}. Air flow was controlled using a mass flow controller (Cole Parmer Model No. EW-32907-73), and each of the analyzers sampled directly from the main sampling line through a

custom designed Teflon manifold. A data logger (National Instruments Compact FieldPoint 2110) and computer within the command center of the FLAME were used to log and process the data.

Figure 4. Rear view of FLAME measurement platform showing sensor equipment configuration. Relaxed eddy accumulation system is also located in the rear of the van and is shown in Figure 3.

All equipment was securely mounted in the rear of the FLAME (Figure 4) and powered using a 4500 W, 60 Hz, 120/240 VAC gasoline generator (Onan GENSET 4500 Series). We recorded data at 10 Hz calculated fluxes according to Equation 1 over 30-min intervals.

4.0 Data Quality Assurance and Control

4.1 Calibration

For the gas and particle analyzers, we developed rigorous calibration protocols according to the manufacturers' recommendations. Calibration of the LI-COR CO_2 analyzer was conducted prior to and twice per week during each field campaign by flowing dry, CO_2-free zero air through the analyzer. Calibration of the NO_x analyzer was conducted every two days during field campaigns by flowing a known concentration of NO_2 through the EcoPhysics CLD 88Y analyzer while simultaneously flowing dry, NO_x free zero air through the analyzer and measuring the span. Similar to the NO_x analyzer, calibration of the CO analyzer was also conducted every two days during the field campaigns by flowing a known concentration of CO through the Teledyne 300E while also flowing dry, CO free zero air through the analyzer and measuring the span. Calibration of the DustTrak 8520 aerosol photometer was conducted daily during the field campaigns by collecting filter samples for gravimetric analysis and

comparing the results with the corresponding time-integrated measurements recorded by the DustTrak.

4.2 Sample Line Testing

The FLAME used a long sampling line in which losses due to deposition to the inside tubing walls were a concern. Ideally the analyzers would be placed near the inlet on top of the tower to minimize the length of sampling lines, but the configuration of the mobile system requires the analyzers to be placed at ground level. Similar geometry has been used at an established flux tower site to measure VOC emissions above a forest with a 12-m sampling line and analyzers at ground level *(90)*. Gas and particle losses were quantified by comparing pollutant concentrations at ground level using both short (< 1 m) and long (14 m) tubing configurations.

Line losses were measured during three non-consecutive days for test periods of three hours each day. Pollutant concentrations were recorded for 30 min with the 14-m sampling line connected at ground level and for the next 30 min without the sampling line, until the end of the test for a total of six sample periods, three periods with tubing, three without. Losses of CO_2 and NO_x were found to be minimal (0.71% and 0.53% respectively). Water vapor losses were eclipsed by humidity variations in the atmosphere during the test periods. CO losses were ~11%. A slight loss in $PM_{2.5}$ was noted, 5 – 6% on two days and 14% on the third. The larger difference during the third day may have been due to the different maximum temperatures, or the amount of moisture in the air. This difference is not large, and the gravimetric method is subject to artifacts, such that line losses in the FLAME are minor and eclipsed by other uncertainties in the eddy covariance method.

4.3 Post-processing

Standard post-processing of the flux measurements included sample line testing, hard spike removal, soft spike removal, lag correction, coordinate rotation, calculation of fluxes and quality assurance of the calculated fluxes *(22, 24, 91)*. For quality assurance, calculated fluxes were subjected to spectral and co-spectral analysis and stationarity testing.

4.3.1 Spike removal

Hard spike removal is a standard quality control procedure for raw instantaneous data. Spikes are typically a result of random electronic spikes or sonic anemometer transducer blockage during events of high precipitation. Hard spikes are removed through both visual inspection of the data, as well as computing the mean and standard deviation of sample data in 1-s windows (10 samples at 10-Hz sampling rate) and removing data points that are more than 3.5 standard deviations from the window mean *(92, 93)*. Data points that are removed are replaced using linear interpolation. If more than four consecutive points are detected, those four points are considered a legitimate signal and are not removed. The spike removal process is continued until no more spikes are discovered within the data.

Soft spike removal is conducted similar to hard spike removal. Soft spikes typically result from large short lived departures from the 15-min mean of 30-min data sets. Data samples are removed if they are more than 3.6 standard deviations from the 15-min mean and contain three or fewer consecutive samples that qualify under the above conditions. If more than three consecutive samples are detected as spikes, the values are considered legitimate and not removed. Samples that are removed are linearly interpolated and replaced. The sample periods are adjusted and the soft spike removal process is repeated until no spikes are detected *(94)*.

4.4 Lag Correction

Due to long distances between the sample location at the top of the mast, and the analyzers located within the van, it was necessary to calculate the lag time between the time of sample collection and the time of sample analysis. Using a flow rate of 20 L min^{-1}, a tubing diameter of 0.0127 m (0.5 in) and a length of 14 m, the lag time can be calculated as approximately 5 s. In an effort to validate this hand calculated value, the cross correlation between C' and w' were calculated and the lag time which maximizes the result was selected *(91, 93)*.

4.5 Coordinate Rotation

We applied a planar-fit three-dimensional coordinate rotation method to align the sonic anemometer's coordinate system with the local mean streamline winds at the end of each

averaging period *(95)*. The purpose of the coordinate rotation is to eliminate errors due to improper alignment of the sonic anemometer sensors in relation to the terrain surface *(91)*. Also, based on measurement platform configurations, actual measurements could be aerodynamically shadowed by the measurement tower *(24)*. However, the configuration of the FLAME is considerably different than typical tower platforms due to its uniquely mobile capabilities. The sonic anemometer was not obstructed by a bulky tower and also had the ability to be rotated into the prevailing wind.

4.6 Spectral and Co-spectral Analysis

Spectral and co-spectral analyses (Figure 5) were conducted on the raw temperature, concentration and vertical wind velocity data. Spectral and co-spectral analyses help to identify weakened raw data samples caused by limited analyzer response times, physical instrument size, instrument and inlet separation distances and general signal processing associated with detrending or mean removal *(23, 24, 96)*.

Figure 5 shows the spectral analysis plot of temperature and CO_2 data from an arbitrarily chosen 30-min data set (9:13 to 9:43) sampled on June 26, 2007 at the intersection of Ferry and Center Streets in Worthington, KY. The spectra clearly obey the -2/3 power decay law expected during unstable atmospheric stratification *(23)*. Figure 5 also shows the co-spectra of the fluctuating (mean-subtracted) components of temperature (T') and CO_2 concentration (CO_2') with the fluctuating components of vertical wind velocity (w'). The co-spectra follow a -4/3 power decay law *(23)*. Ideally, two separate variables being measured independently of one another should have no systematic phase shift and no co-spectral distortion *(24)*. That the two independently measured values exhibit similar power decay characteristics with a -4/3 slope is an excellent indication that our system is fully capable of accurately measuring turbulent fluxes via the eddy covariance method, provided the 30-min data set also passes stationarity testing.

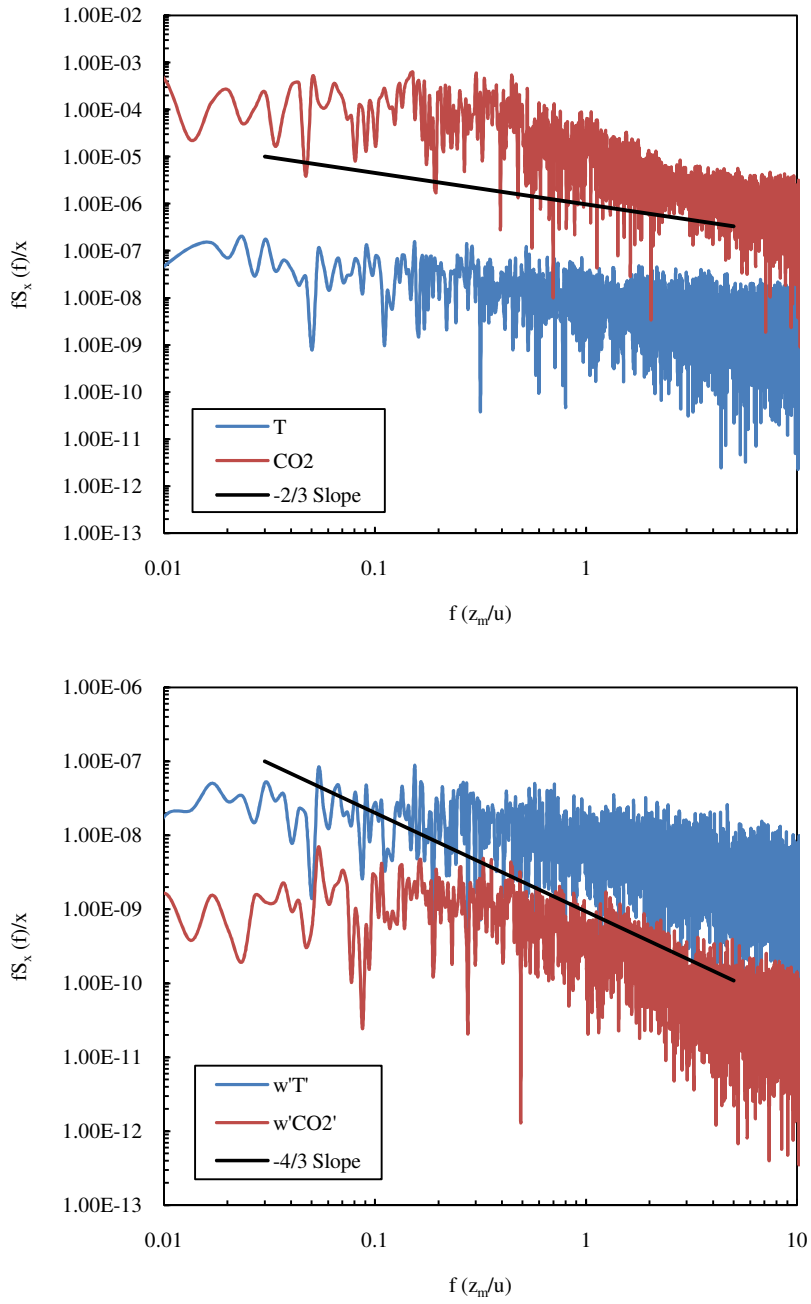

Figure 5. Typical spectral (top) and co-spectral (bottom) analysis plots from a 30-min period. Valid spectra will decay based on the -2/3 and -4/3 slope power law as seen here.

4.7 Stationarity Test

Based on the Monin-Obukhov similarity theory, stationarity of key atmospheric variables is required to ensure the validity of measured fluxes *(97)*. Stationarity implies that the measurement height exceeds the blending height, meaning that the point of measurement is sufficiently high enough above ground for the surface characteristics to be considered

homogeneous *(24, 98)*. One method for determining stationarity of calculated flux values is to calculate the difference between the 30-min average flux from a data set and the average of six consecutive 5-min sub-periods of the same 30-min period (Figure 6). If the difference between the two flux values is greater than 60% then the data set is considered non-stationary and is excluded from further analysis *(22-24, 91)*.

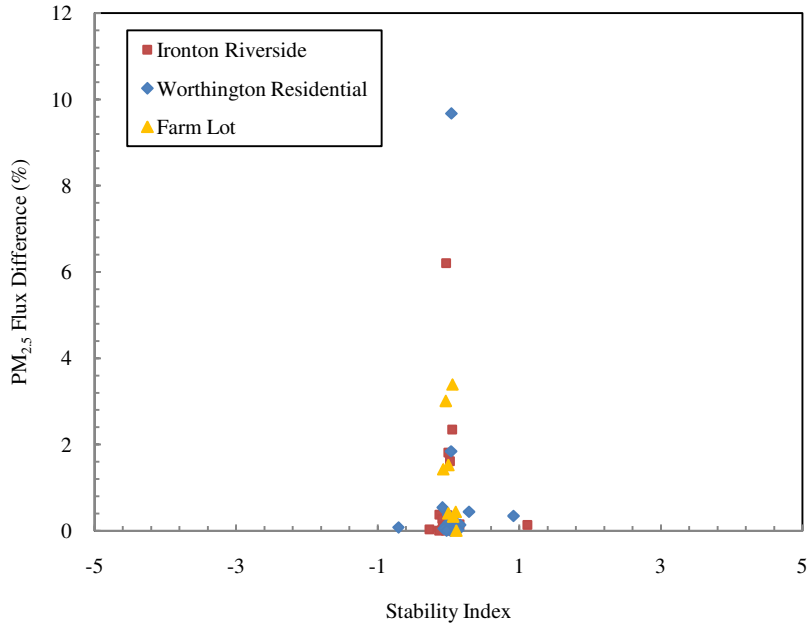

Figure 6. Example stationarity test results from a field campaign.

4.8 VOC Measurement Methods

EPA Methods TO-15 and TO-17 were followed for the sampling and analysis of air toxics. Compounds were trapped on Tenax TA, thermally desorbed, and quantified by gas chromatography with mass spectrometry. Quality assurance and quality control procedures included the collection of laboratory and field blanks in accordance with EPA TO-17 method requirements and storage of sample tubes at less than 4 °C for a period not to exceed 24 hr.

5.0 Measurement of Pollutant Fluxes

5.1 Overall Approach

We deployed the mobile flux system in three areas that have been selected to represent a range of land use types: semi-rural, small urban and large urban. We conducted field

measurements in spring, summer and fall months each year that typically coincide with episodes of high ozone pollution. The small urban area measurement sites focused on schools to allow for educational outreach opportunities.

5.1.1 Semi-rural Area

The City of Worthington, Kentucky located in Greenup County was the focus point for the measurement of small rural industrial area emissions because of its proximity to coal storage and processing facilities as well as coal transport infrastructure such as trains, trailers and barges. It is part of the Huntington-Ashland (West Virginia, Kentucky, and Ohio) metropolitan statistical area, which has a population of 290,000. Covering an area of approximately 8.1 km^2, Worthington has a population of about 1,700 and a median household income of approximately $34,700. Worthington is located along the Ohio River, which maintains a steady amount of barge traffic (3-8 barges hr^{-1} on average) and is the home of various types of manufacturing and industrial processes such as the fabrication, repair and demolition of rail cars, paint pigmentation, industrial abrasives development, steel processing and polystyrene manufacturing. Worthington is also home to a 4 km^2 rail yard used for the loading, unloading and transport of coal from the local coal mines in nearby West Virginia and neighboring areas of Kentucky.

5.1.2 Small Urban Area

The city of Roanoke, Virginia was the focus point for the measurement of small urban area emissions. Roanoke is a small city in southwestern Virginia with a metropolitan area population of approximately 300,000 and a city population of approximately 97,000. Roanoke is located between the Blue Ridge Mountains and the Virginia Allegheny Highlands. Despite its small population Roanoke is considered Western Virginia's center for industry, health, trade, education and travel. However, Roanoke has been described in the past as a "basic" nonattainment area for ozone, i.e., it violates the ozone standard. It had the highest PM concentrations in Virginia in 2002, and in 2005, the Virginia Department of Environmental Quality's monitors at two sites in both Roanoke and neighboring Salem recorded annual PM concentrations above allowable EPA standards. We conducted experiments at three sites near primary and secondary schools to determine the levels of air

toxics to which young students are subjected, in addition to measuring pollutant fluxes.

5.1.3 Large Urban Area

The city of Norfolk, Virginia and its surrounding areas (Chesapeake, Portsmouth and Virginia Beach) were the focal point for the large urban area measurement campaign. Norfolk is located within the Greater Tidewater area of Virginia and has a population of approximately 250,000. The metropolitan area has a population of approximately 1.5 million. Norfolk is a port city with a rich history and is home to a significant amount of industry, including coal processing, rail yard activities, shipping industry, power generation and much more. The area also has a large tourist industry.

Norfolk and its surrounding areas are designated as 1- and 8-hr ozone non-attainment areas, and based on EPA records, during the hot summer months, often experience high levels of particulate matter. Measured fluxes were compared with the National Emission Inventory and an inventory developed for air quality modeling purposes that contains hourly emissions on a 12-km grid. This campaign also focused on using GIS mapping tools and various demographic and land use information to develop a greater knowledge of air quality and its adverse health effects in socioeconomically diverse areas.

5.2 Site Selection

Site selection was based on many factors to capture a wide range of land uses, socioeconomic statuses, traffic patterns and potential for anthropogenic emissions. To achieve spatially integrated results representative of the local scale, we required that the tower be twice the mean height of roughness elements, e.g. buildings or trees *(22)*. When using the mobile eddy covariance system, we sought areas with low one- to two-story buildings and trees no taller than 7 m, extending at least 1 km in all directions. While this requirement limited us from conducting experiments in every location, the mobile system provided much more flexibility than would a taller stationary tower, which must be erected, stabilized with wires, and powered with permission from a land owner. We used a global positioning system to fix our exact latitude, longitude, and altitude.

Selection was also integrated with educational outreach opportunities. We targeted schools and colleges as field sites; these provided safe, geographically and socioeconomically varied locations. When possible, we parked our mobile flux tower at or near schools and offered guided tours of the mobile system to students. During the tour, we described the motivation for our study and the methods we were using. We also prepared and distributed informational flyers explaining the project to students. This outreach activity helped educate students and community members about air pollution and hopefully stimulated excitement about scientific research.

5.3 Source-Receptor Relationship

The connection between sources of emissions and what is measured at a particular site, or receptor, is known as the source-receptor relationship. We employed an existing footprinting model to characterize the source-receptor relationship at our field sites. We used a three-dimensional Lagrangian stochastic footprint model *(99)* to determine the tower's footprint *(37)*, or the area beneath the tower where emissions influence measurements at the top of the tower. The model estimates the two-dimensional source area by solving analytically the advective-diffusion equation. By incorporating measured turbulence variables, the tower height, and surface roughness length, the model estimates the probability that emissions at a certain point in space will contribute to the flux measured at a certain position. From the footprint function, we can estimate the dimensions of the area contributing to observed fluxes and in turn, pinpoint areas within the footprint that contain likely sources of the observed emissions.

6.0 Comparison with existing emission inventories

One of the most important elements of our research is to compare our results to official emission inventories that are used by governmental agencies for air quality management and planning purposes. Our comparison of measurements to the inventory highlighted uncertainties and areas for improvement in the official inventory. The primary source was the EPA's National Emission Inventory, which lists emissions by pollutant, major source category, and county or city. A secondary source was gridded inventories developed for air

quality modeling. These contain estimates of emissions at high spatial and temporal resolution. Good agreement between our measurements and the official inventory added confidence to them. Consistent under or overestimation of emissions in the inventory compared to the measurements indicated certain species and sources that require correction.

7.0 Broader Impacts

Ultimately, this research will lead to improved air quality through the development of more effective control strategies. New air quality regulations are expected to cost over $6.5 billion per year and potentially save $120 billion in health-related expenses *(100)*. More accurate estimates of emissions, and thus improved ability to predict air quality, will ensure that efforts to reduce air pollution are optimized for cost effectiveness. Eddy covariance flux measurements will provide new, real-world data for use in air quality models; and comparison of these measurements to existing estimates of emissions will highlight the uncertainties in them and will help improve methodologies used to predict emissions. The methods developed as part of this project will lay the groundwork for future flux measurements in urban areas.

Broader educational impacts are also associated with the research component of this project. The FLAME was often parked at schools, where we offered tours of the van and descriptions of our research to elementary, secondary and college level students. During field monitoring, the general public asked many questions about the FLAME, what the research entailed, and why it was being done. At all three sampling locations, newspaper agencies visited the site and reported on the FLAME and the research being conducted. During the Norfolk campaign, the FLAME was featured in a TV/internet news story, and public education was achieved through media coverage.

8.0 References

1. Ostro, B. *Outdoor air pollution: Assessing the environmental burden of disease at national and local levels.*; World Health Organization: Geneva, 2004.
2. Samet, J.; Krewski, D., Health effects associated with exposure to ambient air pollution. *J. Toxicol. Env. Heal. A* **2007,** *70*, 227-242.

3. Muller, N. Z.; Mendelsohn, R., Measuring the damages of air pollution in the United States. *J. Environ. Econ. Manag.* **2007,** *54*, 1-14.
4. Dreher, D. B.; Harley, R. A., A fuel-based inventory for heavy-duty diesel truck emissions. *J. Air Waste Manage.* **1998,** *48*, 352-358.
5. Fujita, E. M.; Croes, B. E.; Bennett, C. L.; Lawson, D. R.; Lurmann, F. W.; Main, H. H., Comparison of emission inventory and ambient concentration ratios of CO, NMOG, And NO_x in California South Coast Air Basin. *J. Air Waste Manage.* **1992,** *42*, 264-276.
6. Fujita, E. M.; Watson, J. G.; Chow, J. C.; Magliano, K. L., Receptor model and emissions inventory source apportionments of nonmethane organic gases in California San-Joaquin Valley and San-Francisco Bay Area. *Atmos. Environ.* **1995,** *29*, 3019-3035.
7. Harley, R. A.; McKeen, S. A.; Pearson, J.; Rodgers, M. O.; Lonneman, W. A., Analysis of motor vehicle emissions during the Nashville/Middle Tennessee Ozone Study. *J. Geophys. Res.-Atmos.* **2001,** *106*, 3559-3567.
8. Kasibhatla, P.; Arellano, A.; Logan, J. A.; Palmer, P. I.; Novelli, P., Top-down estimate of a large source of atmospheric carbon monoxide associated with fuel combustion in Asia. *Geophys. Res. Lett.* **2002,** *29*.
9. Kean, A. J.; Sawyer, R. F.; Harley, R. A., A fuel-based assessment of off-road diesel engine emissions. *J. Air Waste Manage.* **2000,** *50*, 1929-1939.
10. Marr, L. C.; Black, D. R.; Harley, R. A., Formation of photochemical air pollution in central California - 1. Development of a revised motor vehicle emission inventory. *J. Geophys. Res.-Atmos.* **2002,** *107*, 4048.
11. Mendoza-Dominguez, A.; Russell, A. G., Emission strength validation using four-dimensional data assimilation: Application to primary aerosol and precursors to ozone and secondary aerosol. *J. Air Waste Manage.* **2001,** *51*, 1538-1550.
12. Singer, B. C.; Harley, R. A., A fuel-based inventory of motor vehicle exhaust emissions in the Los Angeles area during summer 1997. *Atmos. Environ.* **2000,** *34*, 1783-1795.
13. U.S.G.A.O. *Air Pollution: EPA Should Improve Oversight of Emissions Reporting by Large Facilities*; United States General Accounting Office 2001.
14. N.R.C. *Rethinking the Ozone Problem in Urban and Regional Air Pollution*; National Research Council: Washington, D.C., 1991.
15. N.R.C. *Science and Judgement in Risk Assessment*; National Research Council: Washington, D.C., 1994.
16. N.R.C. *Modeling Mobile Source Emissions*; National Research Council: Washington, D.C., 2000.
17. Placet M., e. a. *Emissions Involved in Acidic Deposition Process*; National Acid Precipitation Assessment Program: Washington, D.C., 1990.
18. Baldocchi, D. D., Assessing the eddy covariance technique for evaluating carbon dioxide exchange rates of ecosystems: past, present and future. *Glob. Change Biol.* **2003,** *9*, 479-492.
19. Whitall, D.; Castro, M.; Driscoll, C., Evaluation of management strategies for reducing nitrogen loadings to four US estuaries. *Sci. Total Environ.* **2004,** *333*, 25-36.
20. Winchester, J. W.; Escalona, L.; Fu, J. M.; Furbish, D. J., Atmospheric Deposition and Hydrogeologic Flow of Nitrogen in Northern Florida Watersheds. *Geochim. Cosmochim. At.* **1995,** *59*, 2215-2222.
21. Wu, J. B.; Guan, D. X.; Sun, X. M.; Yu, G. R.; Zhao, X. S.; Han, S. J.; Jin, C. J., Eddy flux corrections for CO_2 exchange in broad-leaved Korean pine mixed forest of Changbai Mountains. *Sci. China Ser. D-Earth Sci.* **2005,** *48*, 106-115.

22. Grimmond, C. S. B.; King, T. S.; Cropley, F. D.; Nowak, D. J.; Souch, C., Local-scale fluxes of carbon dioxide in urban environments: Methodological challenges and results from Chicago. *Environ. Pollut.* **2002,** *116*, 243-254.
23. Martensson, E. M.; Nilsson, E. D.; Buzorius, G.; Johansson, C., Eddy covariance measurements and parameterisation of traffic related particle emissions in an urban environment. *Atmos. Chem. Phys.* **2006,** *6*, 769-785.
24. Velasco, E.; Pressley, S.; Allwine, E.; Westberg, H.; Lamb, B., Measurements of CO_2 fluxes from the Mexico City urban landscape. *Atmos. Environ.* **2005,** *39*, 7433-7446.
25. Pope, C. A.; Burnett, R. T.; Thurston, G. D., Pollution-related mortality and educational level - Reply. *Jama-J. Am. Med. Assoc.* **2002,** *288*, 830-830.
26. Wigle, D. T.; Arbuckle, T. E.; Walker, M.; Wade, M. G.; Liu, S. L.; Krewski, D., Environmental hazards: Evidence for effects on child health. *J. Toxicol. Env. Heal. B* **2007,** *10*, 3-39.
27. Kunzli, N.; Kaiser, R.; Medina, S.; Studnicka, M.; Chanel, O.; Filliger, P.; Herry, M.; Horak, F.; Puybonnieux-Texier, V.; Quenel, P.; Schneider, J.; Seethaler, R.; Vergnaud, J. C.; Sommer, H., Public-health impact of outdoor and traffic-related air pollution: a European assessment. *Lancet* **2000,** *356*, 795-801.
28. Aneja, V. P.; Brittig, J. S.; Kim, D. S.; Hanna, A., Ozone and other air quality-related variables affecting visibility in the southeast United States. *J. Air Waste Manage.* **2004,** *54*, 681-688.
29. Kim, Y. J.; Kim, K. W.; Kim, S. D.; Lee, B. K.; Han, J. S., Fine particulate matter characteristics and its impact on visibility impairment at two urban sites in Korea: Seoul and Incheon. *Atmos. Environ.* **2006,** *40*, S593-S605.
30. Ozer, P.; Laghdaf, M.; Lemine, S. O. M.; Gassani, J., Estimation of air quality degradation due to Saharan dust at Nouakchott, Mauritania, from horizontal visibility data. *Water Air Soil Poll.* **2007,** *178*, 79-87.
31. Russell, K. M.; Galloway, J. N.; Macko, S. A.; Moody, J. L.; Scudlark, J. R., Sources of nitrogen in wet deposition to the Chesapeake Bay region. *Atmos. Environ.* **1998,** *32*, 2453-2465.
32. Nemitz, E.; Hargreaves, K. J.; McDonald, A. G.; Dorsey, J. R.; Fowler, D., Meteorological measurements of the urban heat budget and CO_2 emissions on a city scale. *Environ. Sci. Technol.* **2002,** *36*, 3139-3146.
33. Soegaard, H.; Moller-Jensen, L., Towards a spatial CO_2 budget of a metropolitan region based on textural image classification and flux measurements. *Remote Sens. Environ.* **2003,** *87*, 283-294.
34. Jacob, D. J., *Introduction to Atmospheric Chemistry*. Princeton University Press: Princeton, NJ, 1999.
35. Dorsey, J. R.; Nemitz, E.; Gallagher, M. W.; Fowler, D.; Williams, P. I.; Bower, K. N.; Beswick, K. M., Direct measurements and parameterisation of aerosol flux, concentration and emission velocity above a city. *Atmos. Environ.* **2002,** *36*, 791-800.
36. Grimmond, C. S. B.; Salmond, J. A.; Oke, T. R.; Offerle, B.; Lemonsu, A., Flux and turbulence measurements at a densely built-up site in Marseille: Heat, mass (water and carbon dioxide), and momentum. *J. Geophys. Res.-Atmos.* **2004,** *109*, -.
37. Schmid, H. P., Experimental design for flux measurements: matching scales of observations and fluxes. *Agric. For. Meteorol.* **1997,** *87*, 179-200.

38. Bowling, D. R.; Turnipseed, A. A.; Delany, A. C.; Baldocchi, D. D.; Greenberg, J. P.; Monson, R. K., The use of relaxed eddy accumulation to measure biosphere-atmosphere exchange of isoprene and of her biological trace gases. *Oecologia* **1998,** *116*, 306-315.
39. Beverland, I. J.; Oneill, D. H.; Scott, S. L.; Moncrieff, J. B., Design, construction and operation of flux measurement systems using the conditional sampling technique. *Atmos. Environ.* **1996,** *30*, 3209-3220.
40. Ciccioli, P.; Brancaleoni, E.; Frattoni, M.; Marta, S.; Brachetti, A.; Vitullo, M.; Tirone, G.; Valentini, R., Relaxed eddy accumulation, a new technique for measuring emission and deposition fluxes of volatile organic compounds by capillary gas chromatography and mass spectrometry. *J. Chromatogr. A* **2003,** *985*, 283-296.
41. Graus, M.; Hansel, A.; Wisthaler, A.; Lindinger, C.; Forkel, R.; Hauff, K.; Klauer, M.; Pfichner, A.; Rappengluck, B.; Steigner, D.; Steinbrecher, R., A relaxed-eddy-accumulation method for the measurement of isoprenoid canopy-fluxes using an online gas-chromatographic technique and PTR-MS simultaneously. *Atmos. Environ.* **2006,** *40*, S43-S54.
42. Nie, D.; Kleindienst, T. E.; Arnts, R. R.; Sickles, J. E., The design and testing of a relaxed eddy accumulation system (vol 100, pg 11415, 1995). *J. Geophys. Res.-Atmos.* **1996,** *101*, 4315-4315.
43. Olofsson, M.; Ek-Olausson, B.; Ljungstrom, E.; Langer, S., Flux of organic compounds from grass measured by relaxed eddy accumulation technique. *J. Environ. Monitor.* **2003,** *5*, 963-970.
44. Buzcu-Guven, B.; Fraser, M. P., Comparison of VOC emissions inventory data with source apportionment results for Houston, TX. *Atmos. Environ.* **2008,** *42*, 5032-5043.
45. Cho, S.; Makar, P. A.; Lee, W. S.; Herage, T.; Liggio, J.; Li, S. M.; Wiens, B.; Graham, L., Evaluation of a unified regional air-quality modeling system (AURAMS) using PrAIRie2005 field study data: The effects of emissions data accuracy on particle sulphate predictions. *Atmos. Environ.* **2009,** *43*, 1864-1877.
46. Fu, J. S.; Streets, D. G.; Jang, C. J.; Hao, J. M.; He, K. B.; Wang, L. T.; Zhang, Q., Modeling Regional/Urban Ozone and Particulate Matter in Beijing, China. *J. Air Waste Manage.* **2009,** *59*, 37-44.
47. Ying, Q.; Lu, J.; Allen, P.; Livingstone, P.; Kaduwela, A.; Kleeman, M., Modeling air quality during the California Regional PM10/PM2.5 Air Quality Study (CRPAQS) using the UCD/CIT source-oriented air quality model - Part I. Base case model results. *Atmos. Environ.* **2008,** *42*, 8954-8966.
48. Ying, Q.; Lu, J.; Kaduwela, A.; Kleeman, M., Modeling air quality during the California Regional PM10/PM2.5 Air Quality Study (CPRAQS) using the UCD/CIT Source Oriented Air Quality Model - Part II. Regional source apportionment of primary airborne particulate matter. *Atmos. Environ.* **2008,** *42*, 8967-8978.
49. Xiao, Y. P.; Logan, J. A.; Jacob, D. J.; Hudman, R. C.; Yantosca, R.; Blake, D. R., Global budget of ethane and regional constraints on US sources. *J. Geophys. Res.-Atmos.* **2008,** *113*, D21306.
50. Boersma, K. F.; Jacob, D. J.; Bucsela, E. J.; Perring, A. E.; Dirksen, R.; van der A, R. J.; Yantosca, R. M.; Park, R. J.; Wenig, M. O.; Bertram, T. H.; Cohen, R. C., Validation of OMI tropospheric NO_2 observations during INTEX-B and application to constrain NO_x emissions over the eastern United States and Mexico. *Atmos. Environ.* **2008,** *42*, 4480-4497.
51. Han, K. M.; Song, C. H.; Ahn, H. J.; Park, R. S.; Woo, J. H.; Lee, C. K.; Richter, A.; Burrows, J. P.; Kim, J. Y.; Hong, J. H., Investigation of NO_x emissions and NO_x- related

chemistry in East Asia using CMAQ-predicted and GOME-derived NO_2 columns. *Atmos. Chem. Phys.* **2009,** *9*, 1017-1036.
52. Warneke, C.; McKeen, S. A.; de Gouw, J. A.; Goldan, P. D.; Kuster, W. C.; Holloway, J. S.; Williams, E. J.; Lerner, B. M.; Parrish, D. D.; Trainer, M.; Fehsenfeld, F. C.; Kato, S.; Atlas, E. L.; Baker, A.; Blake, D. R., Determination of urban volatile organic compound emission ratios and comparison with an emissions database. *J. Geophys. Res.-Atmos.* **2007,** *112*, D10S47
53. Ban-Weiss, G. A.; McLaughlin, J. P.; Harley, R. A.; Lunden, M. M.; Kirchstetter, T. W.; Kean, A. J.; Strawa, A. W.; Stevenson, E. D.; Kendall, G. R., Long-term changes in emissions of nitrogen oxides and particulate matter from on-road gasoline and diesel vehicles. *Atmos. Environ.* **2008,** *42*, 220-232.
54. Kopacz, M.; Jacob, D. J.; Henze, D. K.; Heald, C. L.; Streets, D. G.; Zhang, Q., Comparison of adjoint and analytical Bayesian inversion methods for constraining Asian sources of carbon monoxide using satellite (MOPITT) measurements of CO columns. *J. Geophys. Res.-Atmos.* **2009,** *114*, D04305.
55. Kurokawa, J.; Yumimoto, K.; Uno, I.; Ohara, T., Adjoint inverse modeling of NO_x emissions over eastern China using satellite observations of NO_2 vertical column densities. *Atmos. Environ.* **2009,** *43*, 1878-1887.
56. Vivanco, M. G.; Andrade, M. D., Validation of the emission inventory in the Sao Paulo Metropolitan Area of Brazil, based on ambient concentrations ratios of CO, NMOG and NO_x and on a photochemical model. *Atmos. Environ.* **2006,** *40*, 1189-1198.
57. Zhang, J.; Wang, T.; Chameides, W. L.; Cardelino, C.; Blake, D. R.; Streets, D. G., Source characteristics of volatile organic compounds during high ozone episodes in Hong Kong, Southern China. *Atmos. Chem. Phys.* **2008,** *8*, 4983-4996.
58. Song, J.; Vizuete, W.; Chang, S.; Allen, D.; Kimura, Y.; Kemball-Cook, S.; Yarwood, G.; Kiournourtzoglou, M. A.; Atlas, E.; Hansel, A.; Wisthaler, A.; McDonald-Buller, E., Comparisons of modeled and observed isoprene concentrations in southeast Texas. *Atmos. Environ.* **2008,** *42*, 1922-1940.
59. Tian, L. W.; Lucas, D.; Fischer, S. L.; Lee, S. C.; Hammond, S. K.; Koshland, C. P., Particle and gas emissions from a simulated coal-burning household fire pit. *Environ. Sci. Technol.* **2008,** *42*, 2503-2508.
60. Reidy, B.; Dammgen, U.; Dohler, H.; Eurich-Menden, B.; van Evert, F. K.; Hutchings, N. J.; Luesink, H. H.; Menzi, H.; Misselbrook, T. H.; Monteny, G. J.; Webb, J., Comparison of models used for national agricultural ammonia emission inventories in Europe: Liquid manure systems. *Atmos. Environ.* **2008,** *42*, 3452-3464.
61. Hylander, L. D.; Herbert, R. B., Global emission and production of mercury during the pyrometallurgical extraction of nonferrous sulfide ores. *Environ. Sci. Technol.* **2008,** *42*, 5971-5977.
62. Graham, L. A.; Rideout, G.; Rosenblatt, D.; Hendren, J., Greenhouse gas emissions from heavy-duty vehicles. *Atmos. Environ.* **2008,** *42*, 4665-4681.
63. Deutsch, F.; Mensink, C.; Vankerkom, J.; Janssen, L., Application and validation of a comprehensive model for PM_{10} and $PM_{2.5}$ concentrations in Belgium and Europe. *Appl. Math Model.* **2008,** *32*, 1501-1510.
64. Schrooten, L.; De Vlleger, I.; Panis, L. I.; Styns, K.; Torfs, R., Inventory and forecasting of maritime emissions in the Belgian sea territory, an activity-based emission model. *Atmos. Environ.* **2008,** *42*, 667-676.

65. Butler, T. M.; Lawrence, M. G.; Gurjar, B. R.; Van Aardenne, J.; Schultz, M.; Lelieveld, J., The representation of emissions from megacities in global emission inventories. *Atmos. Environ.* **2008,** *42*, 703-719.
66. Nol, L.; Verburg, P. H.; Heuvelink, G. B. M.; Molenaar, K., Effect of land cover data on nitrous oxide inventory in fen meadows. *J. Environ. Qual.* **2008,** *37*, 1209-1219.
67. Cai, H.; Xie, S. D., Estimation of vehicular emission inventories in China from 1980 to 2005. *Atmos. Environ.* **2007,** *41*, 8963-8979.
68. Dalvi, W.; Beig, G.; Patil, U.; Kaginalkar, A.; Sharma, C.; Mitra, A. P., A GIS based methodology for gridding of large-scale emission inventories: Application to carbon-monoxide emissions over Indian region. *Atmos. Environ.* **2006,** *40*, 2995-3007.
69. Symeonidis, P.; Poupkou, A.; Gkantou, A.; Melas, D.; Yay, O. D.; Pouspourika, E.; Balis, D., Development of a computational system for estimating biogenic NMVOCs emissions based on GIS technology. *Atmos. Environ.* **2008,** *42*, 1777-1789.
70. Wilson, S. J.; Steenhuisen, F.; Pacyna, J. M.; Pacyna, E. G., Mapping the spatial distribution of global anthropogenic mercury atmospheric emission inventories. *Atmos. Environ.* **2006,** *40*, 4621-4632.
71. Xu, S. P.; Jaffe, P. R.; Mauzerall, D. L., A process-based model for methane emission from flooded rice paddy systems. *Ecol. Model.* **2007,** *205*, 475-491.
72. Zhang, Q. Y.; Wei, Y. M.; Tian, W. L.; Yang, K. M., GIS-based emission inventories of urban scale: A case study of Hangzhou, China. *Atmos. Environ.* **2008,** *42*, 5150-5165.
73. Matejicek, L.; Engst, P.; Janour, Z., A GIS-based approach to spatio-temporal analysis of environmental pollution in urban areas: A case study of Prague's environment extended by LIDAR data. *Ecol. Model.* **2006,** *199*, 261-277.
74. Weng, Q. H.; Yang, S. H., Urban air pollution patterns, land use, and thermal landscape: An examination of the linkage using GIS. *Environ. Monit. Assess.* **2006,** *117*, 463-489.
75. Briggs, D., The role of GIS: Coping with space (and time) in air pollution exposure assessment. *J. Toxicol. Env. Heal. A* **2005,** *68*, 1243-1261.
76. Gulliver, J.; Briggs, D. J., Time-space modeling of journey-time exposure to traffic-related air pollution using GIS. *Environ. Res.* **2005,** *97*, 10-25.
77. Elbir, T., A GIS based decision support system for estimation, visualization and analysis of air pollution for large Turkish cities. *Atmos. Environ.* **2004,** *38*, 4509-4517.
78. Stuart, A. L.; Mudhasakul, S.; Sriwatanapongse, W., The social distribution of neighborhood-scale air pollution and monitoring protection. In University of South Florida: Tampa, FL, 2007; p 30.
79. Mirabelli, M. C.; Wing, S.; Marshall, S. W.; Wilcosky, T. C., Race, poverty, and potential exposure of middle-school students to air emissions from confined swine feeding operations. *Environ. Health Persp.* **2006,** *114*, 591-596.
80. Ponce, N. A.; Hoggatt, K. J.; Wilhelm, M.; Ritz, B., Preterm birth: The interaction of traffic-related air pollution with economic hardship in Los Angeles neighborhoods. *Am. J. Epidemiol.* **2005,** *162*, 140-148.
81. Salam, M. T.; Li, Y. F.; Langholz, B.; Gilliland, F. D., Early-life environmental risk factors for asthma: Findings from the children's health study. *Environ. Health Persp.* **2004,** *112*, 760-765.
82. Hosgood, H. D.; Berndt, S. I.; Lan, Q., GST genotypes and lung cancer susceptibility in Asian populations with indoor air pollution exposures: A meta-analysis. *Mutat. Res.-Rev. Mutat.* **2007,** *636*, 134-143.

83. Lewtas, J., Air pollution combustion emissions: Characterization of causative agents and mechanisms associated with cancer, reproductive, and cardiovascular effects. *Mutat. Res.-Rev. Mutat.* **2007,** *636*, 95-133.
84. Messerer, A.; Schmatloch, V.; Poschl, U.; Niessner, R., Combined particle emission reduction and heat recovery from combustion exhaust - A novel approach for small wood-fired appliances. *Biomass Bioenerg.* **2007,** *31*, 512-521.
85. Olsson, M.; Kjallstrand, J.; Petersson, G., Specific chimney emissions and biofuel characteristics of softwood pellets for residential heating in Sweden. *Biomass Bioenerg.* **2003,** *24*, 51-57.
86. Williams, I. D.; Bird, A., Public perceptions of air quality and quality of life in urban and suburban areas of London. *J. Environ. Monitor.* **2003,** *5*, 253-259.
87. Pegg, S., Mining and poverty reduction: Transforming rhetoric into reality. *J. Clean Prod.* **2006,** *14*, 376-387.
88. Yen, I. H.; Yelin, E. H.; Katz, P.; Eisner, M. D.; Blanc, P. D., Perceived neighborhood problems and quality of life, physical functioning, and depressive symptoms among adults with asthma. *Am. J. Public Health* **2006,** *96*, 873-879.
89. Schulz, A. J.; Kannan, S.; Dvonch, J. T.; Israel, B. A.; Allen, A.; James, S. A.; House, J. S.; Lepkowski, J., Social and physical environments and disparities in risk for cardiovascular disease: The Healthy Environments Partnership conceptual model. *Environ. Health Persp.* **2005,** *113*, 1817-1825.
90. Schade, G. W.; Goldstein, A. H., Increase of monoterpene emissions from a pine plantation as a result of mechanical disturbances. *Geophys. Res. Lett.* **2003,** *30*.
91. Aubinet, M.; Grelle, A.; Ibrom, A.; Rannik, U.; Moncrieff, J.; Foken, T.; Kowalski, A. S.; Martin, P. H.; Berbigier, P.; Bernhofer, C.; Clement, R.; Elbers, J.; Granier, A.; Grunwald, T.; Morgenstern, K.; Pilegaard, K.; Rebmann, C.; Snijders, W.; Valentini, R.; Vesala, T., Estimates of the annual net carbon and water exchange of forests: The EUROFLUX methodology. In *Advances in Ecological Research, Vol 30*, 2000; Vol. 30, pp 113-175.
92. Hojstrup, J., A statistical-data screening-procedure. *Meas. Sci. Technol.* **1993,** *4*, 153-157.
93. Vickers, D.; Mahrt, L., Quality control and flux sampling problems for tower and aircraft data. *J. Atmos. Ocean Tech.* **1997,** *14*, 512-526.
94. Schmid, H. P.; Grimmond, C. S. B.; Cropley, F.; Offerle, B.; Su, H. B., Measurements of CO_2 and energy fluxes over a mixed hardwood forest in the mid-western United States. *Agric. For. Meteorol.* **2000,** *103*, 357-374.
95. Wilczak, J. M.; Oncley, S. P.; Stage, S. A., Sonic anemometer tilt correction algorithms. *Bound.-Layer Meteor.* **2001,** *99*, 127-150.
96. Massman, W. J.; Lee, X., Eddy covariance flux corrections and uncertainties in long-term studies of carbon and energy exchanges. *Agric. For. Meteorol.* **2002,** *113*, 121-144.
97. Cullen, N. J.; Steffen, K.; Blanken, P. D., Nonstationarity of turbulent heat fluxes at Summit, Greenland. *Bound.-Layer Meteor.* **2007,** *122*, 439-455.
98. Lyons, T. J.; Halldin, S., Surface heterogeneity and the spatial variation of fluxes. *Agric. For. Meteorol.* **2004,** *121*, 153-165.
99. Kljun, N.; Rotach, M. W.; Schmid, H. P., A three-dimensional backward lagrangian footprint model for a wide range of boundary-layer stratifications. *Bound.-Layer Meteor.* **2002,** *103*, 205-226.
100. Raber, L. R., Clean air: Dollars versus lives. *Chem. Eng. News* **1997,** *75*, 28-30.

Chapter 2: Demonstration of a Mobile Flux Laboratory for the Atmospheric Measurement of Emissions (FLAME) to Assess Emissions Inventories

Abstract

The advancement of air quality science and the development of effective air quality management plans require accurate estimates of emissions. In response to the need for new approaches to quantifying emissions, we have designed a mobile Flux Lab for the Atmospheric Measurement of Emissions (FLAME) that uses eddy covariance for the direct measurement of anthropogenic emissions at the neighborhood scale. To demonstrate the FLAME's capabilities, we have deployed it in the Huntington-Ashland region at the borders of Ohio, Kentucky and West Virginia. This area routinely experiences high ozone and fine particulate matter ($PM_{2.5}$) concentrations and is home to a significant amount of industrial activity, including coal storage and transport. Experiments focused on carbon dioxide (CO_2), nitrogen oxides (NO_x) and fine particulate matter ($PM_{2.5}$). Spikes in CO_2 and NO_x concentrations were correlated with the passage of trains and barges through the FLAME's footprint. Calculated barge emission factors ranged from 49 to 76 kg NO_x tonne fuel^{-1} and agreed well with previously published values. Fluxes measured at three sites in the town of Worthington were mainly positive. They ranged between -6.5 to 29 mg m^{-2} s^{-1} for CO_2 and -9.7×10^{-5} to 9.1×10^{-5} mg m^{-2} s^{-1} for $PM_{2.5}$. We illustrate how the measurements can be compared to emissions inventories on a per capita basis for greenhouse gases and countywide for other pollutants. The results show that a mobile eddy covariance system can be used successfully to measure fluxes of multiple pollutants in a variety of settings. This alternative method for estimating emissions can be a useful tool for assessing uncertainties in emissions inventories and for improving their accuracy.

1.0 Introduction

Emissions inventories are considered the foundation of air quality management. However, they may be inaccurate or incomplete due to limitations in the current emissions estimation process. Emissions inventories contain point, nonpoint (area), mobile and biogenic sources.

While air pollutant emissions from point sources such as power plants, chemical plants and oil refineries are continuously measured by the facilities and reported to state environmental agencies, emissions from smaller dispersed sources such as gasoline stations, refuse fires, painting, and yard tools are only estimated. Emissions from such "area" sources are typically calculated by multiplying an emission factor, or the mass of emissions per unit of activity, by the amount of activity conducted.

Considerable uncertainty exists in both emission factors and activity rates. The National Research Council (NRC) has repeatedly called for better quantification of emissions and has stated that the lack of proven methods to test the accuracy and precision of emissions inventories contributes significantly to their uncertainty *(1-3)*. Independent estimates suggest that the government's official emissions inventories may be under or overestimated by a factor of five or more *(4-12)*.

Thanks to the advancement of eddy covariance techniques, the ability to measure surface-atmosphere fluxes has improved over the last two decades *(13-15)*. The majority of eddy covariance applications have taken place over forest, grassland or agricultural canopies in an effort to quantify fluxes of carbon dioxide (CO_2), nitrogenous compounds, ozone and organic compounds *(16-24)*. To a lesser extent, eddy covariance has also been used in urban areas to explore anthropogenic pollutant fluxes *(25-28)*.

Most of the eddy covariance systems currently used for flux measurements are stationary and therefore provide information for an area limited to the tower's footprint, i.e. the area around the measurement site that contributes to the observed fluxes. Also, many of the urban eddy covariance systems measure only one or two pollutants such as CO_2 or particles. To address these limitations, we have developed a mobile eddy covariance system that is capable of measuring the major pollutants that contribute to air pollution: CO_2, fine particulate matter ($PM_{2.5}$), nitrogen oxides (NO_x) and carbon monoxide (CO), with selected volatile organic compounds to be added in the near future. Our Flux Laboratory for the Atmospheric Measurement of Emissions (FLAME) allows for the real-time neighborhood-scale determination of pollutant fluxes and has the abilities to conduct measurements in many different areas and to focus on specific sources by parking downwind of them.

The objective of this research is to demonstrate and validate the use of a mobile eddy covariance system as a tool for the direct measurement of anthropogenic emissions and evaluation of emissions inventories. We conducted a three-day field campaign with the FLAME in the Huntington-Ashland $PM_{2.5}$ non-attainment area at the borders of Kentucky, Ohio and West Virginia, where coal transport is the major industrial activity.

Often overlooked in the national discussion of air quality, such areas of Appalachia deserve greater attention because of sources that may differ from those found in coastal metropolitan areas and socioeconomic factors that raise questions about environmental justice. This initial study focused on rail and barge traffic because compared to motor vehicles, much less research on such sources exists, yet as the on-road fleet becomes cleaner, the contribution of non-road mobile sources to emissions inventories is growing. Additionally, we compared measured fluxes to official inventories to gain insight into their uncertainties. Future work will employ the FLAME in much more extensive field campaigns in order to obtain longer time series and greater statistical power. Here, the intent is to test and validate the system and to demonstrate its capabilities.

2.0 Methods

2.1 Site

In 2006 the Kentucky Division for Air Quality (KDAQ) reported that concentrations of the criteria pollutants ozone (O_3) and $PM_{2.5}$ within Huntington-Ashland were 0.076 ppm (8-hr average) and 14.4 $\mu g\ m^{-3}$ (24-hr average), respectively *(29)*. The value reported for O_3 represents the arithmetic average of the fourth highest values in 2004, 2005 and 2006; however, in 2006, the three highest concentrations in the Huntington-Ashland region were 0.087, 0.083 and 0.081 ppm (245 days measured), which all exceed the new National Ambient Air Quality Standard (NAAQS) of 0.075 ppm. As for $PM_{2.5}$, the region's three-year annual arithmetic mean of 14.4 $\mu g\ m^{-3}$ is lower than the NAAQS of 15 $\mu g\ m^{-3}$; however, in 2005, the reported $PM_{2.5}$ annual arithmetic mean was 16 $\mu g\ m^{-3}$, and in 2006, the reported 98^{th} percentile value was 48.6 $\mu g\ m^{-3}$. The single air quality monitoring station in the small town of Worthington, where we conducted experiments, measures O_3 and SO_2 and is the

third worst in the state for O_3 and the worst for SO_2. With respect to emissions, Worthington houses a railroad and coal hauling facility (CSX Transportation Inc.) which is ranked among the worst 40% emitters of $PM_{2.5}$ in the country *(30)*.

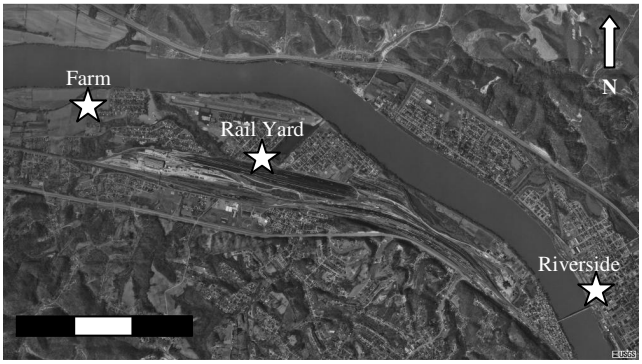

Figure 7. Aerial view of Worthington, KY located along the Ohio River showing three measurement sites.

Figure 7 shows the three sites where we spent one day each conducting measurements on 25-27 July 2007. The sites were selected on the basis of predominant wind direction and expected footprint size to focus on specific types of sources: coal-carrying barges and trains, coal/rail yards and residential activities. The first site (Riverside) was located along the east bank of the Ohio River, 1.6 km east of Worthington in Ironton, Ohio. Here, the predominant wind direction during our experiments was south-southwesterly. Possible emissions sources located within the Riverside footprint were barges along the river, rail traffic approximately 30 m to the east of the measurement site and vehicle traffic. Also, a steel fabrication plant was located approximately 2 km downwind of the measurement site but, based on the footprint size, should not have contributed to the observed fluxes. The second site (Rail Yard) was located near a rail yard in Worthington and experienced east-southeasterly winds. Potential sources within the footprint of this sampling location were a rail yard fabrication plant approximately 200 m to the east, a coal/rail yard adjacent to the site and residential traffic. The third site (Farm) was located along the south bank of the Ohio River and on the north side of a farm, and the predominant wind direction was west-northwesterly. The major anthropogenic source in this site's footprint was an industrial abrasives manufacturing plant approximately 200 m to the southwest.

Footprints for all sites were calculated using the Flux Source Area model (FSAM) *(31, 32)* and meteorological parameters measured on each day. The average footprint sizes

encompassing 90% of the sources for the Riverside, Rail Yard and Farm sites were approximately 700 m × 300 m (length × width), 500 m × 300 m and 400 m × 300 m, respectively. Anthropogenic and natural features within the footprints were no taller than 3 meters.

2.2 Flux measurements and analysis

The FLAME is a customized television news van with an extendable mast that rises to 15.5 m. A sonic anemometer (Applied Technologies SATI-3K) and sample tubing are mounted on a rotating platform on top of the mast. A pump draws air at 20 L min^{-1} through 0.5-inch PTFE conductive tubing (TELEFLEX T1618-08) down to ground level, and gas and particle analyzers subsample the air through a custom designed Teflon manifold. Analyzers inside the van measure CO_2 and water vapor (Li-Cor LI-7000, 0.0017-s response time), NO_x (Eco Physics CLD 88Y, 1-s response time) and $PM_{2.5}$ (DustTrak 8520, 1-s response time). Although the DustTrak is a relatively simplistic method for measuring $PM_{2.5}$, it is the only commercially avaiable instrument with the time response required by eddy covariance, and our previous experience with it has shown its measurements to correlate well with those from more sophisticated particle analyzers, such as an aerosol mass spectrometer and a tapered element oscillation microbalance. A criteria pollutant, $PM_{2.5}$ is important to measure from the standpoint of air quality management because it is the basis of particulate emissions in inventories. Collaborative field campaigns in the future could include other fast-response analyzers such as a condensation particle counter, aerosol mass spectrometer, proton transfer reaction mass spectrometer, and quantum cascade laser to measure a broader suite of particles and gases.

A data logger (National Instruments Compact FieldPoint 2110) records the measurements at 10 Hz. The equipment is powered using a 4500 W gasoline generator (Onan GENSET 4500 Series), whose emissions were determined in a control experiment and subtracted from the fluxes presented here. Because of the high ambient temperatures during the field campaign, the NO_x analyzer functioned only for ~4 h on the first day, after which it overheated.

Quality assurance and control measures included calibration of the analyzers before and

during the field campaign and testing for sampling line losses. Losses of CO_2, NO_x and $PM_{2.5}$ were not significantly different from zero (0.7 ± 0.4%, 0.5 ± 0.8% and 8% ± 5%, respectively), and water vapor losses were eclipsed by humidity variations in the atmosphere during the test periods. Also, gravimetric filter samples of $PM_{2.5}$ were collected during the field campaign for calibration of the DustTrak, an aerosol photometer whose response is dependent on particles' size distribution and optical properties. The factory calibration uses Arizona test dust, which is intended to be representative of a variety of ambient atmospheric aerosols. Previous comparisons of factory-calibrated DustTrak values against gravimetric measurements found no significant difference in the case of a welding school and power plant work site but a factor of 2-3 difference, with the DustTrak higher, in other indoor and outdoor settings *(33-37)*. In the present study, the DustTrak's average concentrations were 12 ± 0.7% higher than the filter-based ones, and because filters may also be subject to sampling artifacts, we have elected to report the factory-calibrated DustTrak $PM_{2.5}$ values rather than correct them to match the filters. It is possible that secondary aerosol could bias the interpretation of $PM_{2.5}$ measurements if there is a vertical gradient in its concentration over the length scales contributing to vertical fluxes; the magnitude of such an effect is unknown.

2.3 Flux Calculation

Standard post-processing of the measurements included hard spike removal, soft spike removal, lag correction, coordinate rotation by the planar fit method, linear detrending, calculation of fluxes and quality assurance of the calculated fluxes through spectral and co-spectral analyses and stationarity testing *(25, 28, 38)*.

Fluxes were calculated over 30-min averaging periods as follows:

$$F_x = \overline{w' C_x'} \qquad \text{(Eq. 1)}$$

The flux F_x (mg m^{-2} s^{-1}) of species x is the time-averaged covariance between the instantaneous deviations of the vertical wind velocity w' (m s^{-1}) and the concentration C_x' (mg m^{-3}), from their linear trends over the averaging period *(13, 28)*. A positive flux represents net transfer upward into the atmosphere from the surface, whereas a negative flux

represents net transfer downward from the atmosphere to the land surface.

The measured flux is a net value, so it represents a combination of emissions to the atmosphere and uptake by surface features. With gases, deposition will usually be small relative to emissions. Of the gases we are considering, NO_2 has the highest dry deposition velocity, 0.1 cm s^{-1} *(39)*. Given a typical urban NO_x concentration of 50 ppb (~100 μg m^{-3} as NO_2) and assuming under worst-case conditions all of it is NO_2, the deposition flux would be ~1 × 10^{-4} mg m^{-2} s^{-1}. During the field campaign, we measured an average NO_x flux of greater than 0.09 mg m^{-2} s^{-1}, which is 900 times larger than the deposition flux. Therefore, it is reasonable to assume that the measured fluxes represent emissions only. On the other hand, deposition may be important for $PM_{2.5}$. Assuming a gravitational settling velocity of 2 × 10^{-4} m s^{-1} for 2.5 μm particles of unit density and a typical $PM_{2.5}$ concentration of 10 μg m^{-3}, we obtain a deposition flux of 2 × 10^{-6} mg m^{-2} s^{-1}. Aside from an outlier during rain, the absolute value of $PM_{2.5}$ fluxes measured during the field campaign ranged between -9.7 × 10^{-5} to 9.1 × 10^{-5} mg m^{-2} s^{-1}, so dry deposition could influence the measurements. The $PM_{2.5}$ fluxes therefore represent a lower limit on emissions.

2.4 Emission Factors

If measured pollutant concentrations are dominated by a single source, they can be used to calculate fuel-based emission factors, the mass of pollutant emitted per mass of fuel consumed. In a study of emissions from barges, Corbett et al. (2001) calculated NO_x emission factors (*EF*) as:

$$EF = \frac{\chi_{NO_x}}{\chi_{CO_2}}\left(\frac{46}{12}\right)(0.87) \qquad \text{(Eq. 2)}$$

where χ_{NO_x} and χ_{CO_2} are the mole fractions of NO_x and CO_2 measured in the undiluted exhaust, $(46/12)$ converts moles to mass with NO_x reported as NO_2, and 0.87 is the mass fraction of carbon in diesel fuel. This equation assumes that all carbon in the fuel is emitted as CO_2. This same equation can also be applied to diluted exhaust plumes, where mole fractions are the above-background values and the two gases are assumed to disperse

similarly in the plume. Applying this equation to the NO_x and CO_2 concentrations obtained at the Riverside site, we can calculate emission factors in units of kilograms of NO_x per metric tonne of fuel (kg NO_x tonne fuel^{-1}) for barges operating under real-world conditions along inland waterways.

2.5 Uncertainties

While it is impossible to quantify uncertainties from eddy covariance data alone, we have followed an empirical approach to ensure the plausibility of the results. This approach to validating flux measurements has provided many investigators with defensible estimates of eddy covariance fluxes *(13, 28, 38)*. Both systematic and random errors may influence measurements and calculations using long data records. Errors may stem from improper equipment setup, inadequate sample amounts and record lengths and inhomogeneity (non-stationarity) *(38, 40)*. Also important to obtaining valid flux measurements are site selection and favorable meteorological conditions. Of course, we have taken every measure possible to minimize such errors.

Spectral and co-spectral analyses were conducted on the raw temperature, CO_2 concentration and vertical wind velocity data. These analyses help to identify weakened raw data samples caused by limited analyzer response times, instrument and inlet separation distances and detrending or mean removal as part of general signal processing *(26, 28, 41)*.

Figure 8 shows spectra of temperature and CO_2 from an arbitrarily chosen 30-min data set sampled between 9:13-9:43 on the second day of the field campaign. The atmosphere was unstable with a Monin-Obukhov length of -21 m. Spectra and co-spectra are plotted versus the normalized frequency, $f \times (z_m/\bar{u})$, where z_m is equal to the measurement height z minus the displacement height z_d and $\bar{u}$ is the average horizontal wind speed. The spectra clearly obey the -2/3 power decay law that is expected during unstable atmospheric conditions *(26)*. Figure 8 also shows the co-spectra of temperature and CO_2 with vertical wind velocity. The data shown were also sampled on the second day of the field campaign between 9:13-9:43. The co-spectra generally obey the -4/3 power decay law *(26)*. Ideally, two separate variables being measured independently of one another should have no systematic phase shift and no

co-spectral distortion *(28)*. That two independently measured values exhibit similar power decay characteristics is an excellent indication that the system is capable of accurately measuring turbulent fluxes via the eddy covariance method, provided the 30-min data set also passes stationarity testing.

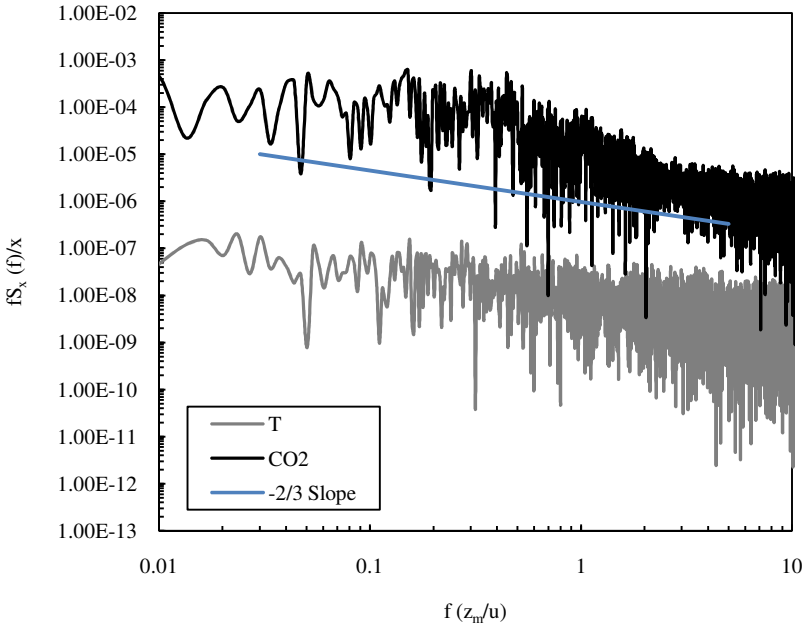

(a)

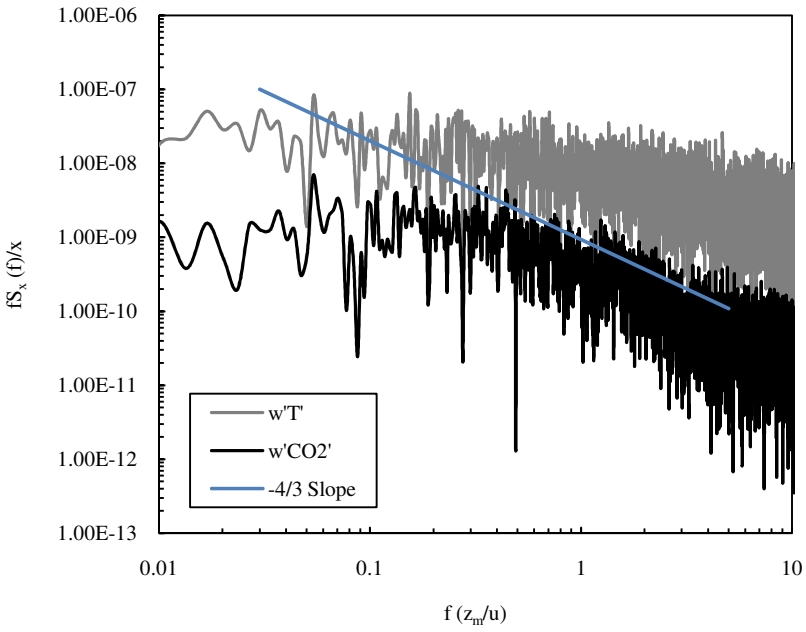

(b)

Figure 8. Power density spectra of temperature (°C) and CO_2 (ppm) (a) and co-spectra of vertical wind velocity (m s^{-1}) (w') with temperature and CO_2 (b). The theoretical -2/3 and -4/3 slopes follow typical data decay rates for turbulent signals and are also shown.

Stationarity has been used extensively in eddy covariance studies in urban settings to validate the homogeneity of measured emissions area surfaces *(13, 14, 25-28, 41-45)*. Based on Monin-Obukhov similarity theory, stationarity of key atmospheric variables is required to ensure that eddy covariance results are valid *(42)*. Stationarity implies that the measurement height exceeds the blending height, the height at which convectively driven turbulence dominates over mechanically driven turbulence.This means that the point of measurement is sufficiently high enough above the surface for its features to appear homogeneous, significantly reducing errors associated with the heterogeneity of the surface *(28, 46)*. One accepted method for determining stationarity is to calculate the difference between the 30-min average flux from a data set and the average of six consecutive 5-min sub-periods of the same 30-min data set. If the difference between the two average values is greater than 60% then the data set is considered non-stationary and is excluded from further analysis *(25, 26, 28, 38)*.

Figure 9 shows the CO_2 and $PM_{2.5}$ flux differences that were calculated using the method described above versus the stability index, $\xi = z_m / L$, where L is the Monin-Obukhov length.

The Monin-Obukhov length is the height at which the production of turbulence by both mechanical and buoyancy forces is equal and is used to provide a measure of the stability of the surface layer. The horizontal axis represents a measure of the average atmospheric stability during the time of measurement. A stability index of less than zero ($\xi < 0$) signifies unstable atmospheric conditions, while a stability index of greater than or equal to zero ($\xi \geq 0$) signifies stable conditions. The figure shows that all 44 CO_2 measurement periods (30 min each) satisfy the conditions of stationarity, with no period having a difference greater than 1.6% from the 5-min averages. The $PM_{2.5}$ differences are less than 12%. The good results are due in part to the fact that we conducted measurements during the daytime hours only and not in the evening, when stationarity conditions are harder to meet.

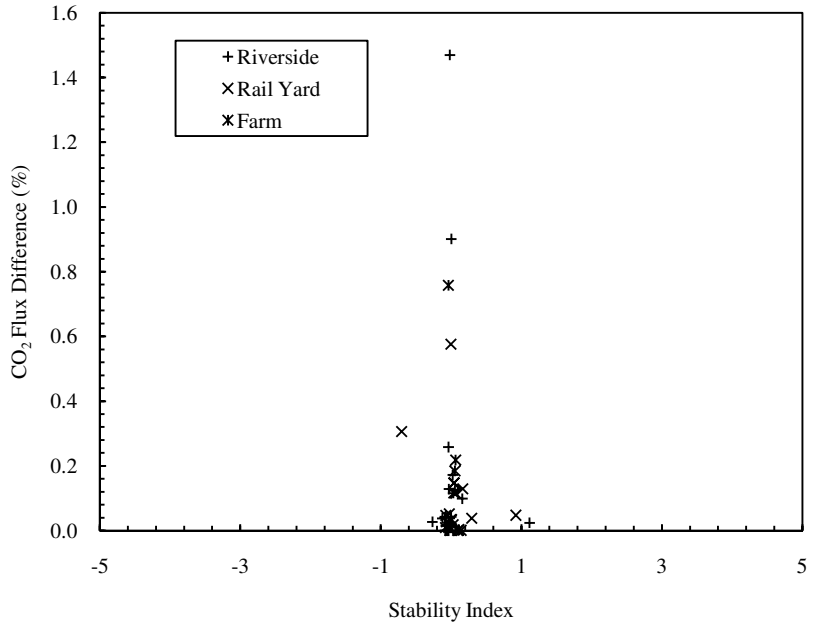

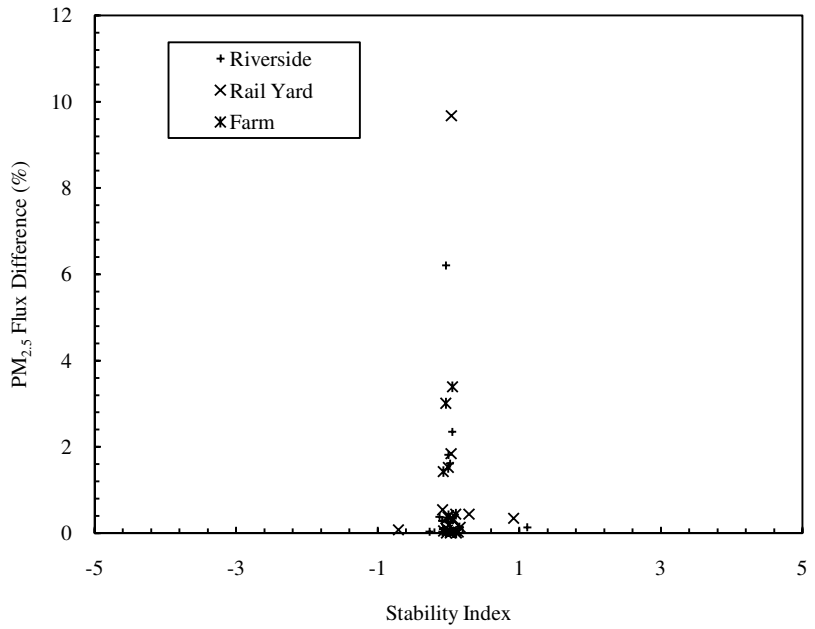

Figure 9. CO_2 and $PM_{2.5}$ flux stationarity test. All flux differences are less than 60%, indicating that all periods can be considered stationary and qualify for further analysis. The stability index is the ratio of the measurement height to the Monin-Obukhov length; a value less than zero signifies unstable conditions, while a value greater than zero signifies stable conditions.

Entire papers have been dedicated to the estimation of uncertainty associated with eddy covariance measurements *(40, 41, 47-51)*. Both systematic and random errors contribute to the total uncertainty. In most cases, such errors are unavoidable, and improving one aspect of the measurement system may negatively affect another. Based on possible sources of error such as instrument noise, calibration, frequency loss and gap filling as described within published research, it is likely that the sytematic error associated with the FLAME's flux measurements is ≤25% and random error is ≤20%.

3.0 Results

3.1 Concentrations

Figures 10 and 11 show 5-min averages of CO_2 and $PM_{2.5}$ concentrations during the entire field campaign. Increases in CO_2 at Riverside appeared to be related to coal-transporting barge or train traffic. For example, the spikes occurring between 11:30-15:00 corresponded well with coal transport traffic, with 12 barges and six trains passing through the footprint between these times. Also, the increase in CO_2 up to nearly 600 ppm, the highest

concentration observed during the field campaign, at 15:00 corresponded to the passage of three barges and a train.

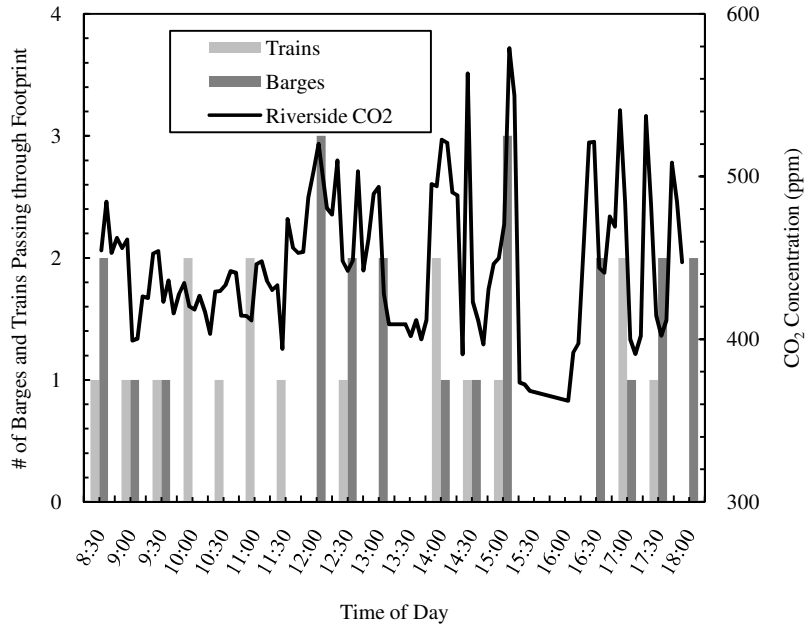

(a)

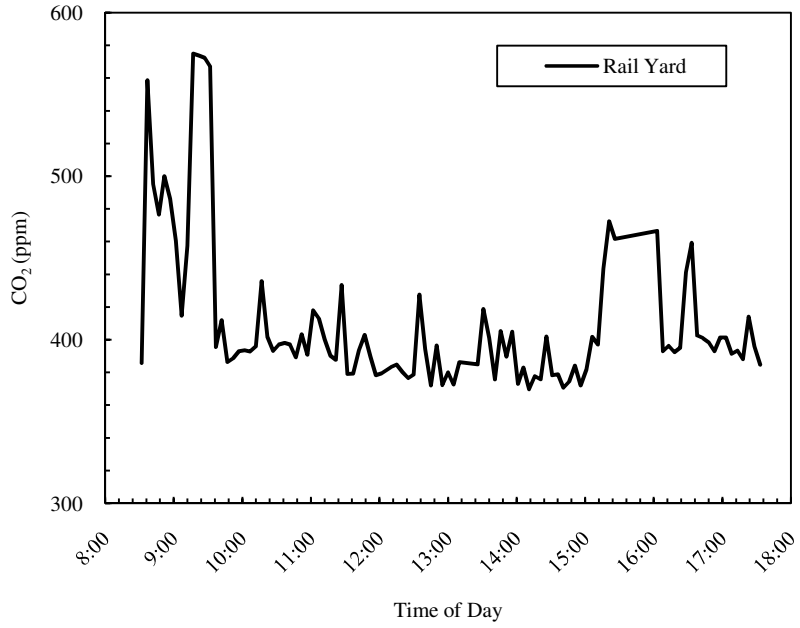

(b)

Figure 10. CO_2 concentrations at Riverside (a) and Rail Yard (b). Barge and train counts are included with the Riverside data.

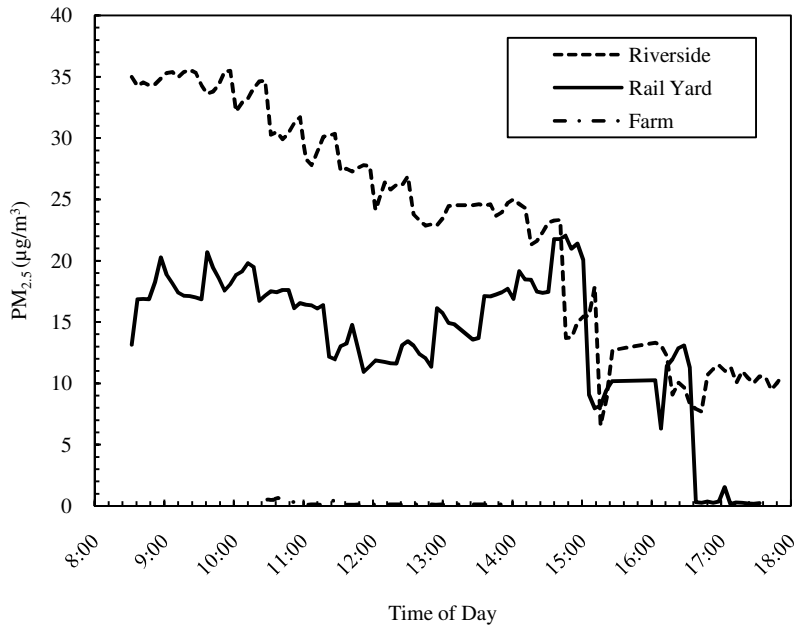

Figure 11. $PM_{2.5}$ concentrations at three locations, each from a different day. The sharp drops in $PM_{2.5}$ concentrations during the afternoon at Riverside and Rail Yard correspond to rain events.

CO_2 concentrations at the Rail Yard site showed a clear diurnal pattern, with higher concentrations between 8:00-9:30 and 15:00-17:00 due to the presence of morning and late afternoon coal transport, construction and commuter traffic passing through the footprint. During these hours, the traffic count along Worthington's main thoroughfare was ~180 vehicles per hour, compared to ~60 per hour during non-rush-hour periods. The Farm CO_2 concentrations (not shown), which were available only between 10:30-14:00, were similar in magnitude and variability to measurements at the Rail Yard site during the same time period. Outside of the rush hour between 10:00-14:00, CO_2 concentrations at the Farm and Rail Yard sites were approximately 58 and 54 ppm lower, respectively, than found at Ironton Riverside, and spikes that rose above the baseline at the Farm site could be directly attributed to slight shifts in wind together with barges passing through the Farm footprint.

Figure 11 shows $PM_{2.5}$ concentrations at the three sites. The Riverside $PM_{2.5}$ concentrations seemed to be correlated with train passage. For instance, between 9:30-13:00, small spikes in $PM_{2.5}$ coincided with eight trains passing by during this period. The overall decrease in $PM_{2.5}$ during the morning was probably due to dilution of the boundary layer as the mixing height rose.

Also, rain began falling at 14:45 and likely caused the ~10 μg m^{-3} drop in $PM_{2.5}$ at this time. At the Rail Yard site, $PM_{2.5}$ concentrations were higher during the morning hours between 8:30-11:00 and after 13:00. A rain event between ~15:00-15:15 on this day resulted in a ~12 μg m^{-3} drop in $PM_{2.5}$. Afterwards, $PM_{2.5}$ recovered but not to its value before the rain began. At 16:30, a significant rain event occurred, and $PM_{2.5}$ concentrations dropped to near zero. Small spikes in $PM_{2.5}$ likely corresponded to traffic as well as production activities at the rail yard fabrication facility. At the Farm, $PM_{2.5}$ remained at or below 1 μg m^{-3}, possibly due to a clean front passing through the region on the third day of the campaign, when measurements at the Farm took place. This $PM_{2.5}$ concentration was later compared with $PM_{2.5}$ ambient concentration data from a control experiment conducted in a location with few to no emission sources. Values obtained during the control experiment also remained at or below 1 μg m^{-3}. Concentrations increased slightly between 10:30-11:00, probably due to stronger wind from the direction of the abrasives manufacturing plant, which fell within the footprint at that time.

3.2 Fluxes

As shown in Figure 12, CO_2 fluxes ranged from -6.5 to 29 mg m^{-2} s^{-1}. Fluxes at Riverside and Rail Yard were predominantly positive, meaning that these areas were net sources of CO_2 to the atmosphere. The large spike in flux between 14:00-15:00 at Riverside probably reflects the heavy train and barge traffic within the footprint (Figure 12). During this period, three barges passed by in less than 30 min. Each took approximately 8-15 min to pass through the footprint and therefore could contribute significantly to the 30-min average fluxes. Six trains passed by between 16:30-18:00, but because they spent only 0.5-2 min in the footprint, their emissions had a lesser impact on the 30-min average flux. Other increases in the Riverside fluxes also corresponded well with the barge and train traffic. The negative fluxes recorded at 16:00 and 18:30 may have been due to the observed rain events.

Fluxes at the Rail Yard site were steadier throughout the day. The string of positive fluxes between the hours of 14:00 and 18:00 was likely a result of the afternoon increase in commuter traffic (250 vehicles per hour). The negative fluxes at the Farm were probably due to uptake of CO_2 by vegetation in the surrounding farmland, along with the absence of CO_2

emissions sources.

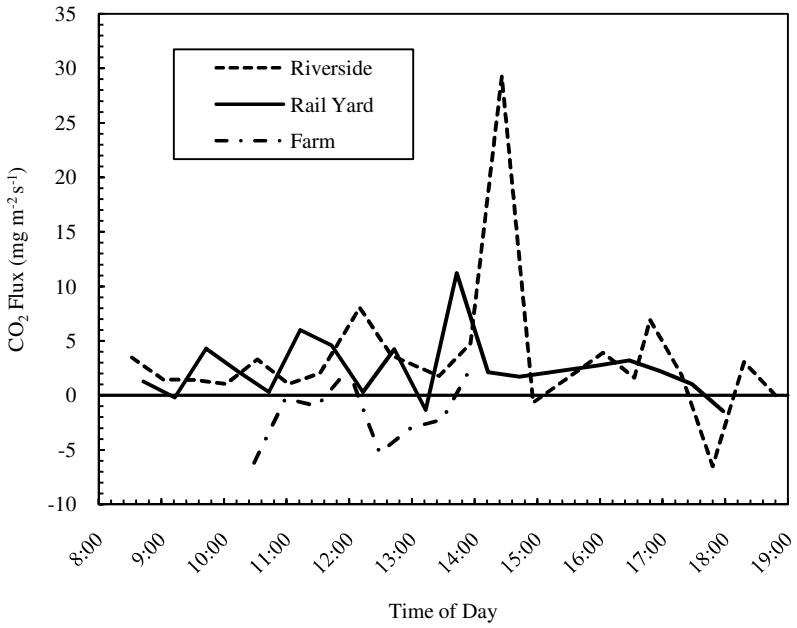

Figure 12. CO_2 fluxes at three locations, each from a different day.

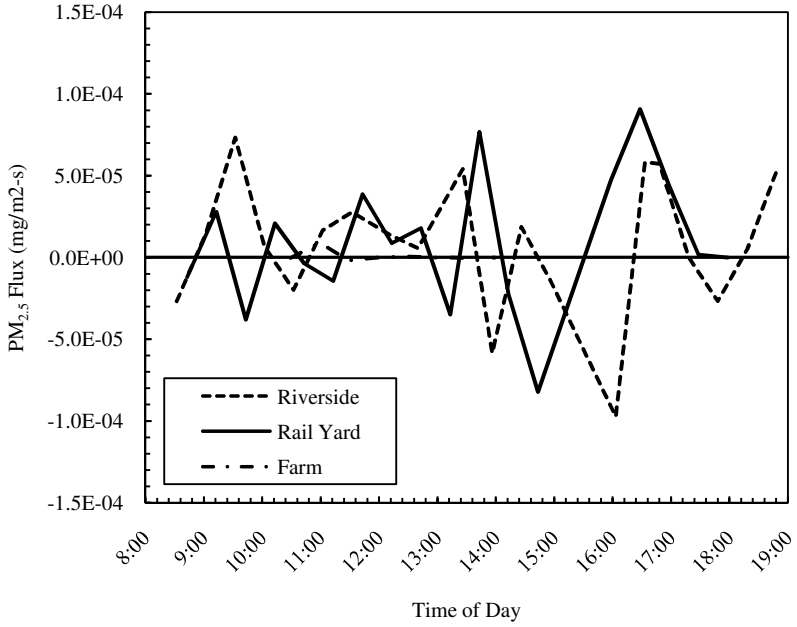

Figure 13. $PM_{2.5}$ fluxes at three locations, each from a different day.

$PM_{2.5}$ fluxes shown in Figure 13 ranged from -2.2×10^{-4} to 1.2×10^{-4} mg m^{-2} s^{-1}. The fluxes at the Riverside site fluctuated around zero and were highest in the afternoon. The positive

fluxes coincided with barge and train traffic. For example, between 9:00-10:30, four trains and two barges passed through the footprint, and the fluxes were 1.1×10^{-5} to 6.0×10^{-5} mg m^{-2} s^{-1}. At approximately 15:00, fluxes dropped below zero due to rain and recovered when the rain ended at ~16:30. Afterwards, fluxes rose to their highest value of the day (8.8×10^{-5} mg m^{-2} s^{-1}) between 17:00-18:00, when three trains and five barges passed through the footprint.

The Rail Yard $PM_{2.5}$ fluxes also fluctuated around zero and were similar in magnitude to those at Riverside. Alternating positive and negative fluxes between 9:30-10:30 may have been associated with significant movement and production of equipment at the rail fabrication plant on hourly intervals with short breaks in between. Lower fluxes between 11:00-14:00 may have resulted from a reduction in production during the typical lunch hours. After 14:00, production increased until the 15:00 rain event, at which point $PM_{2.5}$ fluxes were negative. Following the rain event, Rail Yard operations immediately resumed, subsequently causing a significant increase in positive flux until approximately 16:30 when a more significant rain event brought production to an end for the day.

$PM_{2.5}$ fluxes at the Farm, measured between only 10:00-14:00 because of technical problems, did not exceed 10^{-6} mg m^{-2} s^{-1}. Between 10:00-11:30, the wind speed from the west-southwesterly direction increased, subsequently increasing the footprint to include the industrial abrasives manufacturing plant approximately 200 m to the southwest. It is likely that the positive flux occurring between those hours was a result of emissions from the abrasives plant.

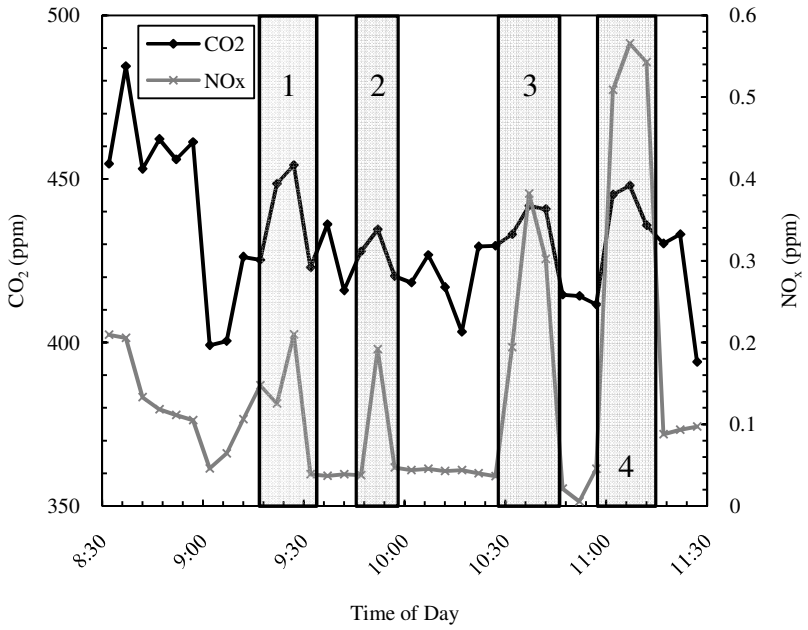

Figure 14. NO_x and CO_2 concentrations at the Riverside site. The four shaded boxes highlight times when barges were passing through the footprint.

4.0 Discussion

4.1 Comparison to Other Urban Studies

That fluxes were mainly positive at the two urbanized sites agrees with results from other cities. In suburban Chicago, Grimmond et al. (2002) reported CO_2 concentrations between 370 and 410 ppm with predominantly positive fluxes ranging up to 1.70 mg m^{-2} s^{-1}; negative fluxes reached -1 mg m^{-2} s^{-1}. The researchers attributed the positive fluxes to motor vehicle emissions and residential use of natural gas and oil and negative fluxes to uptake by vegetation. Of particular interest is that the Chicago study recorded higher fluxes during early morning and late afternoon indicating a possible dependence on commuter traffic; however, in the results from the Railyard site, the fluxes are mostly positive and relatively constant over the course of the day. In Worthington, the flow of traffic, movement of trains and railyard activities in this area were probably more constant in time and less tied to the morning and evening rush hour. Similarly, Velasco et al. (2005) also recorded mostly positive fluxes with CO_2 concentrations ranging from 370 to 430 ppm and fluxes above 1 mg m^{-2} s^{-1} in a mixed-use residential and commercial area of Mexico City. They also reported higher fluxes during the morning and late afternoon rush hours. Both groups noted that the

complexity of urban landscapes as well as the inconsistencies associated with anthropogenic emissions complicated the typical diurnal pattern that is seen in forested emissions measurements.

The CO_2 concentrations in excess of 500 ppm and fluxes in excess of 10 mg m^{-2} s^{-1} measured in Worthington were much larger than those found in the eddy covariance studies in Chicago and Mexico City. The difference is most likely due to the smaller footprint size stemming from differences in tower heights. With heights of 27 and 37 m, the Chicago and Mexico City towers saw anthropogenic contributions from distances greater than 1000 m away. Our study's 15-m tower had a much smaller footprint and therefore was more sensitive to the large sources within it, i.e. a strong source's contribution was not "diluted" by a lack of sources in other areas of the footprint.

Similar to results from Stockholm and Edinburgh where $PM_{2.5}$ concentrations and fluxes were found to correlate well with motor vehicle traffic, $PM_{2.5}$ fluxes observed in this research were found to correlate well with coal transport at Riverside and rail production activities at the Rail Yard. In Stockholm, particle number concentrations were ~10,000 cm^{-3} during the early morning hours and steadily declined to around 5,500 cm^{-3} over the course of the day. Particle number fluxes followed a similar pattern, decreasing from 600 × 10^6 m^{-2} s^{-1} during the morning to ~200 × 10^6 m^{-2} s^{-1} in the late afternoon *(26)*. Similarly, in Edinburgh, aerosol concentrations were ~18,000 cm^{-3} during the early morning hours and declined to around 15,000 cm^{-3} during the afternoon hours *(52, 53)*. Particle number fluxes ranged from ~600 × 10^6 m^{-2} s^{-1} in the morning to approximately 400 × 10^6 m^{-2} s^{-1} in the late afternoon. Negative particle number fluxes were also observed in Stockholm and Edinburgh and ranged up to -20 × 10^6 m^{-2} s^{-1}. In all studies, fluxes were found to correlate with changes in motor vehicle traffic density, whereas in our study, the predominant influence was rail and barge transport of coal. While our $PM_{2.5}$ fluxes were sometimes negative, particle number fluxes in Stockholm and Edinburg were usually positive *(54)*. One reason for the difference is that our measurements included particles up to 2.5 μm, while the other two studies considered particles up to only 0.7 μm. The larger particles are more susceptible to gravitational settling, which produces negative fluxes.

4.2 Emissions Inventory Validation Approaches

The long-term objective of the FLAME is to provide an alternative method for estimating air pollutant emissions. The FLAME's measurements of concentrations and fluxes can be used to validate existing emissions estimates for both individual sources and spatially integrated ones. Improved methods of quantifying emissions will enable state and federal regulatory agencies to produce more accurate inventories and thus improve the regulation of air pollutants. Improved inventories are also needed to advance the science of air quality, as emissions are often the largest source of uncertainty in chemical-transport models. Finally, the FLAME's ability to measure CO_2 fluxes in urban areas is important in the movement toward quantification and regulation of greenhouse gas emissions.

4.3 Barge NO_x Emission Factors

Emissions from boats and ships used for commercial marine transportation of passengers, cargo or coal are a growing concern *(55, 56)*. Research suggests that the global fleet of ocean-going marine vessels emits approximately 3% of the world's carbon budget, which is more than the total carbon emissions from any nation in the world except the US, Russia, China, Japan, India and Germany. Marine emissions are also projected to increase by 75% during the next 20 years *(57-60)*. Emissions from inland waterway vessels, versus ocean-going ones, are especially important because they are more likely to impact populated areas during their operation, yet few measurements of their emission factors exist. Research in the area of marine emissions suggests that in the top 20 states relying on waterway commerce, 54% to 87% of ship NO_x emissions come from commercial marine vessels operating on inland waterways *(61)*.

Corbett et al. (2001) initiated an investigation of NO_x emissions from towboats in the Pittsburgh region along the Ohio River *(55)*. The research was conducted to provide a basic understanding of inland waterway vessel operations and emissions, and more importantly to aid in the development and evaluation of new EPA regulations attempting to limit emissions from marine engines.

Figure 14 shows NO_x concentrations from the Riverside site. Results are presented as 5-min averages and range from 0.011 to 0.021 ppm during the 3-h sampling period. CO_2 values during this same 3-h period are also plotted in Figure 14 and range from 395 to 485 ppm. The four shaded boxes highlight times when barges were passing through the footprint.

Using Corbett's equation above and the baseline-subtracted concentrations of NO_x and CO_2, we calculated emission factors associated with each of the four barges, shown in Table 1. The baseline concentrations were determined by averaging the NO_x and CO_2 concentrations recorded during the 5 min prior to the observed spike in concentration.

Table 1. NO_x emission factors (EF) for four barges.

Barge	Time	5-min Max CO_2 (ppm)	Backgd. CO_2 (ppm)	5-min Max NO_x (ppm)	Backgd. NO_x (ppm)	EF (kg NO_x tonne $fuel^{-1}$)
1	9:27	454	448	0.21	0.13	49
2	9:52	435	428	0.19	0.04	76
3	10:37	442	433	0.38	0.19	72
4	11:07	448	445	0.57	0.51	67
					Mean EF	66±12

Emission factors of the four barges ranged from 49 to 76 kg NO_x tonne $fuel^{-1}$ and averaged 66±12 kg NO_x tonne $fuel^{-1}$. For comparison, emission factors of small tow boats during basic operational modes (full throttle, maneuvering and idle) ranged between 33 and 87 kg NO_x tonne $fuel^{-1}$ *(55, 62, 63)*. Corbett et al. (2001) observed that the emission factor was most stable during periods of engine "full throttle," which is defined as operations occurring during transit between landings or locks on inland river waterways, typically with a barge or group of barges in tow. The portion of the river within the Riverside footprint contained no landings or locks; therefore, we may assume that the barges were in full throttle mode and had stable emission factors.

4.4 Per Capita CO_2 Emissions

As the concern over greenhouse gases continues to rise, regulation of their emissions through trading programs, carbon taxes or other methods is likely to expand. All such approaches require accurate quantification of CO_2 emissions in order to function fairly and effectively. Here, we outline an example of how the FLAME can be used to validate greenhouse gas emissions inventories. At present, such inventories are widely available only at the statewide

level, so although our measurements from a single town over three days are not likely to be representative of the entire state's annual emissions, the example illustrates what can be achieved with a larger data set in the future.

In 2004, the State of Kentucky reported CO_2 emissions of 150 million metric tonnes (Mmt), 93 Mmt of which comes from power generation *(29, 64)*. Not including power generation, the per capita CO_2 emissions in Kentucky are 14 tonne CO_2 person^{-1} yr^{-1}. This is 70% of the 2006 US EPA's nationwide per capita value of 19.92 tonne CO_2 person^{-1} yr^{-1} without including power generation *(65)*. Using the positive CO_2 fluxes measured in this study of 0.68-29 mg m^{-2} s^{-1} and Worthington's area of 3.03×10^6 m^2, it is possible to extrapolate measured flux values to a range of per capita emissions for the city. The resulting range of 13.3-560 tonne CO_2 person^{-1} yr^{-1} is a lower limit because the measured CO_2 fluxes may also reflect uptake of CO_2 by vegetation. The lower end of the range is similar to the statewide reported per capita value of 14 tonne CO_2 person^{-1} yr^{-1}, but the upper end of the range is more than 40 times higher. Granted, the upper end of the range is unlikely to apply statewide because one of our measurement sites was heavily influenced by mobile sources such as barges and trains, which have a higher per capita presence in Worthington. In the future, more intensive field campaigns with the FLAME will produce a much larger set of measurements that more completely represents the land use and demographics of a region.

4.5 $PM_{2.5}$ Emissions Comparison

Table 2 shows the $PM_{2.5}$ emissions inventory for Greenup County, in which Worthington is located, broken down by major source category. This inventory was compiled as part of the Visibility Improvement State and Tribal Association of the Southeast (VISTAS) regional planning organization's air quality modeling program. The inventory suggests that off-highway and "fuel combustion other" sources contribute to approximately 50% of the total. Off-highway emissions consist of boat and rail traffic, and fuel combustion (other) consists of any fuel combustion not attributed to industrial practices, e.g. refuse fires, wood and oil burning. Based on field observations, it is likely that off-highway emissions are significant in this area simply due to the amount of coal transport by rail and barge in the area. In contrast, due to time of year, and drought conditions, very few non-industrial fuel combustion

activities were observed.

Measured positive $PM_{2.5}$ fluxes in Worthington ranged between 1.6×10^{-6} and 9.1×10^{-5} mg m^{-2} s^{-1}. For the sake of comparing the measurements to the county-level reported $PM_{2.5}$ emissions of 354 tons yr^{-1} in 2002, we multiply by the area of Greenup County, realizing that the three measurement sites are unlikely to be representative of the county as a whole. Extrapolated to the entire county, the range of total $PM_{2.5}$ emissions is 290-16,400 tons yr^{-1}, which is 0.8 to 45 times larger than the reported value in 2002. As with our comparison of CO_2 flux measurements to the inventory, this example is meant to be more illustrative than conclusive because of the limited scope of measurements.

One obvious limitation of this comparison stems from the narrow temporal range of our measurements. Eddy covariance experiments were conducted during the daytime hours only, when emissions activity may be greater. A 24-hr measurement of daytime and nighttime fluxes over a larger set of days will provide greater confidence in emissions comparisons.

Table 2. Greenup County $PM_{2.5}$ emissions (tons yr^{-1}) in 2002.

Tier Name	$PM_{2.5}$
Fuel Combustion Electric Utilities	0
Fuel Combustion Industrial	10
Fuel Combustion Other	80
Chemical and Allied Product Manufacturing	17
Other Industrial Processes	26
Solvent Utilization	0
Storage and Transport	2
Waste Disposal and Recycling	60
Highway Vehicles	17
Off-Highway	96
Miscellaneous	43
County Totals	354

5.0 Conclusion

The goals of this research were to design and build a uniquely mobile flux lab capable of measuring neighborhood-scale emissions, to conduct flux measurements in areas with strong anthropogenic influences and to use the results of the field campaign to gain insight into the accuracy of emissions inventories of CO_2, NO_x and $PM_{2.5}$. Over three sites in a small Appalachian town dominated by coal transport, measured CO_2 and $PM_{2.5}$ fluxes ranged

between -6.5 to 29 mg m^{-2} s^{-1} and -9.7 × 10^{-5} to 9.1 × 10^{-5} mg m^{-2} s^{-1} respectively. The findings that a majority of fluxes were positive and that particle concentrations decreased over the course of a day agreed with other eddy covariance studies in urban areas. NO_x emissions associated with barge traffic were quantified in an effort to complement existing research on emissions from inland waterway vessels. Barge emission factors ranged from 49 to 76 kg NO_x tonne $fuel^{-1}$ with a mean of 66±12 kg NO_x tonne $fuel^{-1}$; these values agree well with existing studies of barge, small tow boat and other watercraft diesel engines. As an example of how the FLAME might be used in larger field campaigns in the future to validate emissions inventories, CO_2 and $PM_{2.5}$ fluxes were extrapolated to per capita and county levels and compared with the official inventory. Measured fluxes were up to 60 times higher than annual averages.

Future research with a more sustained field campaign will enable a more complete evaluation of emissions inventories as well as obtain new measurements of sources for which little or no data exist. We recommend several weeks of sampling at evenly spaced sites encompassing a mixture of residential and commercial land uses. Given the 1-km scale of the FLAME's footprint, sites no more than a few kilometers apart will provide nearly complete coverage. In fact, we recently conducted such a field campaign; the results will be presented in a forthcoming publication. The FLAME sampled at 16 evenly spaced sites across a 12 km × 12 km square in the Norfolk, Virginia area. Site selection was intended to facilitate the calculation of per capita emissions, and furthermore, the 12-km square corresponded to a grid cell of an emissions inventory used for air quality modeling. The FLAME will also be fitted with limited VOC measurement capabilities through the use of the "relaxed" eddy accumulation (REA) method *(66-69)*.

6.0 Acknowledgements

This research was supported by a National Science Foundation (NSF) CAREER award (CBET-0547107), NSF Research Experience for Undergraduates grant (CBET-0715162), and a Virginia Tech NSF Advance seed grant. We thank the Virginia Tech Transportation Institute for use of the van and the Cox family for support during the field campaign.

7.0 References

1. NRC *Rethinking the Ozone Problem in Urban and Regional Air Pollution*; National Research Council: Washington, D.C., 1991.
2. NRC *Science and Judgement in Risk Assessment*; National Research Council: Washington, D.C., 1994.
3. NRC *Modeling Mobile Source Emissions*; National Research Council: Washington, D.C., 2000.
4. Dreher, D. B.; Harley, R. A., A fuel-based inventory for heavy-duty diesel truck emissions. *J. Air. Waste Manage.* **1998,** *48*, 352-358.
5. Fujita, E. M.; Croes, B. E.; Bennett, C. L.; Lawson, D. R.; Lurmann, F. W.; Main, H. H., Comparison of emission inventory and ambient concentration ratios of CO, NMOG, and NO_x in California South Coast Basin. *J. Air. Waste Manage.* **1992,** *42*, 264-276.
6. Fujita, E. M.; Watson, J. G.; Chow, J. C.; Magliano, K. L., Receptor model and emissions inventory source apportionments of nonmethane organic gases in California San-Joaquin Valley and San-Francisco Bay Area. *Atmos. Environ.* **1995,** *29*, 3019-3035.
7. Harley, R. A.; McKeen, S. A.; Pearson, J.; Rodgers, M. O.; Lonneman, W. A., Analysis of motor vehicle emissions during the Nashville/Middle Tennessee Ozone Study. *J. Geophys. Res.-Atmos.* **2001,** *106*, 3559-3567.
8. Kasibhatla, P.; Arellano, A.; Logan, J. A.; Palmer, P. I.; Novelli, P., Top-down estimate of a large source of atmospheric carbon monoxide associated with fuel combustion in Asia. *Geophys. Res. Lett.* **2002,** *29*.
9. Kean, A. J.; Sawyer, R. F.; Harley, R. A., A fuel-based assessment of off-road diesel engine emissions. *J. Air. Waste Manage.* **2000,** *50*, 1929-1939.
10. Marr, L. C.; Black, D. R.; Harley, R. A., Formation of photochemical air pollution in central California - 1. Development of a revised motor vehicle emission inventory. *J. Geophys. Res.-Atmos.* **2002,** *107*, 4048.
11. Mendoza-Dominguez, A.; Russell, A. G., Emission strength validation using four-dimensional data assimilation: Application to primary aerosol and precursors to ozone and secondary aerosol. *J. Air. Waste Manage.* **2001,** *51*, 1538-1550.
12. Singer, B. C.; Harley, R. A., A fuel-based inventory of motor vehicle exhaust emissions in the Los Angeles area during summer 1997. *Atmos. Environ.* **2000,** *34*, 1783-1795.
13. Baldocchi, D. D., Assessing the eddy covariance technique for evaluating carbon dioxide exchange rates of ecosystems: past, present and future. In 2003; Vol. 9, pp 479-492.
14. Baldocchi, D. D.; Hicks, B. B.; Meyers, T. P., Measuring Biosphere-Atmosphere Exchanges of Biologically Related Gases with Micrometeorological Methods. *Ecology* **1988,** *69*, 1331-1340.
15. Moncrieff, J. B.; Massheder, J. M.; deBruin, H.; Elbers, J.; Friborg, T.; Heusinkveld, B.; Kabat, P.; Scott, S.; Soegaard, H.; Verhoef, A., A system to measure surface fluxes of momentum, sensible heat, water vapour and carbon dioxide. *J. Hydrol.* **1997,** *189*, 589-611.
16. Barnes, D. H.; Wofsy, S. C.; Fehlau, B. P.; Gottlieb, E. W.; Elkins, J. W.; Dutton, G. S.; Novelli, P. C., Hydrogen in the atmosphere: Observations above a forest canopy in a polluted environment. *J. Geophys. Res.-Atmos.* **2003,** *108*.
17. Goldstein, A. H.; Black, D. G.; Dreyfus, G. B.; Kurpius, M. R.; Lee, A.; Lunden, M. M.; McKay, M.; Schade, G. W., Chemical interactions between the atmosphere and forested ecosystems. *Abstr. Pap. Am. Chem. S.* **2002,** *224*, U303-U303.

18. Goldstein, A. H.; McKay, M.; Kurpius, M. R.; Schade, G. W.; Lee, A.; Holzinger, R.; Rasmussen, R. A., Forest thinning experiment confirms ozone deposition to forest canopy is dominated by reaction with biogenic VOCs. *Geophys. Res. Lett.* **2004,** *31*.
19. Gray, D. W.; Goldstein, A. H.; Lerdau, M. T., Thermal history regulates methylbutenol basal emission rate in Pinus ponderosa. *Plant Cell Environ.* **2006,** *29*, 1298-1308.
20. Potosnak, M. J.; Wofsy, S. C.; Denning, A. S.; Conway, T. J.; Munger, J. W.; Barnes, D. H., Influence of biotic exchange and combustion sources on atmospheric CO_2 concentrations in New England from observations at a forest flux tower. *J. Geophys. Res.-Atmos.* **1999,** *104*, 9561-9569.
21. Whitall, D.; Castro, M.; Driscoll, C., Evaluation of management strategies for reducing nitrogen loadings to four US estuaries. *Sci. Total Environ.* **2004,** *333*, 25-36.
22. Winchester, J. W.; Escalona, L.; Fu, J. M.; Furbish, D. J., Atmospheric Deposition and Hydrogeologic Flow of Nitrogen in Northern Florida Watersheds. *Geochim. Cosmochim. Ac.* **1995,** *59*, 2215-2222.
23. Wofsy, S. C.; Goulden, M. L.; Munger, J. W.; Fan, S. M.; Bakwin, P. S.; Daube, B. C.; Bassow, S. L.; Bazzaz, F. A., Net Exchange of CO_2 in a mid-latitude forest. *Science* **1993,** *260*, 1314-1317.
24. Wu, J. B.; Guan, D. X.; Sun, X. M.; Yu, G. R.; Zhao, X. S.; Han, S. J.; Jin, C. J., Eddy flux corrections for CO_2 exchange in broad-leaved Korean pine mixed forest of Changbai Mountains. *Sci. China Ser. D-Earth Sci.* **2005,** *48*, 106-115.
25. Grimmond, C. S. B.; King, T. S.; Cropley, F. D.; Nowak, D. J.; Souch, C., Local-scale fluxes of carbon dioxide in urban environments: Methodological challenges and results from Chicago. *Environ. Pollut.* **2002,** *116*, 243-254.
26. Martensson, E. M.; Nilsson, E. D.; Buzorius, G.; Johansson, C., Eddy covariance measurements and parameterisation of traffic related particle emissions in an urban environment. *Atmos. Chem. Phys.* **2006,** *6*, 769-785.
27. Velasco, E.; Lamb, B.; Pressley, S.; Allwine, E.; Westberg, H.; Jobson, B. T.; Alexander, M.; Prazeller, P.; Molina, L.; Molina, M., Flux measurements of volatile organic compounds from an urban landscape. *Geophys. Res. Lett.* **2005,** *32*.
28. Velasco, E.; Pressley, S.; Allwine, E.; Westberg, H.; Lamb, B., Measurements of CO_2 fluxes from the Mexico City urban landscape. *Atmos. Environ.* **2005,** *39*, 7433-7446.
29. Keatley, A. *Kentucky Ambient Air Quality Annual Report 2006*; Kentucky Division for Air Quality: Frankfort, 2006.
30. Scorecard.com Pollution Locator: Smog and Particulates: County Report. http://www.scorecard.org/env-releases/cap/county.tcl?fips_county_code=21089
31. Schmid, H. P., Source Areas for Scalars and Scalar Fluxes. *Bound.-Lay. Meteorol.* **1994,** *67*, 293-318.
32. Schmid, H. P. *Flux Source Area Model - FSAM*, 1; Bloomington, 2001.
33. Chang, L. T.; Suh, H. H.; Wolfson, J. M.; Misra, K.; Allen, G. A.; Catalano, P. J.; Koutrakis, P., Laboratory and field evaluation of measurement methods for one-hour exposures to O_3, $PM_{2.5}$, and CO. *J. Air. Waste Manage.* **2001,** *51*, 1414-1422.
34. Chung, A.; Chang, D. P. Y.; Kleeman, M. J.; Perry, K. D.; Cahill, T. A.; Dutcher, D.; McDougall, E. M.; Stroud, K., Comparison of real-time instruments used to monitor airborne particulate matter. *J. Air. Waste Manage.* **2001,** *51*, 109-120.
35. Jiang, M.; Marr, L. C.; Dunlea, E. J.; Herndon, S. C.; Jayne, J. T.; Kolb, C. E.; Knighton, W. B.; Rogers, T. M.; Zavala, M.; Molina, L. T.; Molina, M. J., Vehicle fleet emissions of black

carbon, polycyclic aromatic hydrocarbons, and other pollutants measured by a mobile laboratory in Mexico City. *Atmos. Chem. Phys.* **2005,** *5*, 3377-3387.
36. Kim, J. Y.; Magari, S. R.; Herrick, R. F.; Smith, T. J.; Christiani, D. C., Comparison of fine particle measurements from a direct-reading instrument and a gravimetric sampling method. *J. Occup. Environ. Hyg.* **2004,** *1*, 707-715.
37. Yanosky, J. D.; Williams, P. L.; MacIntosh, D. L., A comparison of two direct-reading aerosol monitors with the federal reference method for $PM_{2.5}$ in indoor air. *Atmos. Environ.* **2002,** *36*, 107-113.
38. Aubinet, M.; Grelle, A.; Ibrom, A.; Rannik, U.; Moncrieff, J.; Foken, T.; Kowalski, A. S.; Martin, P. H.; Berbigier, P.; Bernhofer, C.; Clement, R.; Elbers, J.; Granier, A.; Grunwald, T.; Morgenstern, K.; Pilegaard, K.; Rebmann, C.; Snijders, W.; Valentini, R.; Vesala, T., Estimates of the annual net carbon and water exchange of forests: The EUROFLUX methodology. In *Advances in Ecological Research, Vol 30*, 2000; Vol. 30, pp 113-175.
39. Seinfeld, J. H.; Pandis, S. N., *Atmospheric Chemistry and Physics - From Air Pollution to Climate Change*. 2 ed.; John Wiley & Sons, Inc.: Hoboken, New Jersey, 2006 Vol. 2, p 1203.
40. Vickers, D.; Mahrt, L., Quality control and flux sampling problems for tower and aircraft data. *J. Atmos. Ocean. Tech.* **1997,** *14*, 512-526.
41. Massman, W. J.; Lee, X., Eddy covariance flux corrections and uncertainties in long-term studies of carbon and energy exchanges. *Agr. Forest Meteorol.* **2002,** *113*, 121-144.
42. Cullen, N. J.; Steffen, K.; Blanken, P. D., Nonstationarity of turbulent heat fluxes at Summit, Greenland. *Bound.-Lay. Meteorol.* **2007,** *122*, 439-455.
43. Diem, J. E.; Comrie, A. C., Allocating anthropogenic pollutant emissions over space: application to ozone pollution management. *J. Environ. Manage.* **2001,** *63*, 425-447.
44. Grimmond, C. S. B.; Salmond, J. A.; Oke, T. R.; Offerle, B.; Lemonsu, A., Flux and turbulence measurements at a densely built-up site in Marseille: Heat, mass (water and carbon dioxide), and momentum. *J. Geophys. Res.-Atmos.* **2004,** *109*, -.
45. Guldmann, J. M.; Kim, H. Y., Modeling air quality in urban areas: A cell-based statistical approach. *Geogr. Anal.* **2001,** *33*, 156-180.
46. Lyons, T. J.; Halldin, S., Surface heterogeneity and the spatial variation of fluxes. *Agr. Forest Meteorol.* **2004,** *121*, 153-165.
47. Loescher, H. W.; Law, B. E.; Mahrt, L.; Hollinger, D. Y.; Campbell, J.; Wofsy, S. C., Uncertainties in, and interpretation of, carbon flux estimates using the eddy covariance technique. *J. Geophys. Res.-Atmos.* **2006,** *111*.
48. Hollinger, D. Y.; Richardson, A. D., Uncertainty in eddy covariance measurements and its application to physiological models. *Tree Physiol.* **2005,** *25*, 873-885.
49. Kruijt, B.; Elbers, J. A.; von Randow, C.; Araujo, A. C.; Oliveira, P. J.; Culf, A.; Manzi, A. O.; Nobre, A. D.; Kabat, P.; Moors, E. J., The robustness of eddy correlation fluxes for Amazon rain forest conditions. *Ecol. Appl.* **2004,** *14*, S101-S113.
50. Foken, T.; Wichura, B., Tools for quality assessment of surface-based flux measurements. *Agr. Forest Meteorol.* **1996,** *78*, 83-105.
51. Lenschow, D. H.; Mann, J.; Kristensen, L., How long is long enough when measuring fluxes and other turbulence statistics. *J. Atmos. Ocean. Tech.* **1994,** *11*, 661-673.
52. Dorsey, J. R.; Nemitz, E.; Gallagher, M. W.; Fowler, D.; Williams, P. I.; Bower, K. N.; Beswick, K. M., Direct measurements and parameterisation of aerosol flux, concentration and emission velocity above a city. *Atmos. Environ.* **2002,** *36*, 791-800.

53. Nemitz, E.; Hargreaves, K. J.; McDonald, A. G.; Dorsey, J. R.; Fowler, D., Meteorological measurements of the urban heat budget and CO_2 emissions on a city scale. *Environ. Sci. Technol.* **2002,** *36*, 3139-3146.
54. Coutts, A. M.; Beringer, J.; Tapper, N. J., Characteristics influencing the variability of urban CO_2 fluxes in Melbourne, Australia. *Atmos. Environ.* **2007,** *41*, 51-62.
55. Corbett, J. J.; Robinson, A. L., Measurements of NO_x emissions and in-service duty cycle from a towboat operating on the inland river system. *Environ. Sci. Technol.* **2001,** *35*, 1343-1349.
56. Winebrake, J. J.; Corbett, J. J.; Meyer, P. E., Energy use and emissions from marine vessels: A total fuel life cycle approach. *J. Air. Waste Manage.* **2007,** *57*, 102-110.
57. Corbett, J. J.; Fischbeck, P., Emissions from ships. *Science* **1997,** *278*, 823-824.
58. Corbett, J. J.; Koehler, H. W., Updated emissions from ocean shipping. *J. Geophys. Res.-Atmos.* **2003,** *108*.
59. Eyring, V.; Kohler, H. W.; Lauer, A.; Lemper, B., Emissions from international shipping: 2. Impact of future technologies on scenarios until 2050. *J. Geophys. Res.-Atmos.* **2005,** *110*.
60. Eyring, V.; Kohler, H. W.; van Aardenne, J.; Lauer, A., Emissions from international shipping: 1. The last 50 years. *J. Geophys. Res.-Atmos.* **2005,** *110*.
61. Corbett, J. J.; Fischbeck, P. S., Emissions from waterborne commerce vessels in United States continental and inland waterways. *Environ. Sci. Technol.* **2000,** *34*, 3254-3260.
62. Carlton, J. S.; Danton, S. D.; Gawen, R. W.; Lavender, K. A.; Mathieson, N. M.; Newell, A. G.; Reynolds, G. L.; Webster, A. D.; C.M.R., W.; A.A., W., Marine Exhaust Emissions Research. *Lloyd's Register Engineering Services: London* **1995**.
63. Sierra-Research *Analysis of Commercial Marine Vessels Emissions and Fuel Consumption Data*; U.S. Environmental Protection Agency, Office of Mobile Sources: Ann Arbor, Michigan, 2000.
64. USEIA *Official Energy Statistics from the U.S. Government*; Department of Energy: 2006.
65. USEPA *Inventory of U.S. Greenhouse Gas Emissions and Sinks: 1990-2006* 2008; p 473.
66. Ciccioli, P.; Brancaleoni, E.; Frattoni, M.; Marta, S.; Brachetti, A.; Vitullo, M.; Tirone, G.; Valentini, R., Relaxed eddy accumulation, a new technique for measuring emission and deposition fluxes of volatile organic compounds by capillary gas chromatography and mass spectrometry. *J. Chromatogr. A* **2003,** *985*, 283-296.
67. Graus, M.; Hansel, A.; Wisthaler, A.; Lindinger, C.; Forkel, R.; Hauff, K.; Klauer, M.; Pfichner, A.; Rappengluck, B.; Steigner, D.; Steinbrecher, R., A relaxed-eddy-accumulation method for the measurement of isoprenoid canopy-fluxes using an online gas-chromatographic technique and PTR-MS simultaneously. *Atmos. Environ.* **2006,** *40*, S43-S54.
68. Skov, H.; Brooks, S. B.; Goodsite, M. E.; Lindberg, S. E.; Meyers, T. P.; Landis, M. S.; Larsen, M. R. B.; Jensen, B.; McConville, G.; Christensen, J., Fluxes of reactive gaseous mercury measured with a newly developed method using relaxed eddy accumulation. *Atmos. Environ.* **2006,** *40*, 5452-5463.
69. Valverde-Canossa, J.; Ganzeveld, L.; Rappengluck, B.; Steinbrecher, R.; Klemm, O.; Schuster, G.; Moortgat, G. K., First measurements of H_2O_2 and organic peroxides surface fluxes by the relaxed eddy-accumulation technique. *Atmos. Environ.* **2006,** *40*, S55-S67.

8.0 Supporting Information

8.1 Pollutant Concentrations

Table 3 summarizes the average concentrations of each pollutant measured during the field campaign. CO_2 and $PM_{2.5}$ were measured on all three days, and NO_x was measured for three hours on the first day of the campaign only.

Table 3. Calculated standard deviations for daily recorded measurements of CO_2, $PM_{2.5}$ and NO_x at three sample locations during field campaign.

Location	Average Measured Concentrations			Standard deviation		
	CO_2 (ppm)	$PM_{2.5}$ ($\mu g\ m^{-3}$)	NO_x (ppm)	CO_2 (ppm)	$PM_{2.5}$ ($\mu g\ m^{-3}$)	NO_x (ppm)
Ironton Riverside	448	24	0.14	± 35	± 8	± 0.03
Worthington Residential	410	14	N/A	± 31	± 5	N/A
Cox Farm Lot	397	0.17	N/A	± 18	± 0.077	N/A

The relative standard deviations of CO_2 at the Ironton Riverside and Worthington Residential sites are low (< 11%) and at the Farm Lot, it is even lower, less than 6%. However, the variabilities in $PM_{2.5}$ at all measurement sites is relatively high (33 – 45%). The reason for this variability may have been the extreme changes in concentrations before and after rain events or the large drop in $PM_{2.5}$ over the course of the day due to dilution of the boundary layer as the mixing height rises. The NO_x variability is approximately 20% over the three-hour measurement period.

Chapter 3: Validation of Urban Air Pollution Emission Inventories by Eddy Covariance

Abstract

Eddy covariance flux measurements of carbon dioxide (CO_2), nitrogen oxides (NO_x), and fine particulate matter ($PM_{2.5}$) were conducted in Norfolk, Virginia, to describe quantitatively urban air pollutant emissions and to validate official inventories used for regulatory purposes and air quality modeling. The daytime average of positive (upward) fluxes, which defines a lower bound on emissions, for CO_2, NO_x and $PM_{2.5}$ across 16 sites ranged between 0.7-3.1, 5.6×10^{-4}-1.2×10^{-2} and 5.4×10^{-6}- 3.0×10^{-4} mg m^{-2} s^{-1}, respectively, with tremendous spatial and temporal variability at the neighborhood scale. Larger fluxes of all pollutants occurred in areas with heavier vehicle traffic, and the highest $PM_{2.5}$ fluxes were associated with construction activity. From the positive fluxes, we estimated summer, daytime emission rates of 800,640±75,000 (standard error) kg hr^{-1} for CO_2, 1,470±325 kg hr^{-1} for NO_x and 32±12 kg hr^{-1} for $PM_{2.5}$ from the 139 km^2 city. Within the precision and limitations of the eddy covariance method, the measurements agree with official CO_2 and NO_x emission inventories but suggest that $PM_{2.5}$ emissions may be overstated. Emissions were also compared with a high-resolution air quality modeling inventory. The range of hourly rates of NO_x and $PM_{2.5}$ emissions were very similar between the inventory and flux measurements.

1.0 Introduction

Air pollution emission inventories are critical tools for improving air quality, but they are known to contain large uncertainties that can limit progress toward scientific and policymaking goals. Emissions from non-point sources are especially uncertain because of the dearth of methods for independently verifying them. To estimate such emissions, inventories rely on emission factors, but these are often based on measurements from a very small sample size and may not be representative of the population of sources. Independent estimates suggest that fine particulate matter inventories, for example, may be inaccurate by an order of magnitude *(1)*.

A host of techniques has been used to validate, invalidate, or estimate emission inventories indirectly, including applying receptor models to observed concentrations *(2)*, incorporating inventories into air quality models and comparing predictions with atmospheric measurements *(3-7)* or satellite observations *(8-10)*, comparing pollutant ratios within the inventory to ambient ones *(11)*, conducting on-road studies for mobile sources *(12)* and applying inverse methods using three-dimensional air quality models *(13, 14)*, to highlight a handful of the most recent publications. However, none of these methods directly measures the flux of emissions to the atmosphere.

Eddy covariance, widely used in the biogeosciences to measure surface-atmosphere exchange fluxes, can be used as a powerful tool for validating emission inventories and identifying missing and/or erroneous components in them *(15)*. Previous work has demonstrated the successful use of eddy covariance towers to measure fluxes in urban locations such as Chicago, Mexico City and Edinburgh *(16-18)*. Although towers enable high measurement heights, they are locked into a single location and require infrastructure and permissions that can be difficult to obtain. We have overcome this challenge by employing a van with a telescoping mast as the eddy covariance platform, thereby gaining the advantage of being able conduct measurements anywhere that is accessible to vehicles and favorable topographically to the method. In a recent pilot study, we demonstrated this approach for measuring fluxes of carbon dioxide (CO_2), nitrogen oxides (NO_x) and fine particulate matter ($PM_{2.5}$) in an area of Appalachia dominated by sources associated with coal transport *(15)*.

The objective of this research is to determine the magnitude and spatial and temporal variability in air pollutant fluxes at the neighborhood scale for comparison to official emission inventories used for regulatory purposes and air quality modeling. Measurements that are in agreement with the inventory will add confidence to the estimates, and those that differ will highlight segments in need of further refinement. Using a mobile eddy covariance system, we measured surface-atmosphere exchange fluxes of CO_2, NO_x and $PM_{2.5}$ during a month-long field campaign in the Norfolk, Virginia area. We compared results with the Environmental Protection Agency's (EPA) emission inventory and with a high-resolution gridded inventory developed for air quality modeling. These alternative estimates of

emissions can provide insight into uncertainties in inventories and prioritize further development of inventorying methods.

2.0 Methods

2.1 Site

The field campaign took place in Norfolk, Virginia, and also included parts of the surrounding cities of Chesapeake, Portsmouth and Virginia Beach. The area is designated non-attainment for ozone and often experiences high levels of $PM_{2.5}$ during the summer. For eddy covariance, a uniform fetch is most desirable, but urban areas are spatially heterogeneous and therefore require a sampling approach to achieve spatially representative measurements. Sixteen sampling locations were chosen to be approximately evenly spaced across a 12-km × 12-km square that coincided with the grid cell of highest emissions in the region in an inventory developed by the Visibility Improvement State and Tribal Association of the Southeast (VISTAS) regional planning organization for modeling air quality.

Figure 16 in the Supporting Information shows a map of the 16 sampling locations (SL), superimposed on land use categories according to the US Department of Agriculture. Most sites were located in residential/industrial areas with varying amounts of pavement, grassland and crops nearby. Terrain was typically flat with low building and tree heights (<10 m). Sampling took place on Mondays through Thursdays for four weeks in June 2008, beginning at 7:00 and ending at 17:00. Ten sites were within or adjacent to residential neighborhoods. The remaining six sites were located within commercial areas, e.g. malls, golf courses, restaurants, small businesses, warehouses and universities. Industrial areas consisted of ship painting, coal processing or other facilities, and their vehicle traffic was dominated by delivery trucks. Sampling locations are described in greater detail in the Supporting Information.

"Footprints" at each site were calculated using the Flux Area Source Model (FSAM) *(19)*, an analytical solution of the advection-diffusion equation. The footprint describes the source probability distribution, or the extent of the area influencing measured fluxes. Footprint

lengths measured 2.6-3.6 km upwind.

2.2 Flux Measurements

The mobile Flux Laboratory for the Atmospheric Measurement of Emissions (FLAME) is a customized television news van with a mast that extends to 15.5 m above ground. A sonic anemometer (Applied Technologies SATI-3K) and sample tubing are mounted on a rotating platform on top of the mast. Fast analyzers inside the van measure CO_2 by infrared absorption (Li-Cor LI-7000), NO_x by chemiluminescence (Eco Physics CLD 88Y) and $PM_{2.5}$ by light scattering (TSI DustTrak 8520). A slower analyzer measures carbon monoxide (CO) (Teledyne Instruments Model 300E), but its response time is too slow to be used for calculating fluxes.

Data quality control and standard post-processing of the measurements includes hard spike removal, soft spike removal, lag correction, coordinate rotation by the planar fit method, linear detrending, calculation of fluxes and quality assurance of the fluxes through spectral and co-spectral analyses and stationarity testing *(16, 18, 20)*. Additional details are contained in a previous publication *(15)* and the Supporting Information.

Fluxes are calculated over 30-min averaging periods as

$$F_x = \overline{w' C_x'} \qquad \text{(Eq. 1)}$$

The flux F_x of species x is the time-averaged covariance between the instantaneous deviations of the vertical wind velocity w' and the concentration C_x' from their means over the averaging period *(18, 21)*. A positive flux represents net transfer upward into the atmosphere from the surface. Although it is impossible to quantify uncertainties accurately from eddy covariance data alone, on the basis of previous work dedicated to the estimation of such uncertainties *(22-28)*, it is likely that the systematic error in fluxes is ≤ 25% and random error is ≤ 20%.

3.0 Results

Weather during the campaign was hot and humid with daily high temperatures of 25 to 40 °C. There was no precipitation, and skies were typically clear. Due to practical considerations and the difficulty in measuring nighttime fluxes under very stable atmospheric conditions, the results presented here reflect daytime measurements only, between 7:00-17:00.

3.1 Campaign Concentrations

Table 4 shows CO_2, NO_x, CO and $PM_{2.5}$ concentrations (mixing ratios for gases) measured at all 16 sites. Time series can be found in the Supporting Information. The first 1.5 hr of measurements at SL 10 were excluded from further analysis because high CO and $PM_{2.5}$ from wildfires ~60 km to the south exceeded instrumental limits.

Table 4. Daytime average±standard deviation of 30-min CO_2, NO_x, CO and $PM_{2.5}$ concentrations between 7:00-17:00.

Date	Site	CO_2 (ppm)	NO_x (ppb)	CO (ppb)	$PM_{2.5}$ (μg m^{-3})
06/02/08	SL 1	486±28	54±75	360±70	9.6±1.8
06/03/08	SL 2	585±56	24±23	460±80	8.6±4.9
06/04/08	SL 3	528±43	26±64	300±80	1.1±0.4
06/05/08	SL 4	539±65	24±18	650±30	19±23
06/09/08	SL 5	477±61	31±60	450±90	1.0±0.3
06/10/08	SL 6	520±53	36±48	440±140	1.0±0.5
06/11/08	SL 7	560±61	24±21	570±260	15±20
06/12/08	SL 8	573±55	34±33	490±170	16±15
06/16/08	SL 9	516±74	33±40	390±130	5.3±4.6
06/17/08	SL 10	604±88	89±48[a,b]	490±640	3.3±0.3[b]
06/18/08	SL 11	531±62	61±44	440±130	13±29
06/19/08	SL 12	606±80	56±45	430±140	8.0±4.9
06/23/08	SL 13	587±89	46±17	360±40	6.4±3.8
06/24/08	SL 14	464±45	22±14	370±30	6.9±1.1
06/25/08	SL 15	525±42	26±24	360±80	2.3±2.7
06/26/08	SL 16	499±40	22±7	390±110	1.7±0.6

[a] Lower bound since concentrations exceeded the analyzer's maximum range of 5000 ppb for ~40 s in 8.5 hours.
[b] Excludes the first 90 min of measurements, when concentrations exceeded analyzers' upper limits.

Concentrations showed substantial spatial and temporal variability across the 12 km × 12 km

area. At each site, average daytime CO_2 concentrations ranged between 464 and 606 ppm, much higher than the current global background of ~380 ppm. Such an "urban CO_2 dome" has been reported in Phoenix, where citywide CO_2 concentrations in excess of 650 ppm were 75% higher than in the surrounding rural areas *(29, 30)*. Average NO_x concentrations at each site ranged between 22 and 89 ppb. The location with the highest NO_x, SL 10, was 0.5 km downwind of the interchange of four highways and 0.7 km downwind of a construction site. CO concentrations ranged from 300 to 650 ppb, and $PM_{2.5}$ concentrations averaged 1 to 19 $\mu g\ m^{-3}$ across sites. Construction at a nearby golf course at SL 4 and heavy commercial traffic at SL 7 and 8 were the likely sources of $PM_{2.5}$ at these sites, where concentrations exceeded the annual standard of 15 $\mu g\ m^{-3}$ but not the 24-hr standard of 35 $\mu g\ m^{-3}$. Among the four pollutants, the highest daytime average concentrations occurred at three different sites; both CO and $PM_{2.5}$ were maximal at SL 4. The spread of maxima across different sites and the different ratios of pollutants to each other indicate that there were differences in the sources influencing each site.

CO_2 was relatively stable over the daytime hours, whereas CO, NO_x and $PM_{2.5}$ tended to be higher in the morning. The latter three pollutants had more variable temporal patterns across sites and days than did CO_2. At any single site, the relative standard deviation of the 20 30-min CO_2 concentrations was 6-15%, and that of site-averaged 30-min concentrations was only 3%. In contrast, the relative standard deviations of 30-min CO, NO_x and $PM_{2.5}$ at any single site were 8-130%, 30-243% and 13-134%, respectively. Sites with larger amounts of commercial and industrial traffic, i.e. a relatively large fraction of diesel-powered vehicles, such as SL 1, 10, 11, and 12, had the largest spikes in NO_x and $PM_{2.5}$. Sites with heavier traffic throughout much of the day, SL 4 and 7, had CO spikes of 1500-2500 ppb.

3.2 Campaign Fluxes

For quality assurance purposes, spectral and co-spectral plots of CO_2 and temperature with vertical wind velocity, as well as stationarity tests of all pollutants, were reviewed. As in previous work with the FLAME *(15)*, slopes of frequency-weighted spectral and co-spectral plots were found to match theoretically expected values of -2/3 and -4/3, respectively *(18, 25, 31)*. All differences between 30-min and 5-min fluxes were well below the criterion of

60% *(18, 20, 25).*

Table 5 presents average fluxes over the 10 hr of measurements each day and the average of positive fluxes only for CO_2, NO_x (as NO_2) and $PM_{2.5}$ at all 16 sites.

Table 5. Daytime average ± standard deviation fluxes (mg m^{-2} s^{-1}) of all periods and of positive ones (+) only.

Date	Site	All CO_2	+CO_2	All NO_x (as NO_2)	+NO_x (as NO_2)	All $PM_{2.5}$	+$PM_{2.5}$
6/02	SL 1	0.4±1.9	1.6±2.1	$-1.8\pm5.6 \times 10^{-3}$	$2.8\pm2.3 \times 10^{-3}$	$0.5\pm2.0 \times 10^{-5}$	$1.8\pm1.0 \times 10^{-5}$
6/03	SL 2	0.7±1.9	1.7±1.7	$1.8\pm1.5 \times 10^{-3}$	$1.8\pm1.5 \times 10^{-3}$	$-2.1\pm6.3 \times 10^{-5}$	$2.0\pm3.8 \times 10^{-5}$
6/04	SL 3	0.4±1.4	1.1±1.0	$1.5\pm2.9 \times 10^{-3}$	$2.1\pm3.2 \times 10^{-3}$	$0.2\pm1.4 \times 10^{-5}$	$1.0\pm1.2 \times 10^{-5}$
6/05	SL 4	0.1±3.0	1.8±1.2	$0.6\pm1.3 \times 10^{-3}$	$1.2\pm1.3 \times 10^{-3}$	$1.4\pm4.5 \times 10^{-4}$	$3.0\pm6.1 \times 10^{-4}$
6/09	SL 5	0.6±1.9	1.9±1.6	$0.9\pm3.6 \times 10^{-3}$	$2.0\pm3.5 \times 10^{-3}$	$0.4\pm1.0 \times 10^{-5}$	$7.7\pm9.0 \times 10^{-6}$
6/10	SL 6	1.2±1.8	1.9±1.4	$3.5\pm2.2 \times 10^{-3}$	$3.5\pm2.2 \times 10^{-3}$	$1.3\pm1.6 \times 10^{-5}$	$1.4\pm1.6 \times 10^{-5}$
6/11	SL 7	0.5±2.5	1.9±1.7	$1.3\pm1.6 \times 10^{-3}$	$1.6\pm1.6 \times 10^{-3}$	$0.7\pm4.0 \times 10^{-4}$	$2.8\pm5.8 \times 10^{-4}$
6/12	SL 8	0.4±3.1	2.5±1.5	$1.7\pm2.5 \times 10^{-3}$	$2.3\pm2.4 \times 10^{-3}$	$-0.2\pm2.3 \times 10^{-4}$	$1.2\pm2.1 \times 10^{-4}$
6/16	SL 9	0.4±1.3	1.2±1.0	$1.1\pm1.3 \times 10^{-3}$	$1.4\pm1.2 \times 10^{-3}$	$1.5\pm2.4 \times 10^{-5}$	$2.9\pm2.0 \times 10^{-5}$
6/17	SL 10[a]	1.0±1.7	1.5±1.7	$0.4\pm1.6 \times 10^{-2}$ [b]	$1.4\pm1.6 \times 10^{-2}$ [b]	$0.9\pm2.1 \times 10^{-5}$	$1.9\pm1.6 \times 10^{-5}$
6/18	SL 11	-0.2±2.8	1.6±1.2	$1.9\pm1.8 \times 10^{-3}$	$2.3\pm1.5 \times 10^{-3}$	$1.4\pm1.5 \times 10^{-5}$	$1.7\pm1.3 \times 10^{-5}$
6/19	SL 12	1.5±4.4	3.1±5.5	$2.4\pm3.1 \times 10^{-3}$	$3.0\pm3.0 \times 10^{-3}$	$2.8\pm5.0 \times 10^{-5}$	$3.2\pm5.1 \times 10^{-5}$
6/23	SL 13	0.3±3.0	1.9±1.7	$3.1\pm3.4 \times 10^{-3}$	$3.8\pm3.2 \times 10^{-3}$	$1.4\pm1.5 \times 10^{-5}$	$1.8\pm1.4 \times 10^{-5}$
6/24	SL 14	-0.5±1.6	1.0±1.1	$4.0\pm5.6 \times 10^{-4}$	$5.6\pm5.0 \times 10^{-4}$	$-0.07\pm1.3 \times 10^{-5}$	$1.1\pm0.7 \times 10^{-5}$
6/25	SL 15	-0.3±1.5	0.7±0.8	$1.4\pm1.6 \times 10^{-3}$	$1.5\pm1.6 \times 10^{-3}$	$2.9\pm3.2 \times 10^{-5}$	$3.8\pm2.8 \times 10^{-5}$
6/26	SL 16	0.7±1.0	1.0±0.8	$0.8\pm1.2 \times 10^{-3}$	$1.0\pm1.2 \times 10^{-3}$	$0.4\pm8.2 \times 10^{-6}$	$5.4\pm6.7 \times 10^{-6}$
Average	All	0.44±0.52	1.6±0.6	$1.5\pm1.4 \times 10^{-3}$	$2.7\pm2.6 \times 10^{-3}$	$2.0\pm3.9 \times 10^{-5}$	$5.9\pm9.4 \times 10^{-5}$

[a] Excludes the first 90 min of measurements, when the measurements exceeded analyzer maximum.
[b] Lower bound since concentrations exceeded the analyzer's maximum range of 5000 ppb for ~40 s in 8.5 h.

Fluxes represent net surface-atmosphere exchange, and values less than zero mean that emissions were exceeded by uptake at the surface. In situations when downward fluxes were significant, e.g. uptake of CO_2 by photosynthesizing plants or gravitational deposition of larger particles, positive fluxes more closely isolate anthropogenic emissions. Histograms showing the distribution of fluxes at all sites are shown in the Supporting Information. All averages except CO_2 at SL 11, 14 and 15; NO_x at SL 1 and $PM_{2.5}$ at SL 2, 8 and 14 were positive, indicating that most areas of Norfolk were net sources to the atmosphere. As expected, this observation agrees with previous findings that urban areas are sources of emissions *(15, 18, 31-35)*.

The relative standard deviations in fluxes shown in Table 5 across sites were 118% for CO_2, 87% for NO_x and 185% for $PM_{2.5}$. The large values indicate that emissions were highly spatially heterogeneous. Not surprisingly, CO_2 fluxes were highest, 1.0-1.5 mg m^{-2} s^{-1}, at those sites with the greatest amount of traffic: SL 6, 10 and 12. SL 6 was ~1.3 km north and downwind of downtown Norfolk and its commuter traffic. At this site, 75% of the 30-min fluxes were positive. SL 10 was located adjacent to heavy industrial activity as well as a major highway interchange, and 80% of its 30-min fluxes were positive. The largest flux of the campaign, 19.5 mg m^{-2} s^{-1}, occurred at SL 12 at 8:00. This site was adjacent to Interstate 64 (I-64). Yet only 55% of the 30-min fluxes at SL 12 were positive, possibly because the site was also adjacent to a major waterway and near large areas of vegetation, which may have been a sink for CO_2. SL 14 was adjacent to an older, wooded residential neighborhood and experienced the lowest average CO_2 fluxes.

Some of the highest NO_x fluxes were experienced at SL 6 and 10, highly commercial and industrial locations. SL 6 was adjacent to heavy commercial activity, the I-64/264 interchange and downtown Norfolk, and all of its NO_x fluxes were positive. SL 10 was adjacent to numerous industrial shipbuilding and painting operations, and 55% of its fluxes were large and positive. SL 1 was adjacent to a large body of water, a large football practice field and a wooded residential area and had the lowest average fluxes of the campaign, negative in fact, indicating that deposition outweighed emissions. SL 14 was located in a mostly residential area and saw very little diesel or commercial traffic; it had the second

lowest NO_x fluxes.

For $PM_{2.5}$, SL 4 and SL 7 experienced some of the highest fluxes during the campaign. Although only 50% of fluxes measured at SL 4 were positive, they were large; nearby construction activity probably led to dust suspension. At SL 7, only 40% of the measured fluxes were positive, but construction activity and commercial traffic were high in this area, likely causing higher positive fluxes.

One factor common to all of the sites with higher fluxes was that they were located in areas with denser populations and with a significant amount of diesel vehicle traffic. Out of the 320 half-hourly fluxes of each pollutant measured during the campaign (317 for NO_x and $PM_{2.5}$), 192, 254, and 207 were greater than zero for CO_2, NO_x, and $PM_{2.5}$, respectively. Among the three pollutants, CO_2 had the largest fraction of negative fluxes because it has a major removal mechanism: photosynthetic uptake.

Diurnal patterns of fluxes of CO_2, NO_x and $PM_{2.5}$ are shown in Figure 15. The thick black line shows fluxes averaged across all 16 sites, and the colored lines highlight SL 4, 7, 10, and 12 because they exhibited some of the larger fluxes during the campaign. Fluxes were highly variable by location and time of day. For example, some sites had higher fluxes in the morning (7:30 – 9:30) and late afternoon (14:30 – 17:00), most likely attributable to rush hour traffic. Most sites, however, experienced anthropogenic activity throughout the day and also showed large spikes in fluxes at non-rush-hour times, too.

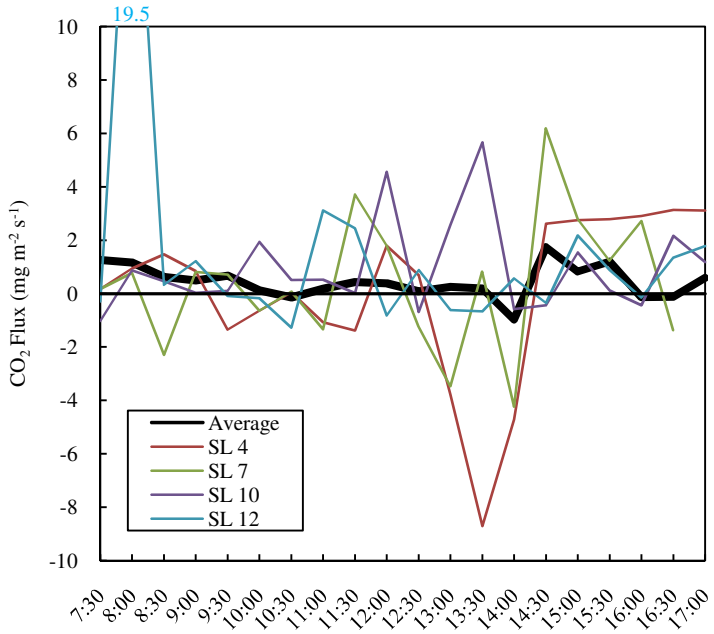
19.5
10
8
6
4
2
0
-2
-4
-6
-8
-10
CO2 Flux (mg m-2 s-1)
Average
SL 4
SL 7
SL 10
SL 12
7:30
8:00
8:30
9:00
9:30
10:00
10:30
11:00
11:30
12:00
12:30
13:00
13:30
14:00
14:30
15:00
15:30
16:00
16:30
17:00

(a)

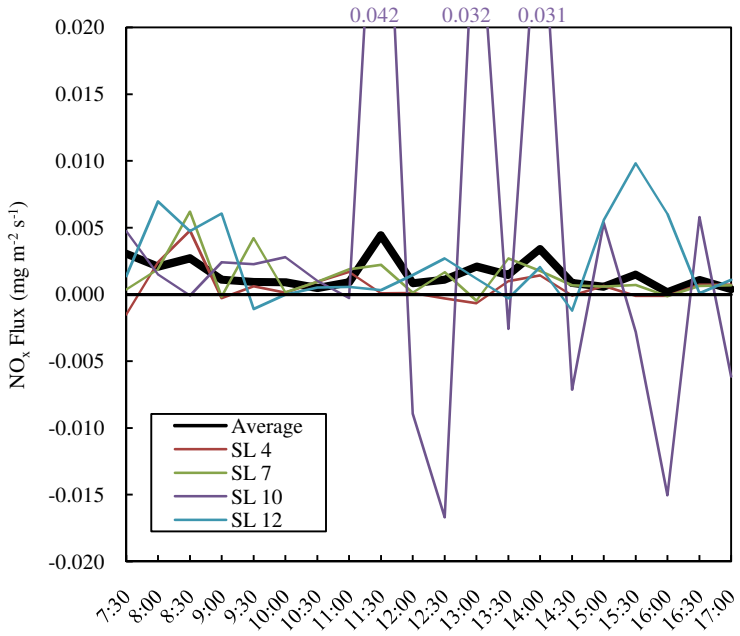
0.042
0.032
0.031
0.020
0.015
0.010
0.005
0.000
-0.005
-0.010
-0.015
-0.020
NOx Flux (mg m-2 s-1)
Average
SL 4
SL 7
SL 10
SL 12
7:30
8:00
8:30
9:00
9:30
10:00
10:30
11:00
11:30
12:00
12:30
13:00
13:30
14:00
14:30
15:00
15:30
16:00
16:30
17:00

(b)

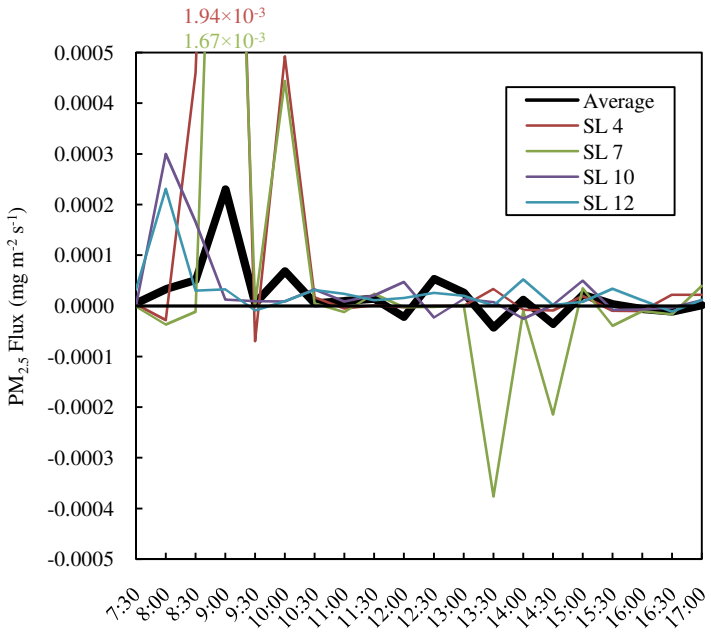

Figure 15. Average half-hourly (a) CO2, (b) NOx and (c) PM2.5 fluxes across all 16 sample locations (thick black line) and at four selected sites.

(c)

CO_2 fluxes were highest between 7:30-8:30 and 14:30-15:30, periods of greater traffic, and most negative at 14:00, at the dip between lunch time and afternoon rush hour traffic when photosynthetic uptake is high. Large downward fluxes at SL 4 were likely due to uptake by the golf course near this site.

NO_x fluxes were highest between 11:30-14:30. These hours correspond to the period of greatest heavy-duty diesel truck activity, a major source of NO_x emissions *(36)*. SL 10's fluxes had large fluctuations, possibly due to heavy diesel-powered truck traffic (> 100 trucks per day) in this industrial area and/or the proximity of a major interchange less than 200 m away. Fluxes at SL 10 represented a lower limit because recorded NO_x concentrations exceeded the analyzer's maximum of 5000 ppb for ~40 s during the day. The only loss process for NO_x is dry deposition, and, assuming a deposition velocity of 0.1 cm s^{-1} *(37)*, this flux would be 1.5×10^{-6} mg m^{-2} s^{-1} at most, orders of magnitude lower than observed values. $PM_{2.5}$ fluxes were largest between 8:30-9:30 and negative in the early afternoon. Peaks in the morning at SL 4 and 7 correlated with construction activity near SL 4 and delivery truck traffic associated with warehouses near SL 7.

4.0 Discussion

The predominantly positive CO_2, $PM_{2.5}$ and NO_x fluxes confirm that the Norfolk area is a net source of air pollutant emissions. CO_2 fluxes in Norfolk are similar to those measured in other urban areas using eddy covariance. For example, a study at a single site in Chicago measured fluxes of -0.7 to 1.7 mg m^{-2} s^{-1}, a range very similar to -0.9 to 1.8 mg m^{-2} s^{-1} in Norfolk; and the overall average CO_2 fluxes are exactly the same, 0.44 mg m^{-2} s^{-1} *(16)*. Average CO_2 fluxes in Mexico City of 0.41 mg m^{-2} s^{-1} are also similar *(18)*. A mobile eddy covariance system in Denmark measured positive-only CO_2 fluxes of 0.22 – 4.4 mg m^{-2} s^{-1} *(34)*, similar in magnitude to the range obtained in Norfolk.

The large spatial and diurnal variability in emissions over the 16 sampling locations, if we can assume that day-to-day differences were minor, presents a challenge for modeling air quality at high spatial resolution, i.e. grid cells of a few kilometers. Capturing fine spatial and temporal features in emissions will be needed in order to simulate atmospheric chemistry at the neighborhood scale. This level of accuracy could be important for reproducing nonlinearities in ozone sensitivity to precursors *(38)* and predicting individuals' exposure to air pollution.

Flux measurements during the field campaign are thought to represent mobile, area, and biogenic sources and not stationary point sources. Of the 55 point sources registered by the Virginia Department of Environmental Quality (VADEQ), only two fell within site footprints: Old Dominion University (ODU) near SL 1 and Military Circle Mall near SL 8. Neither the VADEQ listing nor field reconnaissance provided further information about the sources. The NO_x emissions from these sources amounted to 1.2% and 0.12% of the positive NO_x fluxes at the two sampling locations, if we multiply the measurements by an assumed footprint area of 3 km^2. The $PM_{2.5}$ emissions were reported to be zero. Therefore, the point sources should have very little effect on the overall flux measurements.

By comparing the measured fluxes with EPA's National Emission Inventory (NEI) as well as with a gridded inventory designed for air quality modeling, it is possible to validate the

inventory and/or to gain insight into its uncertainties. In order to approximate emissions more closely, this analysis focuses on only the positive fluxes. Because deposition may also be occurring when fluxes are positive, the measured values represent a lower bound on actual emissions.

Presently, the NEI does not include greenhouse gases, so we gathered estimates of CO_2 emissions from EPA's compilation of state greenhouse gas emission inventories. Virginia's inventory for the year 2005 reported total emissions of 181×10^6 metric tons of CO_2 equivalents *(39)*. Subtracting the 36% of emissions related to electricity generation (power plants whose emissions are not captured by the FLAME) and scaling by the fraction of Norfolk's population to the whole state's, 3%, we obtain a CO_2 emission rate of 4.0×10^5 kg hr^{-1} for the city, assuming that CO_2 dominates emissions of greenhouse gases. The Vulcan project *(40)*, a high resolution CO_2 inventory, reported total emissions of 3.3×10^5 kg hr^{-1}, or 1.4 kg hr^{-1} per person, for Norfolk. The average emissions measured by the FLAME, calculated by multiplying CO_2 fluxes (the average of positive ones only across all 16 sites) by the area of Norfolk (139 km^2) were 8×10^5 kg hr^{-1}, or 3.4 kg hr^{-1} per person, twice as high as in the inventory. If emissions during the 14 evening and nighttime hours not monitored during the field campaign were zero, in the most extreme case, the measured fluxes would produce an emission rate of 3.3×10^5 kg hr^{-1}. Within the precision and limitations of the eddy covariance method, the measurements of CO_2 fluxes agree well with inventories.

For NO_x and $PM_{2.5}$, we compared measured fluxes with the NEI for area and mobile source emissions for 2002, the most recent year for which estimates are available *(41)*. Biogenic emissions of these pollutants are negligible. Measured NO_x fluxes corresponded to an emission rate of 1,470 kg hr^{-1} as NO_2 over Norfolk, 27% lower than the NEI value of 2,026 kg hr^{-1}. If nighttime emissions were zero, then the measured fluxes would imply an emission rate of 613 kg hr^{-1} averaged over a full day. As with CO_2, measured fluxes corroborate the inventory within experimental uncertainties. Further searches for EPA-reported NO_x emissions for Norfolk revealed major inconsistencies in two separate reports published by EPA Region III *(42, 43)*. A report published in 1997 projects NO_x emissions from area and mobile sources in the Norfolk area to be 15 kg hr^{-1} in 2008, whereas a very similar report

from 2007 lists mobile and area source NO_x emissions of 4,000 kg hr^{-1}, 267 times higher. An error in units may have corrupted the earlier report, highlighting the need for extreme care in developing inventories.

For $PM_{2.5}$, measured emissions of 32 kg hr^{-1} are 3.5 times lower than the NEI value of 111 kg hr^{-1} or even lower if we scale our estimate downward and assume zero emissions at night. On average, deposition should account for downward fluxes of 1.5×10^{-6} mg m^{-2} s^{-1} (0.8 kg hr^{-1} over Norfolk) for NO_x and 7.7×10^{-6} mg m^{-2} s^{-1} (4 kg hr^{-1}) for $PM_{2.5}$. Adjusting the measured fluxes upward to account for deposition and the official inventory downward to account for trends in emissions between 2002 (year of the inventory) and 2008 (year of the field campaign) would bring the two estimates closer together but probably not enough to overcome a factor of >3.5 difference. These results support the suggestion that emissions of fugitive dust, which comprises nearly half of $PM_{2.5}$ in the NEI, are greatly overestimated *(1)*.

The final comparison is with an emission inventory for air quality modeling with 2002 as the base year. The inventory, developed using the Sparse Matrix Operator Kernel Emissions (SMOKE) modeling system, contains hourly emission rates of various criteria, particulate and toxic pollutants at 12-km resolution. The measurement sites selected in this field campaign were designed to cover a 12 km ×12 km square aligned with the SMOKE inventory's grid. Emission rates of NO_x and $PM_{2.5}$ in mol s^{-1} or g s^{-1} were extracted from the corresponding grid cell on Mondays through Thursdays between 7:00 – 17:00 in the month of June. Emission rates were then averaged over the 10-hr period and converted to kg hr^{-1}. Similarly, fluxes from the 16 sites were averaged and converted to kg hr^{-1} over the 144 km^2 square. Measured and modeled $PM_{2.5}$ emissions of 34 and 41 kg hr^{-1}, respectively, differ by only 18%. Modeled emissions of NO_x were 1,022 kg hr^{-1}, which is 51% lower than the measurement-based estimate of 1,542 kg hr^{-1}. In the inventory, hourly emissions of NO_x and $PM_{2.5}$ between 7:00 – 17:00 were 393 – 1,330 and 15 – 54 kg hr^{-1}, respectively, very similar to the measured hourly positive fluxes of 384 – 2,461 and 7 – 49 kg hr^{-1}. Mobile eddy covariance flux measurements can provide independent, measurement-based validation of emission inventories.

5.0 Acknowledgements

This research was supported by a National Science Foundation (NSF) CAREER award (CBET-0547107), NSF Research Experience for Undergraduates grant (CBET-0715162), and a Virginia Tech NSF Advance seed grant. We thank H. Rakha and the Virginia Tech Transportation Institute for use and maintenance of the van, the City of Norfolk and the Woolard family for support during the field campaign.

6.0 Supporting Information Available

Supporting information contains detailed descriptions of sample locations, quality control and post-processing of data, time series of pollutant concentrations and histograms of 30-min fluxes at all sites.

7.0 References

1. Simon, H.; Allen, D. T.; Wittig, A. E., Fine particulate matter emissions inventories: Comparison's of emissions estimates with observations from recent field programs. *J. Air Waste Manage.* **2008,** *58*, 320-343.
2. Buzcu-Guven, B.; Fraser, M. P., Comparison of VOC emissions inventory data with source apportionment results for Houston, TX. *Atmos. Environ.* **2008,** *42*, 5032-5043.
3. Cho, S.; Makar, P. A.; Lee, W. S.; Herage, T.; Liggio, J.; Li, S. M.; Wiens, B.; Graham, L., Evaluation of a unified regional air-quality modeling system (AURAMS) using PrAIRie2005 field study data: The effects of emissions data accuracy on particle sulphate predictions. *Atmos. Environ.* **2009,** *43*, 1864-1877.
4. Fu, J. S.; Streets, D. G.; Jang, C. J.; Hao, J. M.; He, K. B.; Wang, L. T.; Zhang, Q., Modeling Regional/Urban Ozone and Particulate Matter in Beijing, China. *J. Air Waste Manage.* **2009,** *59*, 37-44.
5. Ying, Q.; Lu, J.; Allen, P.; Livingstone, P.; Kaduwela, A.; Kleeman, M., Modeling air quality during the California Regional PM10/PM2.5 Air Quality Study (CRPAQS) using the UCD/CIT source-oriented air quality model - Part I. Base case model results. *Atmos. Environ.* **2008,** *42*, 8954-8966.
6. Ying, Q.; Lu, J.; Kaduwela, A.; Kleeman, M., Modeling air quality during the California Regional PM10/PM2.5 Air Quality Study (CPRAQS) using the UCD/CIT Source Oriented Air Quality Model - Part II. Regional source apportionment of primary airborne particulate matter. *Atmos. Environ.* **2008,** *42*, 8967-8978.
7. Xiao, Y. P.; Logan, J. A.; Jacob, D. J.; Hudman, R. C.; Yantosca, R.; Blake, D. R., Global budget of ethane and regional constraints on US sources. *J. Geophys. Res.-Atmos.* **2008,** *113*, D21306.
8. Boersma, K. F.; Jacob, D. J.; Bucsela, E. J.; Perring, A. E.; Dirksen, R.; van der A, R. J.; Yantosca, R. M.; Park, R. J.; Wenig, M. O.; Bertram, T. H.; Cohen, R. C., Validation of OMI

tropospheric NO_2 observations during INTEX-B and application to constrain NO_x emissions over the eastern United States and Mexico. *Atmos. Environ.* **2008,** *42*, 4480-4497.
9. Han, K. M.; Song, C. H.; Ahn, H. J.; Park, R. S.; Woo, J. H.; Lee, C. K.; Richter, A.; Burrows, J. P.; Kim, J. Y.; Hong, J. H., Investigation of NO_x emissions and NO_x- related chemistry in East Asia using CMAQ-predicted and GOME-derived NO_2 columns. *Atmos. Chem. Phys.* **2009,** *9*, 1017-1036.
10. Zhao, T. X. P.; Loeb, N.; Laszlo, I.; Zhou, M. In *Study of Global Component Aerosol Direct Radiative Effect by Combining Satellite Measurement and Model Simulations*, International Radiation Symposium (IRC/IAMAS), Foz do Iguacu, BRAZIL, Aug 03-08, 2008; Nakajima, T.; Yamasoe, M. A., Eds. Foz do Iguacu, BRAZIL, 2008; pp 601-604.
11. Warneke, C.; McKeen, S. A.; de Gouw, J. A.; Goldan, P. D.; Kuster, W. C.; Holloway, J. S.; Williams, E. J.; Lerner, B. M.; Parrish, D. D.; Trainer, M.; Fehsenfeld, F. C.; Kato, S.; Atlas, E. L.; Baker, A.; Blake, D. R., Determination of urban volatile organic compound emission ratios and comparison with an emissions database. *J. Geophys. Res.-Atmos.* **2007,** *112*, D10S47
12. Ban-Weiss, G. A.; McLaughlin, J. P.; Harley, R. A.; Lunden, M. M.; Kirchstetter, T. W.; Kean, A. J.; Strawa, A. W.; Stevenson, E. D.; Kendall, G. R., Long-term changes in emissions of nitrogen oxides and particulate matter from on-road gasoline and diesel vehicles. *Atmos. Environ.* **2008,** *42*, 220-232.
13. Kopacz, M.; Jacob, D. J.; Henze, D. K.; Heald, C. L.; Streets, D. G.; Zhang, Q., Comparison of adjoint and analytical Bayesian inversion methods for constraining Asian sources of carbon monoxide using satellite (MOPITT) measurements of CO columns. *J. Geophys. Res.-Atmos.* **2009,** *114*, D04305.
14. Kurokawa, J.; Yumimoto, K.; Uno, I.; Ohara, T., Adjoint inverse modeling of NO_x emissions over eastern China using satellite observations of NO_2 vertical column densities. *Atmos. Environ.* **2009,** *43*, 1878-1887.
15. Moore, T. O.; Doughty, D. C.; Marr, L. C., Demonstration of a mobile Flux Laboratory for the Atmospheric Measurement of Emissions (FLAME) to assess emissions inventories. *J. Environ. Monitor.* **2009,** *11*, 259-268.
16. Grimmond, C. S. B.; King, T. S.; Cropley, F. D.; Nowak, D. J.; Souch, C., Local-scale fluxes of carbon dioxide in urban environments: Methodological challenges and results from Chicago. *Environ. Pollut.* **2002,** *116*, 243-254.
17. Nemitz, E.; Hargreaves, K. J.; McDonald, A. G.; Dorsey, J. R.; Fowler, D., Meteorological measurements of the urban heat budget and CO_2 emissions on a city scale. *Environ. Sci. Technol.* **2002,** *36*, 3139-3146.
18. Velasco, E.; Pressley, S.; Allwine, E.; Westberg, H.; Lamb, B., Measurements of CO_2 fluxes from the Mexico City urban landscape. *Atmos. Environ.* **2005,** *39*, 7433-7446.
19. Schmid, H. P. Flux Source Area Model - FSAM. http://www.indiana.edu/~climate/SAM/SAM_FSAM.html
20. Aubinet, M.; Grelle, A.; Ibrom, A.; Rannik, U.; Moncrieff, J.; Foken, T.; Kowalski, A. S.; Martin, P. H.; Berbigier, P.; Bernhofer, C.; Clement, R.; Elbers, J.; Granier, A.; Grunwald, T.; Morgenstern, K.; Pilegaard, K.; Rebmann, C.; Snijders, W.; Valentini, R.; Vesala, T., Estimates of the annual net carbon and water exchange of forests: The EUROFLUX methodology. *Adv Ecol Res* **2000,** *30*, 113-175.
21. Baldocchi, D. D., Assessing the eddy covariance technique for evaluating carbon dioxide exchange rates of ecosystems: past, present and future. *Glob. Change Biol.* **2003,** *9*, 479-492.

22. Massman, W. J.; Lee, X., Eddy covariance flux corrections and uncertainties in long-term studies of carbon and energy exchanges. *Agric. For. Meteorol.* **2002,** *113*, 121-144.
23. Loescher, H. W.; Law, B. E.; Mahrt, L.; Hollinger, D. Y.; Campbell, J.; Wofsy, S. C., Uncertainties in, and interpretation of, carbon flux estimates using the eddy covariance technique. *J. Geophys. Res.-Atmos.* **2006,** *111*, D21S90.
24. Hollinger, D. Y.; Richardson, A. D., Uncertainty in eddy covariance measurements and its application to physiological models. *Tree Physiol.* **2005,** *25*, 873-885.
25. Vickers, D.; Mahrt, L., Quality control and flux sampling problems for tower and aircraft data. *Journal of Atmospheric and Oceanic Technology* **1997,** *14*, 512-526.
26. Kruijt, B.; Elbers, J. A.; von Randow, C.; Araujo, A. C.; Oliveira, P. J.; Culf, A.; Manzi, A. O.; Nobre, A. D.; Kabat, P.; Moors, E. J., The robustness of eddy correlation fluxes for Amazon rain forest conditions. *Ecol. Appl.* **2004,** *14*, S101-S113.
27. Foken, T.; Wichura, B., Tools for quality assessment of surface-based flux measurements. *Agric. For. Meteorol.* **1996,** *78*, 83-105.
28. Lenschow, D. H.; Mann, J.; Kristensen, L., How Long is Long Enough When Measuring Fluxes and Other Turbulence Statistics. *J. Atmos. Ocean Tech.* **1994,** *11*, 661-673.
29. Balling, R. C.; Cerveny, R. S.; Idso, C. D., Does the urban CO_2 dome of Phoenix, Arizona contribute to its heat island? *Geophys. Res. Lett.* **2001,** *28*, 4599-4601.
30. Idso, C. D.; Idso, S. B.; Balling, R. C., An intensive two-week study of an urban CO_2 dome in Phoenix, Arizona, USA. *Atmos. Environ.* **2001,** *35*, 995-1000.
31. Martensson, E. M.; Nilsson, E. D.; Buzorius, G.; Johansson, C., Eddy covariance measurements and parameterisation of traffic related particle emissions in an urban environment. *Atmos. Chem. Phys.* **2006,** *6*, 769-785.
32. Grimmond, C. S. B.; Salmond, J. A.; Oke, T. R.; Offerle, B.; Lemonsu, A., Flux and turbulence measurements at a densely built-up site in Marseille: Heat, mass (water and carbon dioxide), and momentum. *J. Geophys. Res.-Atmos.* **2004,** *109*, D24101.
33. Guldmann, J. M.; Kim, H. Y., Modeling air quality in urban areas: A cell-based statistical approach. *Geogr. Anal.* **2001,** *33*, 156-180.
34. Soegaard, H.; Moller-Jensen, L., Towards a spatial CO_2 budget of a metropolitan region based on textural image classification and flux measurements. *Remote Sens. Environ.* **2003,** *87*, 283-294.
35. Weng, Q. H.; Yang, S. H., Urban air pollution patterns, land use, and thermal landscape: An examination of the linkage using GIS. *Environ. Monit. Assess.* **2006,** *117*, 463-489.
36. Marr, L. C.; Black, D. R.; Harley, R. A., Formation of photochemical air pollution in central California - 1. Development of a revised motor vehicle emission inventory. *J. Geophys. Res.-Atmos.* **2002,** *107*, 4048.
37. Seinfeld, J. H.; Pandis, S. N., *Atmospheric Chemistry and Physics - From Air Pollution to Climate Change*. Second ed.; John Wiley & Sons, Inc.: Hoboken, New Jersey, 2006
38. Cohan, D. S.; Hu, Y. T.; Russell, A. G., Dependence of ozone sensitivity analysis on grid resolution. *Atmos. Environ.* **2006,** *40*, 126-135.
39. VADEQ Greenhouse Gas Emission Inventory for Virginia. http://www.deq.virginia.gov/export/sites/default/info/documents/Climate.Ballou.GHGInventory.5.pdf
40. Gurney, K. R.; Mendoza, D.; Zhou, Y.; Seib, B.; Fischer, M.; Can, S.; Geethakumar, S.; Miller, C. The Vulcan Project: High Resolution Fossil Fuel Combustion CO_2 Emissions fluxes for the United States. http://www.purdue.edu/eas/carbon/vulcan/research.html

41. USEPA AirData. http://www.epa.gov/air/data/geosel.html
42. Caprio, A. *Maintenance Plan for the Norfolk-Virginia Beach-Newport News (Hampton Roads), Virginia 8-Hour Ozone Area*; Environmental Protection Agency: Norfolk, Virginia, 2007.
43. Lewis, J. *Maintenance Plan for the Hampton Roads, Virginia Ozone Area*; Environmental Protection Agency: Philadelphia, Pennsylvania, 1997.

8.0 Supporting Information

8.1 Sample Location Descriptions

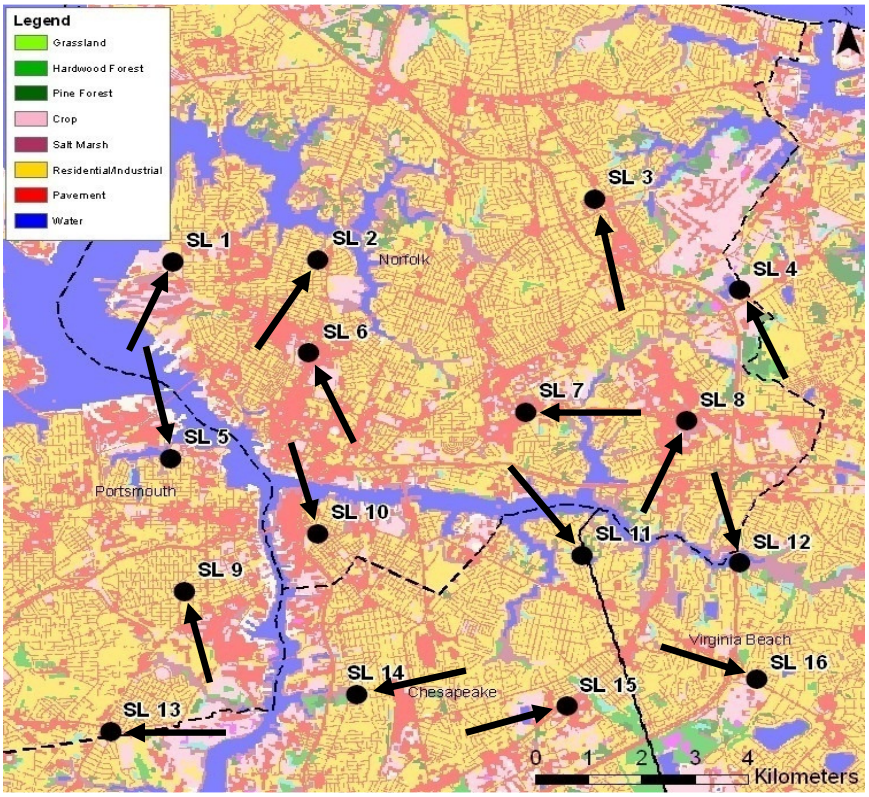

Figure 16. Sampling locations (SL) and land use. City boundaries are outlined, and arrows show the predominant wind direction and approximate footprint length at each site.

8.1.1 Sample Location 1

SL 1 was located within the parking lot of Lambert's Point Golf Course just southwest of Old Dominion University on the corner of West 43rd Street and Powhatan Avenue. Winds were predominantly westerly and southerly. This site was located ~0.2 km northeast of a Norfolk Southern railyard terminal and 0.1 km from the Hampton Roads Sanitation District's Powhatan Avenue Sewage Treatment Plant. Vehicle activity at this location was busy at most

times during the day due to traffic in and out of the treatment plant and a nearby school.

8.1.2 Sample Location 2

SL 2 was a public boat ramp near the intersection of Llewellyn Avenue and Delaware Avenue. Winds were predominantly southwesterly. Other than a few local shops and fast food restaurants, this location was mostly residential. Traffic was mostly steady with heavier volumes during the morning, lunchtime, and evening rush hours.

8.1.3 Sample Location 3

SL 3 was in a shopping center parking lot at the intersection of Norview Avenue and North Military Highway. Winds were predominantly easterly, ranging from northeasterly to southeasterly. A strip mall with various boutiques and fast food restaurants was located ~0.1 km east of the sample location, and gas stations were located 0.15 and 2.0 km to the southeast. Although high in residential density, this area can also be considered very commercial due to its proximity to both the Norfolk International Airport (1.8 km to the east) and Interstate 64 (I-64) (0.7 km to the west). Many hotels, corporations and commercial businesses front Military Highway, and traffic in this location was steady at all hours.

8.1.4 Sample Location 4

SL 4 was located in a motel parking lot on Northampton Boulevard. Winds were predominantly easterly, ranging from northeasterly to southeasterly. I-64 was located ~0.5 km to the southwest of the FLAME. A private school, Norfolk Academy was located 0.6 km directly south of the measurement location. Directly east of the FLAME was the Lake Wright Golf Course. A dense commercial district with gas stations, restaurants and shopping was located 0.9 km to the northeast. Also, the airport was located ~0.75 km to the north. To the south and southeast of the FLAME was dense housing, making this a mixed zoning area.

8.1.5 Sample Location 5

SL 5 was located in the parking lot of the Portsmouth Boat Club at 20 Elm Avenue in Portsmouth. Winds were predominantly northerly, ranging from northwesterly to northeasterly. The Portsmouth Naval Hospital Facility was located ~0.7 km east of the

sample location. Also, located 0.4 km to the northwest was a Virginia Port Authority container shipping facility, where heavy equipment and tug boat operations were taking place. A barge/container painting operation was also to the northwest. A dense, older low income residential neighborhood was located ~0.1 km south of the FLAME, and a new school was being constructed ~0.3 km to the southwest. Zoning for this area appeared mostly residential; however, the area northeast of the site was highly industrial.

8.1.6 Sample Location 6

SL 6 was located on the northeast corner of the intersection of 19th Street and Granby Street in the southwest corner of the Doumar's Barbecue parking lot. Winds were multi-directional, varying between easterly, northeasterly, southerly, and southwesterly. Ghent Elementary and Maury High School were located ~0.4 km to the southwest of the sample location. This particular location consisted mainly of commercial businesses such as restaurants, shops and boutiques. It was also 1.5 km north of the Norfolk City Center and 2 km north of the Norfolk Harbor. This area contains much shopping and is the center of tourist activity in Norfolk. Also, a large cemetery was located 0.5 km to the southeast of the site. Dense commercial areas were located to the northwest, and the older, densely populated upscale neighborhood of Ghent was located to the west. Traffic in this location was steady throughout the day; however, due to all of the restaurants and businesses located in the area, lunchtime traffic was very heavy.

8.1.7 Sample Location 7

SL 7 was located in the parking lot of a packaging company on the northeast corner of the intersection of East Virginia Beach Boulevard and Ingleside Road. Winds were typically easterly. This area was a mix of warehouse and residential buildings. Ingleside Elementary was located ~0.1 km to the south, and Interstate 264 (I-264) was ~1 km to the south. Traffic at this location was light in comparison to other sample locations, but typical rush-hour traffic patterns were observed, and diesel traffic appeared quite a bit heavier in this region simply because of the number of warehouses.

8.1.8 Sample Location 8

SL 8 was located at the intersection of North Military Highway and East Virginia Beach Boulevard in the northern portion of the Military Circle Mall parking lot. Winds in this location were southerly and southwesterly, and traffic in this area was steady throughout the day. This area was considered commercial, with some densely populated residential neighborhoods 0.6 km east and 0.7 km south of the sample location. Traffic was especially heavy during the lunch hour and after 5:00 PM. The junction of I-64 and I-264 was located ~1.3 km southeast of the sample location, and this junction is known to accommodate heavy traffic during rush hours. A relatively large amount of diesel traffic was present in this area due to its proximity to the warehouse district, as well as the high number of commercial businesses in the area.

8.1.9 Sample Location 9

SL 9 was located in the southwest corner of the Jefferson Street Public Park at the intersection of Jefferson Street and Pearl Street in Portsmouth. Winds were southeasterly and southerly at this location. The area is considered “middle income residential” according to city zoning. Brighton Elementary is located ~0.25 km south of the sample location, and a large port shipping operation and commercial area is located ~1.1 km southeast of the sample location. This location is 0.8 km south of I-264, and traffic in this area tends to be heavy due to the numerous industrial and commercial port operations occurring in this area.

8.1.10 Sample Location 10

SL 10 was located at the intersection of East Berkley Avenue and South Main Street. The FLAME was parked at the southeast corner of this intersection, in the northwest corner of the Farm Fresh parking lot. Winds in this location were northerly, ranging between northwesterly and northeasterly. This sample location was located 0.5 km southeast of the intersection of a number of major highways in this area, including I-264, I-464, Highway 337 and Highway 460. This location was close to downtown, and 0.7 km northwest of the sample location was a large port authority shipping operation with ongoing construction at the time. Also, ~0.6 km north of the site was an industrial ship painting facility, a dredging operation

and a number of other industrial port operations. A fuel storage facility was located 0.95 km east of the FLAME. This area is zoned as industrial and residential with a few commercial facilities such as strip shopping malls. Traffic in this location was typically very heavy due to the proximity of downtown Norfolk and the industry located nearby; the fraction of diesel-powered traffic was especially high in this area. The residential area 0.1 km to the north of this location appeared to be low income housing.

8.1.11 Sample Location 11

SL 11 was located in the northern area of the Elizabeth River Baptist Church parking lot at the intersection of Little Beaver Road and Sparrow Road in Chesapeake. Wind direction was variable, ranging between west, north, and east. This area was mostly residential, and traffic was light. This location was adjacent to a pungent smelling pond which was densely covered with algae. Also located <0.8 km to the east, west and north, was a major recreational waterway with a large amount of boating traffic.

8.1.12 Sample Location 12

SL 12 was located at the end of a residential cul-de-sac on Lancelot Drive in Chesapeake. Winds were predominantly easterly. Residential traffic was very light, but the FLAME was located <0.1 km east of I-64, which carried traffic at all times during the day. The area was densely residential with very little commercial zoning nearby, and the FLAME was parked ~0.25 km south of a major recreational waterway, similar to SL 11. Boating traffic here was also heavy.

8.1.13 Sample Location 13

SL 13 was located on the southeast corner of the intersection of Victory Boulevard and George Washington Highway in Portsmouth. Winds were predominantly easterly. This area is zoned as residential, with some commercial strip shopping as well as local fast food restaurants. The Portsmouth Naval Shipyard was located ~2.1 km east of the FLAME. Traffic in this area was steady throughout the day but was particularly heavy during typical rush-hour times due to the proximity of the Naval Shipyard. Diesel-powered vehicle traffic was also high in this area along Victory Boulevard traveling both to and from the Naval

Shipyard.

8.1.14 Sample Location 14

SL 14 was located in an abandoned parking lot off of Bainbridge Boulevard in Chesapeake. Winds were predominantly easterly, southeasterly and southerly. The area was mostly residential with a small amount of commercial businesses such as restaurants and retail. There was no substantial industrial activity in the area, and traffic was light. I-464 was located 0.46 km west of the sample location, and Oscar Smith Middle School as well as a new high school which was under construction, were adjacent to the east. A Norfolk Southern Railyard Facility was located 0.65 km to the east.

8.1.15 Sample Location 15

SL 15 was located in the northern corner of a McDonald's parking lot at the intersection of South Military Highway and Smith Avenue in Chesapeake. Winds were southwesterly at this location. This area was mostly commercial with car dealerships, fast food restaurants and warehouses lining Military Highway and surrounding streets. A large residential area was located 0.15 km north of the site. Traffic in this area was steady throughout the day, with greater activity during the early morning and late afternoon hours to and from the nearby naval base.

8.1.16 Sample Location 16

SL 16 was located at the University Shoppes center at the intersection of Strickland Boulevard and Indian River Road. Winds were predominantly northerly and northeasterly in this location. Regent University was located 0.25 km southwest of the sample location, and most of the area is zoned as residential. The site was ~0.5 km southeast of the I-64 and Indian River interchange. Traffic on these routes was heavy during rush hours. Other nearby features included a fuel station, restaurants and strip malls within 0.1 km. Local construction was occurring in the neighborhood to the north of the sample location, and diesel traffic as well as increased levels of traffic in and out of the neighborhood was thought to be associated with this activity.

8.2 Quality Control and Post Processing of Data

During the field campaign, we collected data for 10 hr on each of 16 days, Mondays through Thursdays for four weeks between 2-26 June 2008. A data acquisition system consisting of a logger and program developed in LabView 8.0 saved CO_2, H_2O vapor, $PM_{2.5}$, NO_x, CO, wind velocity (u, v and w), and temperature (T) at 10 Hz to plain text files in 30-min increments. Each 30-min data set consisted of ~18,000 data points. Quality assurance and control measures included calibration of all analyzers before and during the field campaign and testing for sampling line losses. Losses of CO_2 and NO_x were 0.52% and 0.57% respectively, and water vapor losses were eclipsed by humidity variations in the atmosphere during the test periods. There was a slight loss in $PM_{2.5}$ (8% ± 5%). The results have not been corrected for line losses, as they fall within the uncertainties of the eddy covariance method. Also, gravimetric filter samples of $PM_{2.5}$ were collected during the field campaign for calibration of the DustTrak, an aerosol photometer whose response is dependent on particles' optical properties. The DustTrak's average concentrations were 11±0.3% higher than the filter-based ones, and because filters may also be subject to sampling artifacts, we have elected to report the factory-calibrated DustTrak $PM_{2.5}$ values rather than correct them to match the filters.

Standard post-processing of the measurements included hard spike removal, soft spike removal, lag correction, coordinate rotation by the planar fit method, linear detrending, calculation of fluxes and quality assurance of the calculated fluxes through spectral and co-spectral analyses and stationarity testing *(1-3)*. Figure 17 shows spectra of NO_x, CO_2 and $PM_{2.5}$ and co-spectra of w with NO_x, CO_2 and $PM_{2.5}$ from a randomly selected period (SL3 7:15-7:45). Slopes of -2/3 and -4/3 of spectral and co-spectral plots, respectively, conform to previously published results *(3-5)*. Figure 18 shows the percent difference between 30-min and 5-min fluxes, an indicator of stationarity. Differences were well below the stationarity criterium of 60%, and all stationarity indices were between -1 and 1 *(1, 3, 5)*.

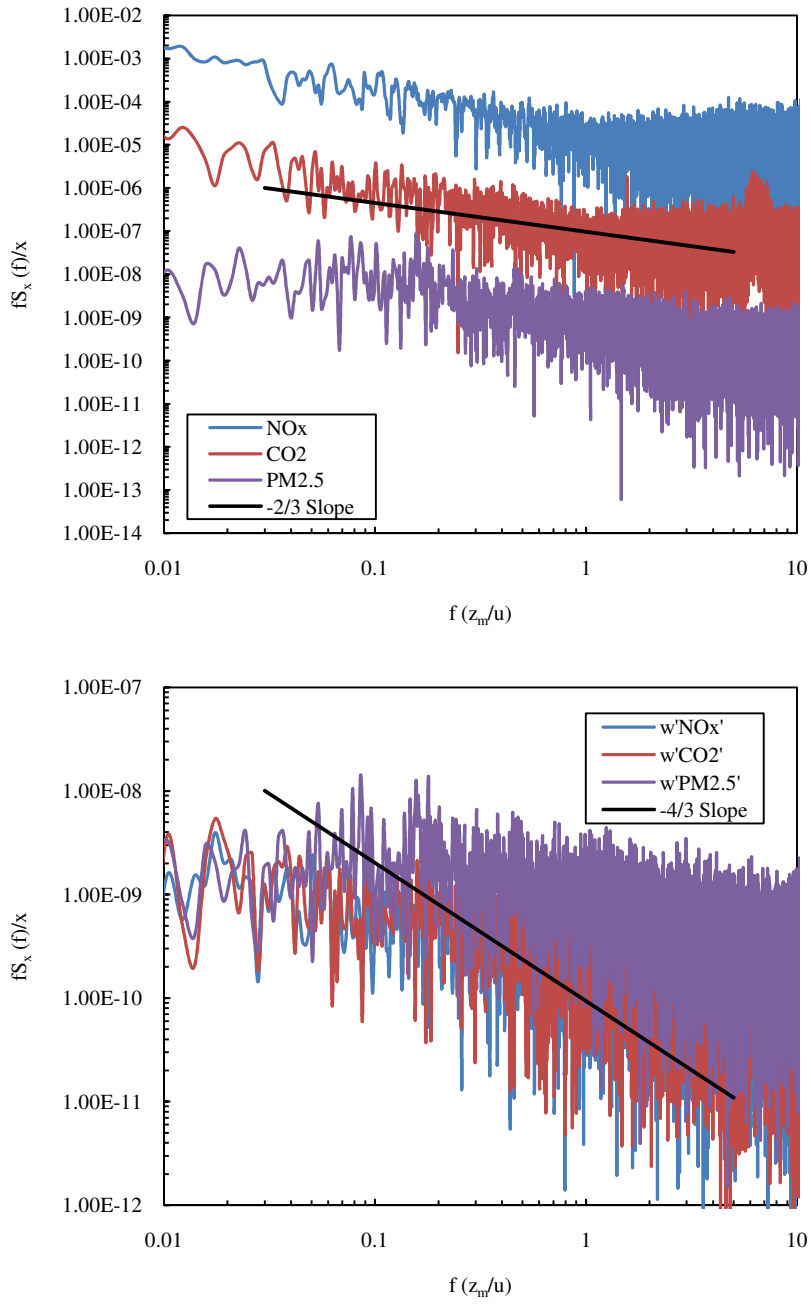

Figure 17. Spectral (top) and co-spectral (bottom) graphs from SL 3. Lines with -2/3 and -4/3 slopes show theoretically expected values.

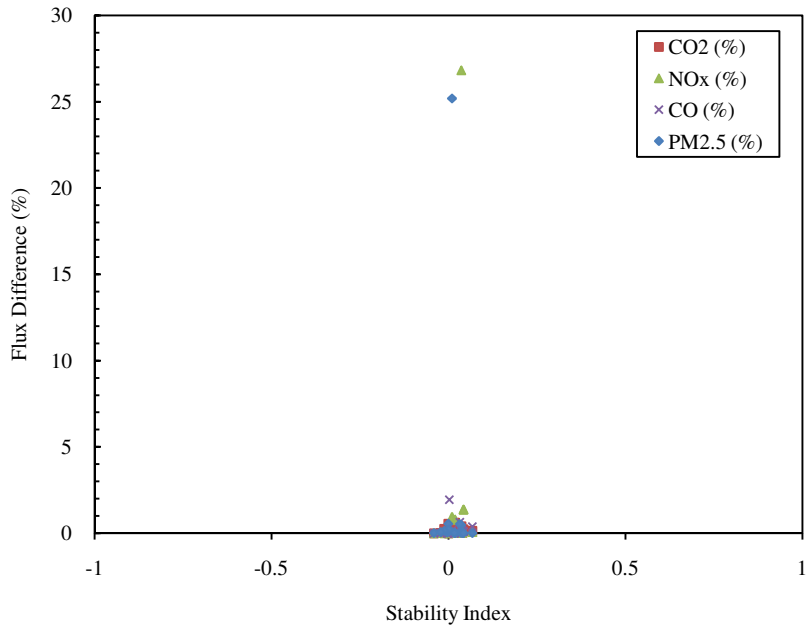

Figure 18. Stationarity test from SL 3 showing differences between 30-min and 5-min fluxes.

8.3 Campaign Concentrations

As shown in Figure 19, daytime CO_2 concentrations averaged over all 16 sites ranged between 500 and 560 ppm and were lowest at 7:30 and after 16:00. Time series from SL 4, 7, 10 and 12 are shown separately to illustrate the diversity of concentrations measured at individual sites; these were among the dirtiest. Concentrations at these four sites ranged between 400 and 750 ppm. These sites were located near busy intersections or interstates, so vehicle activity was the likely source of elevated levels of CO_2.

In similar format, Figure 20 shows that average NO_x concentrations across all sites ranged between 20 and 120 ppb, while individual concentrations at the four chosen sites ranged between 10 and 190. Site-averaged concentrations were highest at the beginning of the day, 7:30 and had a later peak at 15:00. A clear diurnal pattern is visible at SL 10 and 12 with higher concentrations at 7:30, 12:00 and 16:00. These temporal patterns are indicative of rush-hour traffic. Diesel-powered vehicle traffic was influential at these sites.

Figure 21 shows that site-averaged CO concentrations ranged between 0.3 and 0.8 ppm, and

those at the individual sites in the figure ranged between 0.2 and 2.7 ppm. Many of the largest spikes occurred in areas of heavy traffic, and some corresponded with isolated occurrences of smoke drifting through the area from fires in eastern North Carolina. CO concentrations were highest in the morning and then leveled off at ~0.4 ppm for the remainder of the day.

Figure 22 shows $PM_{2.5}$ concentrations observed during the campaign. SL 4, 7, 10 and 12 had some of the highest levels of $PM_{2.5}$. A site-averaged diurnal pattern in $PM_{2.5}$ was not evident, but large spikes in the morning at some of the sites were associated with smoke from brush and forest fires mentioned previously. In particular, smoke was visible at SL 4, 7 and 12 at 9:00 and at SL 10 during the early morning hours. These were the only occurrences of observed smoke during the campaign and should not have affected vertical fluxes because the smoke was already vertically well-mixed by the time it reached Norfolk.

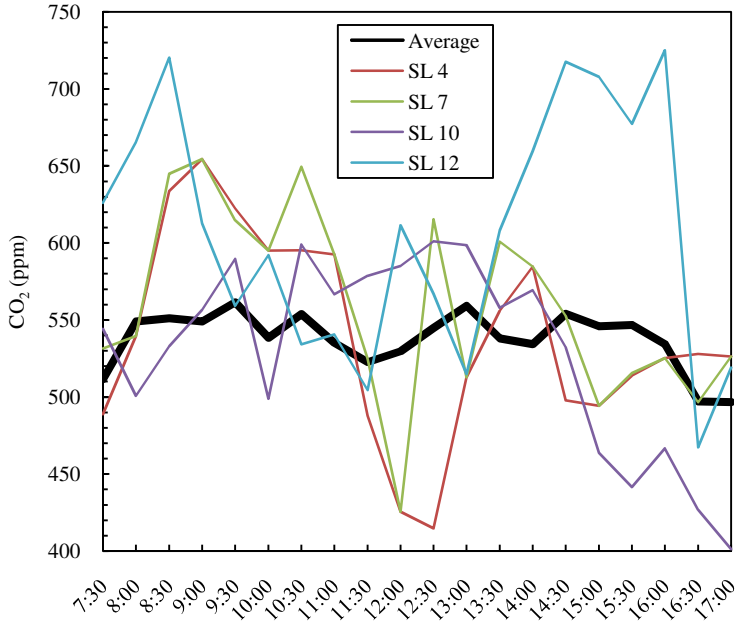

Figure 19. Daytime CO_2 concentrations averaged across all sites and at SL 4, 7, 10 and 12.

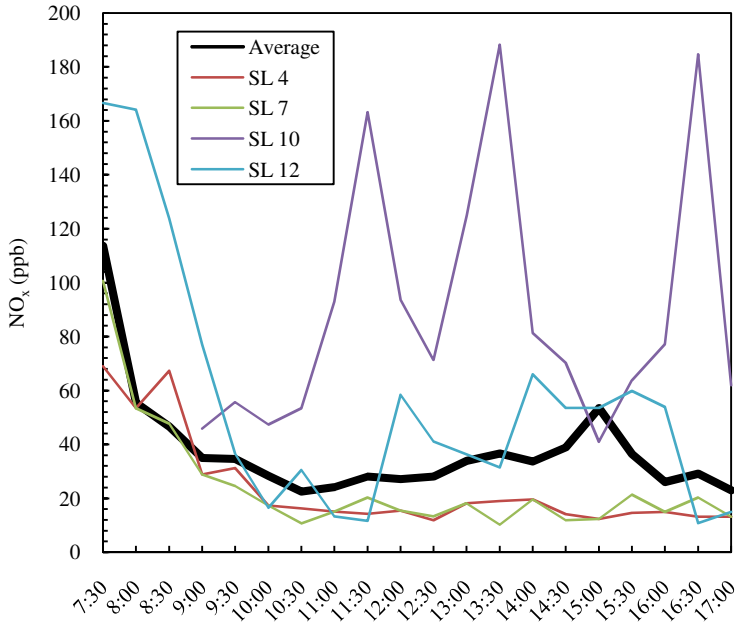

Figure 20. Daytime NO_x concentrations averaged across all sites and at SL 4, 7, 10 and 12.

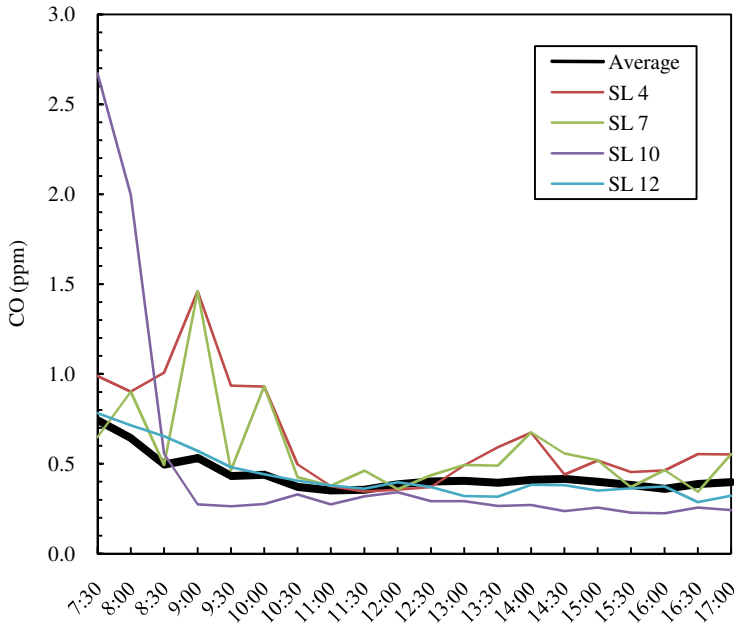

Figure 21. Daytime CO concentrations averaged across all sites and at SL 4, 7, 10 and 12.

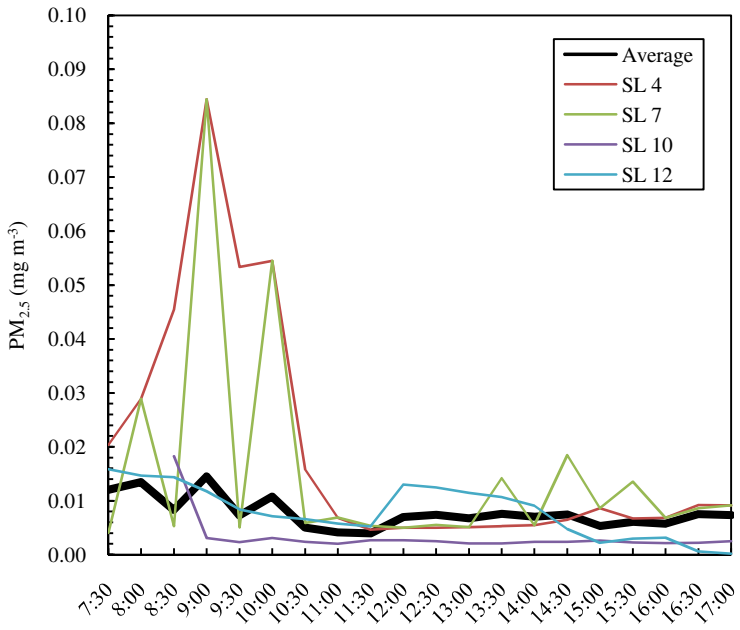

Figure 22. Daytime $PM_{2.5}$ concentrations averaged across all sites and at SL 4, 7, 10 and 12.

8.4 Campaign Fluxes (Additional Information)

Histograms of 30-min fluxes by site, shown in Figures 23, 24 and 25, reveal which sites contributed most to positive or negative fluxes. Sixty percent of the fluxes were positive. SL 6 and 8 accounted for approximately 21% of the CO_2 fluxes above 1 mg m^{-2} s^{-1}. These two sites were near popular shopping areas that had steady vehicle traffic throughout the day. For NO_x, SL 6, 11 and 13 accounted for more than 36% of NO_x fluxes above 0.01 mg m^{-2} s^{-1}, and 80% of the measured NO_x fluxes were positive. SL 11 was located within a residential neighborhood and adjacent to a major recreational waterway with boating traffic. SL 13 was adjacent to the Naval Shipyard, which experienced diesel-powered delivery truck traffic and rush-hour traffic throughout the day. SL10, which was located adjacent to shipyard industrial production facilities was especially dominant above 0.01 to 0.05 mg m^{-2} s^{-1}, accounting for more than 37% of measured fluxes within this range. Finally, $PM_{2.5}$ fluxes were 65% positive with SL 5, 6 and 16 accounting for more than 30% of fluxes ranging between 2×10^{-5} and 2×10^{-4} mg m^{-2} s^{-1}. Also, SL 4 accounted for more than 37% of positive fluxes above 2×10^{-3} mg m^{-3}. SL 5 was located within the parking lot of a boating club which experienced a consistent boating traffic, and SL 16 was at the intersection of a major I-64 interchange. At SL 4, samples were taken adjacent to a golf course, which was undergoing construction during the day.

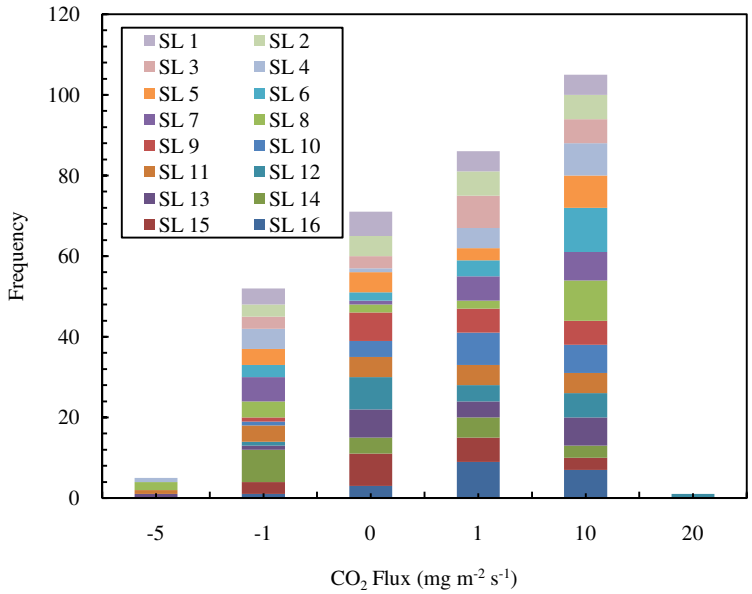

Figure 23. Histogram of 30-min CO_2 fluxes at all sites. Values on the x-axis are the upper limits of the bins.

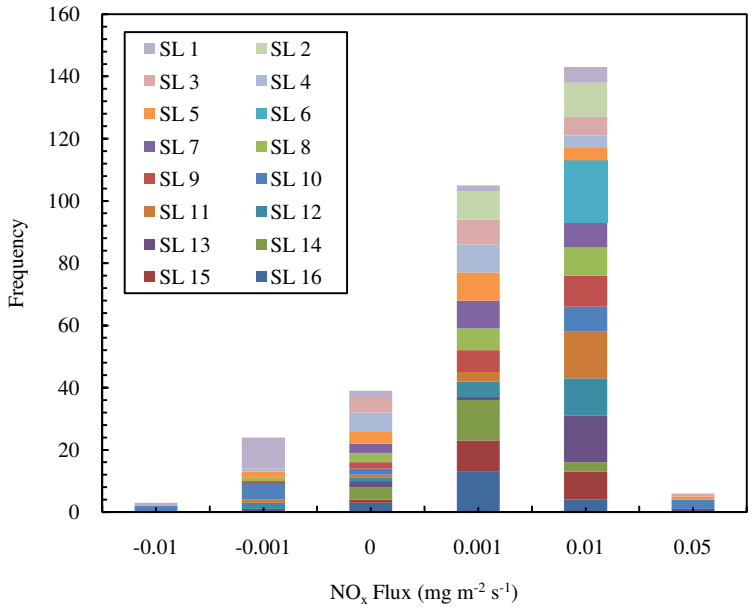

Figure 24. Histogram of 30-min NO_x fluxes at all sites. Values on the x-axis are the upper limits of the bins.

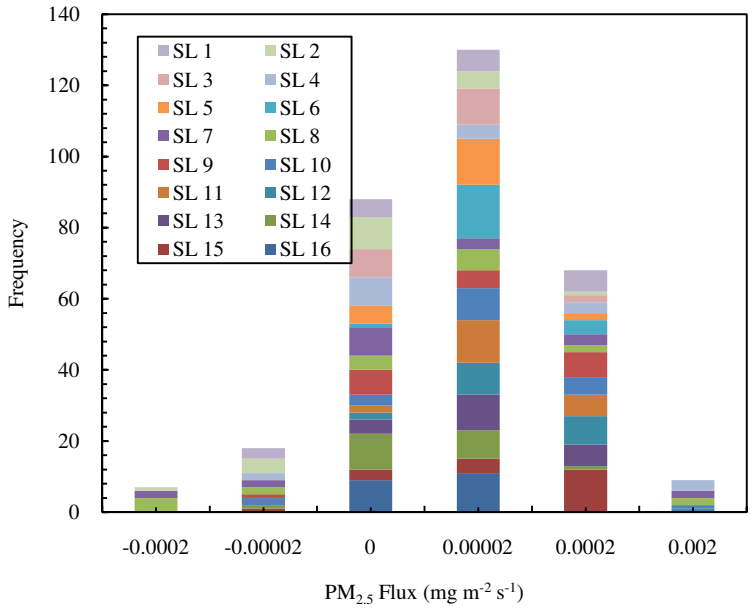

Figure 25. Histogram of 30-min $PM_{2.5}$ fluxes at all sites. Values on the x-axis are upper limits of the bins.

8.5 Supporting Information References

1. Aubinet, M.; Grelle, A.; Ibrom, A.; Rannik, U.; Moncrieff, J.; Foken, T.; Kowalski, A. S.; Martin, P. H.; Berbigier, P.; Bernhofer, C.; Clement, R.; Elbers, J.; Granier, A.; Grunwald, T.; Morgenstern, K.; Pilegaard, K.; Rebmann, C.; Snijders, W.; Valentini, R.; Vesala, T., Estimates of the annual net carbon and water exchange of forests: The EUROFLUX methodology. In *Advances in Ecological Research, Vol 30*, 2000; Vol. 30, pp 113-175.
2. Grimmond, C. S. B.; King, T. S.; Cropley, F. D.; Nowak, D. J.; Souch, C., Local-scale fluxes of carbon dioxide in urban environments: Methodological challenges and results from Chicago. *Environ. Pollut.* **2002,** *116*, 243-254.
3. Velasco, E.; Pressley, S.; Allwine, E.; Westberg, H.; Lamb, B., Measurements of CO2 fluxes from the Mexico City urban landscape. *Atmos. Environ.* **2005,** *39*, 7433-7446.
4. Martensson, E. M.; Nilsson, E. D.; Buzorius, G.; Johansson, C., Eddy covariance measurements and parameterisation of traffic related particle emissions in an urban environment. *Atmos. Chem. Phys.* **2006,** *6*, 769-785.
5. Vickers, D.; Mahrt, L., Quality control and flux sampling problems for tower and aircraft data. *J. Atmos. Ocean. Tech.* **1997,** *14*, 512-526.

Chapter 4: Eddy-Covariance Measurement of VOC, CO_2, NO_x and $PM_{2.5}$ Emissions and Exposure Levels Near Schools

Abstract

Eddy covariance flux measurements of volatile organic compounds (VOCs), carbon dioxide (CO_2), nitrogen oxides (NO_x) and fine particulate matter ($PM_{2.5}$) were conducted near seven schools in Roanoke, Virginia, to describe quantitatively the air quality experienced by children and nearby air pollutant emissions. Daytime average VOC fluxes of 2,2,4-trimethylpentane, toluene, ethylbenzene, xylenes (m-, o- and p-) and styrene ranged between 8.9×10^{-5} and 1.4×10^{-3} mg m^{-2} s^{-1}. Among the species measured, emissions of toluene were highest and those of styrene were lowest. The correlation in time between spikes in fluxes and school bus activity suggests that idling buses are a large source of emissions of air toxics. Positive (upward) fluxes, which define a lower bound on emissions, for CO_2, NO_x and $PM_{2.5}$ across the three sites ranged between 1.3-1.4, 1.5×10^{-3}-1.8×10^{-3} and 0.82×10^{-3}-1.0×10^{-3} mg m^{-2} s^{-1}, respectively. If we assume that these fluxes were representative of the city as a whole, then the positive fluxes would translate to daytime emission rates of 275, 474, 88, 147 and 39 kg hr^{-1} for 2,2,4-trimethylpentane, toluene, ethylbenzene, xylenes (m-, o- and p-), and styrene, respectively, which was between 5 and 17 times higher than reported by the Environmental Protection Agency (EPA). The large differences between VOC fluxes measured at schools in this study and emissions predicted by EPA suggest that schools are "hot spots" for air toxic emissions or that the official inventory for Roanoke may be underestimated.

1.0 Introduction

Most children spend about half of their waking hours at school, so there is considerable concern about schools' air quality and its effects on health. To date, many studies have quantified the exposure of children at schools to pollutants such as carbon monoxide (CO), carbon dioxide (CO_2), nitrogen oxides (NO_x), fine particulate matter ($PM_{2.5}$) and various volatile organic compounds (VOCs) indoors *(1-8)*. While these studies have typically measured ambient and personal concentrations, they have not, for the most part, identified

the sources of pollution. This next step, including quantification of the sources, must be achieved in order to implement strategies most effectively to improve schools' air quality.

Typically, indoor air pollution is directly proportional to the air pollution levels outdoors *(9)*, but the results of source apportionment for a region cannot blindly be applied to an individual school because of the large spatial variability in emission rates and resulting pollutant concentrations at the neighborhood scale *(10)*. Research conducted on the emissions associated with school bus idling and exposure of children to these emissions has shown that children are subjected to $PM_{2.5}$, NO_x and particulate elemental carbon levels that are 2 to 4 times higher than typical background ambient concentrations *(11)*. Additionally, research conducted in the South Coast Air Basin (SoCAB) of California showed that, while commuting on a school bus, children are subjected to emissions that are 10^5 to 10^6 times higher than the average SoCAB resident *(12)*. A separate study of school bus caravans in Los Angeles found that NO_2 concentrations inside buses were 8 to 11 times higher than ambient ones *(13)*. Very little research has been conducted on outdoor emissions of VOCs near schools. These compounds dominate the list of 187 pollutants considered to be "air toxics" or "hazardous air pollutants" by the US Environmental Protection Agency (EPA).

Emission inventories are an important tool in prediction, management and protection of air quality. Because they are used to make regulatory and planning decisions that could have tremendous economic and societal impacts, defining their accuracy and uncertainty is crucial. Among the pollutants routinely present in emissions inventories, VOCs are especially problematic. Emissions of the other pollutants are dominated by large point sources and/or motor vehicles, which are either measured continuously or have been studied extensively, respectively. VOCs, however, are not subject to regulatory monitoring at point sources and are emitted by a diverse array of sources including non-point or area-wide activities such as refueling, painting, and lawn mowing, that have limited data on their emissions.

On the basis of discrepancies in measured and/or modeled versus reported VOC emissions, VOC emission inventories are being questioned by a number of researchers *(14-20)*. For

example, aircraft observations of petrochemical plant plumes in Texas suggested that alkene and propene emissions were underestimated by factors of 25-70 *(21)*. Flux measurements in Mexico City generally agreed with the inventory for alkenes, toluene, and acetone but were over two times smaller for C_2-benzenes *(22)*. Also, a study of vehicular emissions in China between 1980 and 2005 revealed discrepancies of greater than 15% in reported versus measured NMOC emissions *(23)*. All these studies acknowledge that VOC emission factors in inventories are highly uncertain.

One method of measuring emissions directly is to apply a micrometeorological technique, eddy covariance, for quantifying surface-atmosphere exchange fluxes. The method has been widely used over soils, crops, and forests but less so over developed areas *(22, 24-27)*. We recently added the ability to measure speciated VOCs to our mobile Flux Laboratory for the Atmospheric Measurement of Emissions (FLAME), which uses eddy covariance for the direct measurement of pollutant fluxes at the neighborhood scale *(10, 28)*. Because most VOCs cannot be measured readily at the temporal resolution required by eddy covariance, we have developed a relaxed eddy accumulation (REA) system for the FLAME.

REA measurement of VOCs was originally proposed in 1977 *(29)* and later modified in 1990 *(30)*. It is a conditional sampling technique that determines fluxes by collecting the positive (updraft) and negative (downdraft) vertical air fluctuations into separate reservoirs. This is typically only possible when stationarity conditions are met, i.e. the average of vertical wind velocity (w) over the sampling period closely approaches zero *(31)*. REA sampling of anthropogenic VOCs has proven to be a valuable tool for air quality scientists; and because it does not require costly fast-response instrumentation, it has gained popularity as an approved method for trace gas flux measurement *(32)*. Although REA has been used extensively to measure VOC fluxes over forest, peatland, agricultural and grassland canopies *(31-37)*, the method has not yet been applied to measurement of urban area fluxes.

While studies have shown that students are subjected to high concentrations of pollutants from diesel emissions while commuting to school, none have yet quantified sources of outdoor pollution near schools. Also, due to discrepancies noted in past research involving

comparisons of measured emissions to published emission inventories *(10, 28)*, further research should be conducted to validate reported data. The goals of this research are to measure concentrations and fluxes of VOCs, CO_2, NO_x and $PM_{2.5}$ to describe sources of air pollutant emissions affecting schools. Taking advantage of the FLAME's mobility, we conducted measurements at three different sites encompassing seven schools in southwestern Virginia. To our knowledge, this research represents the first time that emission rates near schools have been measured.

2.0 Methods

2.1 Site

The field campaign was conducted in Roanoke, Virginia, a small city in southwestern Virginia with a metropolitan area population of approximately 300,000. Roanoke has been identified as a nonattainment area for the 8-hr ozone standard and in 2007, had the highest three-year annual average $PM_{2.5}$ concentration in Virginia, 14.5 $\mu g\ m^{-3}$, just shy of the standard of 15.0 $\mu g\ m^{-3}$. Experiments were conducted at three sites that were adjacent to seven primary and secondary schools: William Fleming High School (WFHS), William Ruffner Middle School (WRMS), Addison Aerospace Magnet Middle School (AAMM), Lincoln Terrace Elementary School (LTES), Patrick Henry High School (PHHS), Roanoke Valley Governor's School (RVGS) and Raleigh Court Elementary School (RCES). Sample locations were chosen based on proximity to schools (200 to 300 m) as well as representative sources of anthropogenic emissions, e.g. vehicle traffic, general construction and commercial activity,experienced in small urban areas. Sites were approximately 4 km apart.

Measurements took place for 10 hr beginning at 7:00 and ending at 17:00 on Monday, Wednesday and Thursday of each week for three weeks between 20 October and 6 November 2008. Sample Locations (SL) were located within or close to neighborhoods and schools of various economic statuses. The neighborhoods can be further divided into three categories: upper income (SL 1), low to middle income (SL 2) and commercial (SL 2 and 3). Commercial regions included malls, golf courses, restaurants, hotels, small businesses and warehouses.

2.1.1 Sample Location 1 (SL 1)

SL 1 was located within the parking lot of a public library (Raleigh Court Library). Patrick Henry High School, Roanoke Valley Governor's School and Raleigh Court Elementary School were next to the library. Traffic in this location was steady throughout the day. Higher volume traffic, including buses and personal vehicles, occurred between the hours of 7:30 and 8:30 and 15:00 and 16:00, which are typical drop off and pick up times of students. Wind direction at this location was variable.

2.1.2 Sample Location 2 (SL 2)

SL 2 was located within a parking lot of a public park, adjacent to Lincoln Terrace Elementary School (320 m) and Addison Magnet Middle School (340 m). Traffic in this location was steady during the morning and late afternoon hours due to its proximity to residential neighborhoods and residents heading to and from work. The site was 4 km from the Roanoke Airport and directly under a landing and takeoff pattern for most of the air traffic in the area. Similar to SL 1, traffic was heaviest during the early morning and afternoon hours. A busy intersection of the city's major highway (I-581) and a main thoroughfare was 500 m to the northwest. Wind direction was predominantly north-northwesterly at this site.

2.1.3 Sample Location 3 (SL 3)

SL 3 was located on a cul-de-sac adjacent to William Ruffner Middle School (125 m) and William Fleming High School (400 m). Traffic in this location was very steady throughout the entire day and had a high fraction of diesel-powered trucks, as this area was more commercial in nature compared to the other two sites. It was surrounded by many businesses, including a strip mall, big box store, gas stations and hotels and a construction site 50 m to the northwest. It was also 440 m from I-581, and 550 m from its intersection with a major thoroughfare leading to both the airport and the largest shopping mall in the area. Wind direction ranged between northerly and southeasterly.

2.2 Equipment

The FLAME is a customized television news van with an extendable mast that rises to 15.5 m. A sonic anemometer (Applied Technologies SATI-3K) and sample tubing are mounted on a rotating platform on top of the mast. A pump draws air at 20 L min^{-1} through 12.7 mm PTFE conductive tubing (TELEFLEX T1618-08) down to ground level, and gas and particle analyzers subsample the air through a custom designed Teflon manifold. Analyzers inside the van measure CO_2 and water vapor (Li-Cor LI-7000, 0.0017-s response time), NO_x (Eco Physics CLD 88Y, 1-s response time) and $PM_{2.5}$ (DustTrak 8520, 1-s response time). A data logger (National Instruments Compact FieldPoint 2110) records the measurements at 10 Hz. The equipment is powered using a gasoline generator, whose emissions are negligible at approximately 0.15% of the overall fluxes.

VOC measurement is accomplished through the use of a REA system with sorbent tubes. The REA design was based on previously tested eddy accumulation systems *(31, 32, 34, 37-41)*. Air was sub-sampled from the main line and pulled through the sorbent tubes at 100 mL min^{-1} for 30 min (approximately 15 min per tube). Updrafts were collected in one tube and downdrafts in another. A third tube was used to measure instances of near-zero (deadband) vertical wind. A LabView 8.0 program controlled three fast-response valves attached to each sorbent tube on the basis of vertical wind velocity with a lag time of 5.2 s to account for residence time in the sample tubing. Also, a deadband threshold of $\pm 0.6\sigma$ was used to ensure proper separation of the reservoirs in an effort to obtain reliable VOC fluxes *(31)*.

VOCs were collected on 3-mm I.D., Silco-coated thermal desorption tubes packed with 100 mg of Tenax TA 60/80 mesh sorbent (Scientific Instrument Services, Inc.) and analyzed for 2,2,4-trimethylpentane, toluene, hexanal, tetrachlorethylene, ethylbenzene, m-, o- and p-xylene, and styrene by thermal desorption (Scientific Instrument Services TD-5) followed by gas chromatography (30 m Zebron ZB-5MS column) with mass spectrometry (Shimadzu Model 2110 GC/MS). The injection port was held at 250 °C with split injection at a ratio of 20:1. The linear velocity was 50.0 cm s^{-1}. The oven was held at 50 °C for 2.00 min, and then ramped at 25.0 °C min^{-1} to 250 °C. The mass spectrometer scanned m/z ratios of 33 to 300.

VOC calibration standards were prepared in decane and diluted to final concentrations of 2, 10, 25 and 50 ppm. Spent tubes were purged with nitrogen gas while being heated to 35 °C for 15 min, 100 °C for 30 min, and 300 °C for 3 h. After conditioning, the tubes were allowed to cool, while still under purge, then disconnected and resealed.

2.3 Quality Control and Post Processing of Data

During the field campaign, we collected nine, 10-h data sets, grouped in 30-min increments, containing CO_2, H_2O vapor, $PM_{2.5}$, NO_x, CO, vertical wind velocity (*w*), and temperature (T). VOC samples were taken every two hours between 8:00 and 17:00 for a total of five measurements per day and a campaign total of 45 half-hourly samples.

Quality assurance and control of VOC measurements included providing heat cured (300° C) and capped (blank) thermal desorption (TD) tubes prior to measurment. Tubes were run in the field with a backup tube in series to test for breakthrough (which was 0% for all tubes), and tubes were resealed and stored in a cool environment (< 4° C) until sampling. GC/MS controls included blanks before and after sample runs and calibration standards after every third sample to ensure that analyte peaks were within an acceptable and measurable range during testing. Calibration curves for each species had R^2 values of at least 97.4%. Error propogation was conducted on all VOC concentration and flux calculations.

For other pollutants, we calibrated all analyzers before and during the field campaign and testing for sampling line losses. The FLAME's losses of CO_2 and NO_x have been previously measured as 0.7±0.4% and 0.5±0.8% respectively, and water vapor losses are typically eclipsed by humidity variations in the atmosphere during the test periods. $PM_{2.5}$ losses were slight (8±5%) *(28)*. The results have not been corrected for line losses, as they fall within the uncertainties of the eddy covariance method, discussed below. Previous efforts to calibrate the DustTrak aerosol photometer against gravimetrically determined $PM_{2.5}$ samples produced a difference of no more than 12% between the two methods, and we have elected to report the factory-calibrated DustTrak $PM_{2.5}$ values.

Standard post-processing of the measurements included hard spike removal, soft spike

removal, lag correction, coordinate rotation by the planar fit method, linear detrending, calculation of fluxes and quality assurance of the calculated fluxes through spectral and co-spectral analyses and stationarity testing *(42-44)*. One randomly chosen set of spectral and cospectral analysis plots (3 November 2008, 16:20–16:50 at SL 3) of NO_x, CO_2 and $PM_{2.5}$ as well as a randomly chosen stationarity plot (23 October 2008) of all concentrations measured that day are shown in Figures 26 and 27, respectively. Slopes of spectral and co-spectral plots were found to conform to theoretically expected values of of -2/3 and -4/3, respectively *(44-46)*. Stationarity plots showed that species' 30-min and 5-min flux differences fell below the criterion of 60% and all stationarity indexes between -5 and 5 *(42, 44, 46)*. Favorable stationarity results ensure valid measurement of VOCs and other pollutants *(30, 31, 47, 48)*.

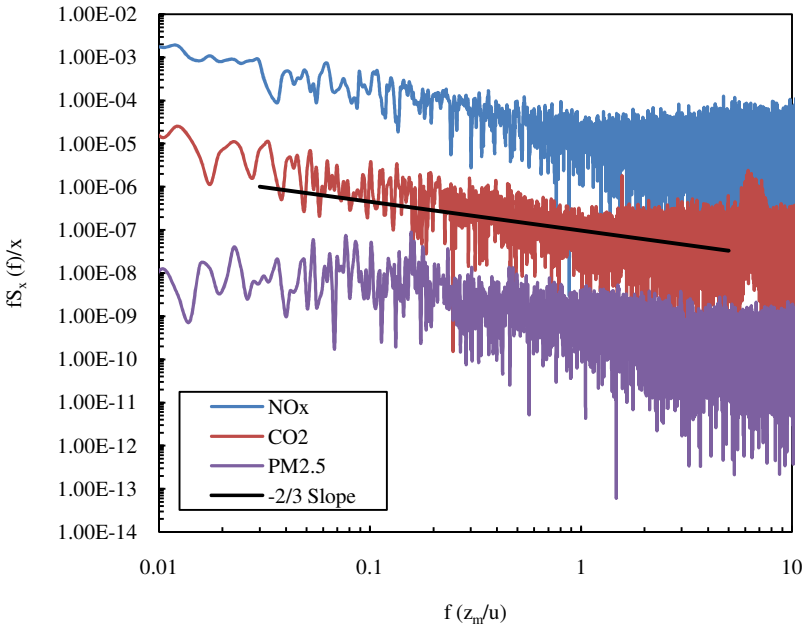

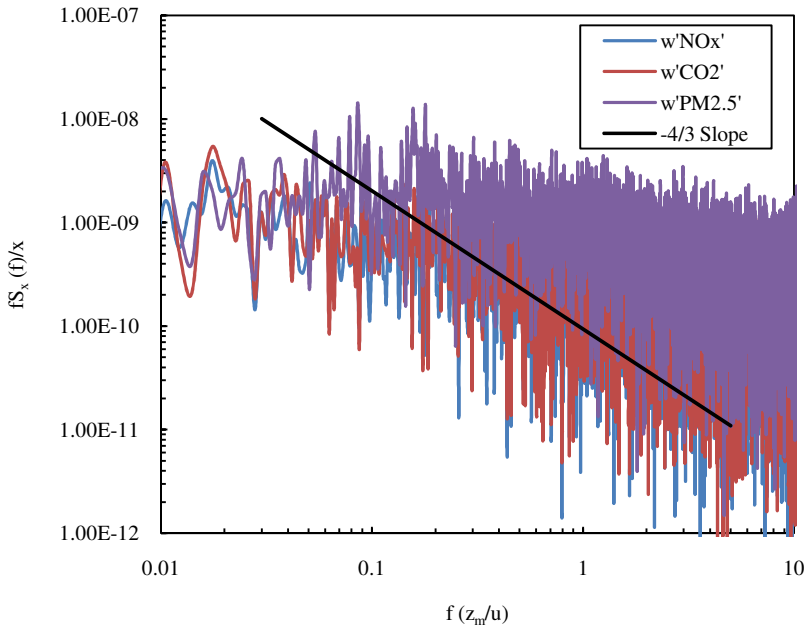

Figure 26. Spectral (top) and co-spectral (bottom) plots from measurements taken at SL 3. Black lines show theoretically expected -2/3 and -4/3 slopes.

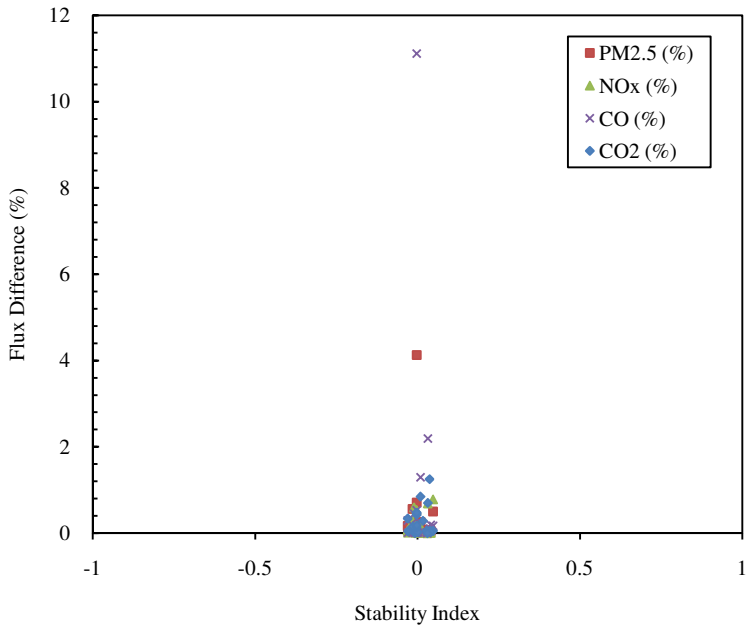

Figure 27. Stationarity test from SL 1 showing that all 30-min and 5-min flux differences are below 12%.

2.4 Calculation of Fluxes

Using the updraft (C_{up}) and downdraft (C_{down}) concentrations measured in the REA system, VOC fluxes were calculated as:

$$F_x = \beta\sigma_w\left(\overline{C}_{up} - \overline{C}_{down}\right) \quad \text{(Eq. 1)}$$

where β is a dimensionless empirical coefficient having a constant value of 0.56 *(31)* and σ_w is the standard deviation of the vertical wind speed.

Fluxes of CO_2, $PM_{2.5}$ and NO_x were calculated over 30-min averaging periods as follows:

$$F_x = \overline{w'C_x'} \quad \text{(Eq. 2)}$$

The flux F_x of species x is the time-averaged covariance between the instantaneous deviations of the vertical wind velocity w' and the concentration C_x', from their linear trends over each 30-min period *(44, 49)*. A positive flux represents net transfer upward into the atmosphere from the surface, whereas a negative flux represents net transfer downward from the atmosphere to the land surface.

The measured flux is a net value, so it represents a combination of emissions to the atmosphere and uptake by surface features. With gases, deposition will usually be small relative to emissions. Of the gases we are considering, NO_2 has the highest dry deposition velocity, 0.1 cm s^{-1} *(50)*. Given a typical urban NO_x concentration of 50 ppb (~100 μg m^{-3} as NO_2) and assuming under worst-case conditions all of it is NO_2, the deposition flux would be ~1×10^{-4} mg m^{-2} s^{-1}.

Although it is impossible to accurately quantify uncertainties from eddy covariance data alone, we followed an empirical approach to test the plausibility of the fluxes through spectral and co-spectral analyses of the variables and stationarity testing *(42)*. Entire papers have been dedicated to the estimation of uncertainty associated with eddy covariance measurements. *(46, 51-56)* They acknowledged that systematic and random errors are unavoidable and that improving one aspect of the measurement system may negatively affect another. Based on possible sources of error such as instrument noise, calibration and frequency loss, it is likely that the systematic error associated with the FLAME's flux measurements is ≤25% and random error is ≤20%.

3.0 Results

3.1 Concentrations

3.1.1 VOCs

This research has produced the first measurements of VOCs in southwestern Virginia. VOCs are routinely monitored at only three Photochemical Assessment Monitoring Stations (PAMS) in Virginia along the Washington-Richmond corridor. Table 6 shows the three-day average VOC concentrations measured at SL 1, 2 and 3 during the Roanoke campaign. Toluene concentrations at each site ranged between 12.1±16.9 and 45.5±35.8 μg m^{-3}. The major sources of toluene are gasoline and solvent use and industrial processes. Concentrations of 2,2,4-trimethylpentane, also known as isooctane, were similar and ranged between 12.2±13.7 and 32.4±22.7 μg m^{-3} at each site. This compound is associated with gasoline-related emissions. Ethylbenzene concentrations were between 6.9±3.9 and 12.2±5.3 μg m^{-3}, and xylenes and styrene concentrations ranged between 10.4±6.8 and 18.5±9.4 μg m^{-3} and between 3.7±1.9 and 6.3±2.4 μg m^{-3}, respectively. Ethylbenezene is typically used in the production of styrene and as a solvent. Xylene is an isomer of ethylbenzene, and is found in trace amounts in fuel. Styrene is used in the production of rubber and occurs naturally in low levels in plants.

Figures 28, 29 and 30 display VOC concentrations throughout the day, every two hours, at each site. At SL 1, high concentrations of toluene and 2,2,4-trimethylpentane (>120 and >80 μg m^{-3}, respectively) occurred during the early morning hours and at 14:00. This site was within ~100 m of three schools, and 8:00 and 14:00 coincided with busy bus and car activity for drop-off and pick-up of the students. SL 2 was closer to a residential neighborhood which experienced some morning and afternoon commuter traffic, that possibly accounted for spikes in concentrations during those times. Also, the FLAME was parked within a municipal park where people visited the park at odd hours for recreational purposes. SL 3 was located 100 m southeast of an elementary school and 200 m southeast of a high school which on the morning of the first day (3 Nov) saw very high isooctane and toluene concentrations (>80 μg m^{-3}) likely due to bus traffic and directly downwind location of the

site from the buses. High concentrations (>20 µg m^{-3}) were not experienced again until the third day (6 Nov) when wind direction shifted to northeasterly, from the direction of I-581 (~500 m upwind).

Table 6. Average ± standard deviation of VOC concentrations measured at each site.

	2,2,4-Trimethylpentane (µg m^{-3})	Toluene (µg m^{-3})	Ethylbenzene (µg m^{-3})	Xylenes (µg m^{-3})	Styrene (µg m^{-3})
SL 1	32.4±22.7	45.5±35.8	12.2±5.3	18.5±9.4	6.3±2.4
SL 2	18.5±18.9	30.3±29.9	9.1±5.3	13.3±8.5	5.2±2.3
SL 3	12.2±13.7	12.1±16.9	6.9±3.9	10.4±6.8	3.7±1.9

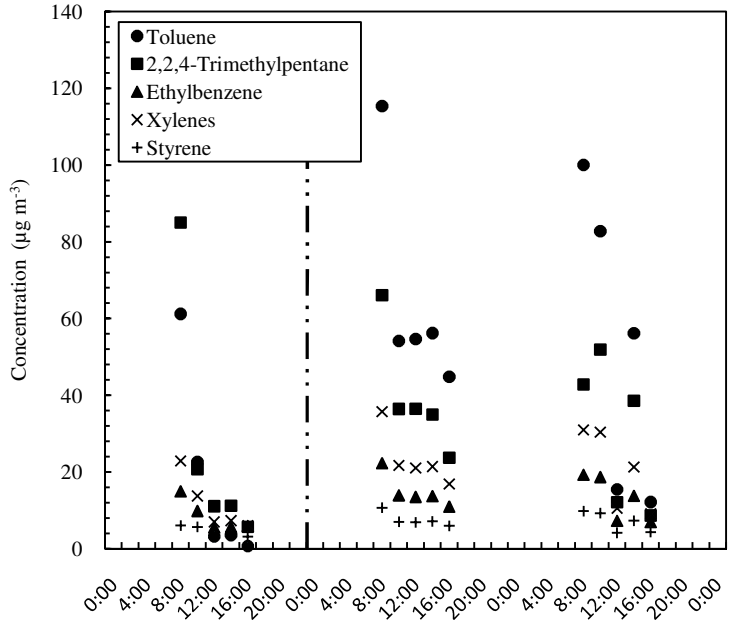

Figure 28. VOC concentrations measured at SL 1 on 20, 22 and 23 October (vertical line separates the 20th and 22nd).

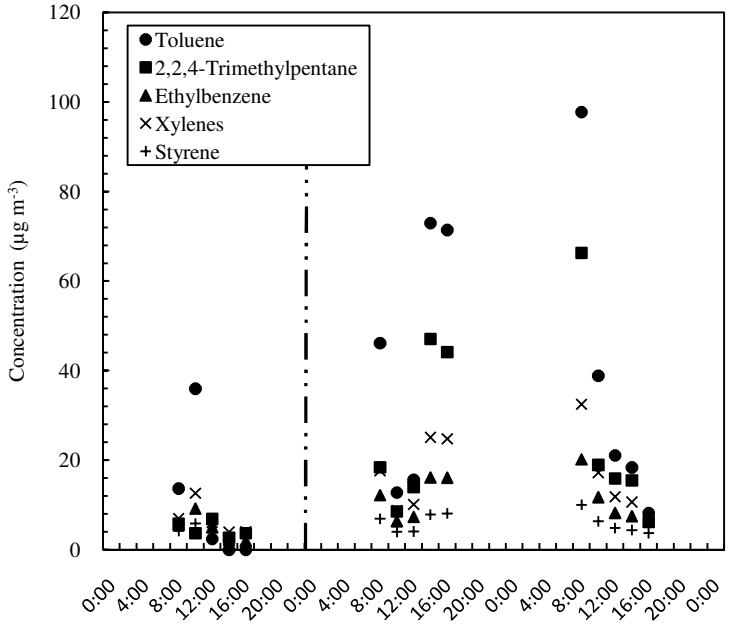

Figure 29. VOC concentrations measured at SL 2 on 27, 29 and 30 October (vertical line separates the 27th and 29th).

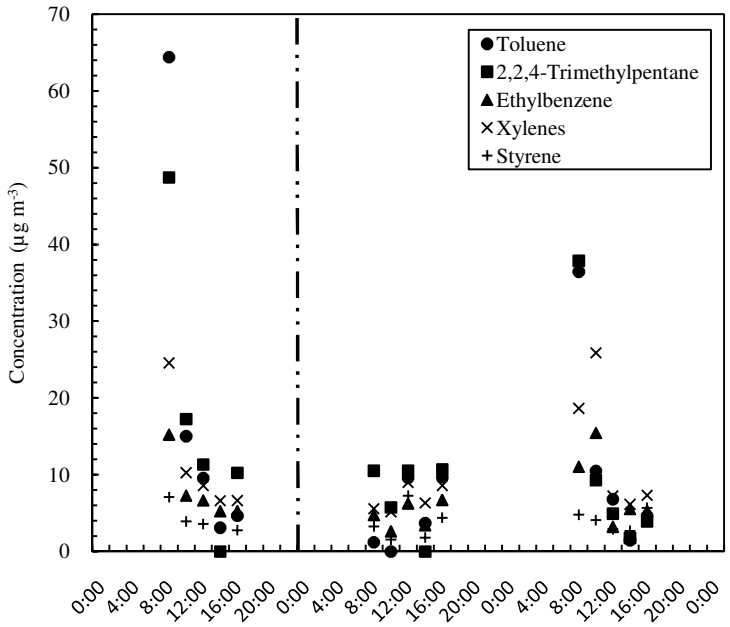

Figure 30. VOC concentrations measured at SL 3 on 3, 5 and 6 November (vertical line separates the 3rd and 5th).

3.1.2 CO_2, NO_x and $PM_{2.5}$

Table 7 shows the three-day average concentrations of CO_2, NO_x and $PM_{2.5}$ at each site. Average 30-min CO_2 concentrations were 476±43, 464±23 and 484±22 ppm at SL 1, 2 and 3

respectively, 84-104 ppm higher than typical global background concentrations of ~380 ppm. Daytime NO_x concentrations were 59±55, 39±47 and 53±52 ppb at SL 1, 2 and 3 respectively. Typical NO_x background concentrations are 18 – 25 ppb *(57)*. $PM_{2.5}$ concentrations ranged from 6±4 to 10±5 μg m^{-3} with an average concentration across all sites of 8±7 μg m^{-3}. Currently the Virginia Department of Environmental Quality (DEQ) maintains two particulate matter sampling stations, which together recorded an average $PM_{2.5}$ concentration of 9 μg m^{-3} during the fourth quarter of 2008. This is very similar to the average $PM_{2.5}$ concentrations measured at SL 1, 2 and 3 combined. In particular, SL 1 was located approximately 20 m southwest of one of the DEQ's $PM_{2.5}$ sites, which recorded a fourth quarter mean of 9.7 μg m^{-3}, while average concentrations measured at SL 1 over the three day period were 9.0 μg m^{-3}. Average CO_2 concentrations measured in Roanoke were approximately 2% lower than those measured in Norfolk using the FLAME. NO_x and $PM_{2.5}$ concentrations in Roanoke were 25% and 3% higher respectively *(10)*. NO_x and $PM_{2.5}$ concentrations at SL 1 and 3 were likely higher because of their closer proximity to more schools, which experienced increased commuter traffic and diesel-powered school bus traffic during the early mornings.

Figures 31, 32 and 33 show the diurnal patterns of CO_2, NO_x, and $PM_{2.5}$ at each site individually and averaged across all sites (thick black line). In contrast to results from a previous campaign in Norfolk, Virginia, where 16 sites were spaced approximately 4 km apart *(10)*, the diurnal concentration profiles were much more similar between sites. One feature common to all of the sites was higher concentrations during the morning hours before ~10:00. Since SL 1 and 3 were located closer to schools, the higher NO_x and $PM_{2.5}$ concentrations at these sites may be related to early morning bus idling during student drop-off. Concentrations tend to tail off during the day and do not seem to spike during the afternoon hours since bus pick-up in the afternoons is sporadic and does not occur all at once as in the mornings. Growth of the mixing depth throughout the day also promotes greater dilution of emissions. The dip in CO_2 concentrations in the early afternoon may be due to photosynthetic uptake by plants.

Table 7. Average ± standard deviation of 30-min concentrations of CO_2, NO_x and $PM_{2.5}$ at each site.

	CO_2 (ppm)	NO_x (ppb)	$PM_{2.5}$ ($\mu g\ m^{-3}$)
SL 1	476±43	59±55	8.8±6.9
SL 2	464±23	39±47	5.5±3.5
SL 3	484±22	53±52	10.1±4.6

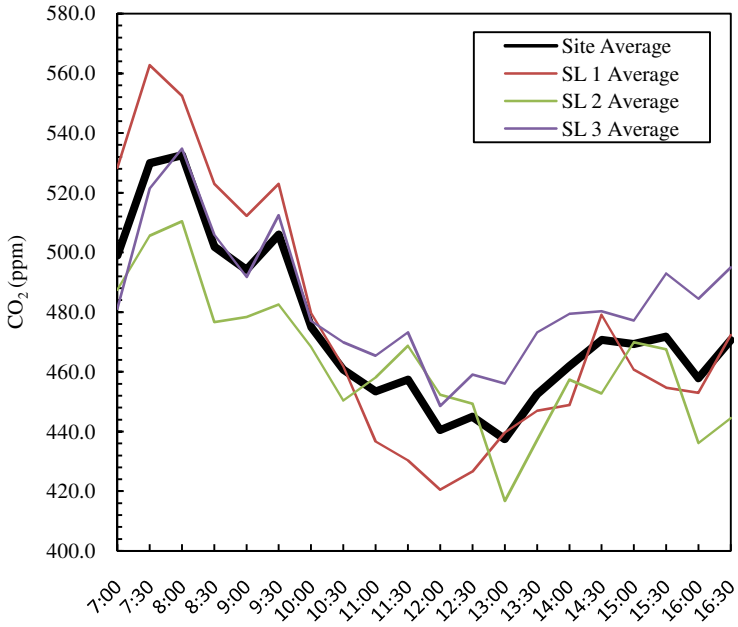

Figure 31. Diurnal profile of CO_2 averaged over all sites (thick black line) and at individual sites.

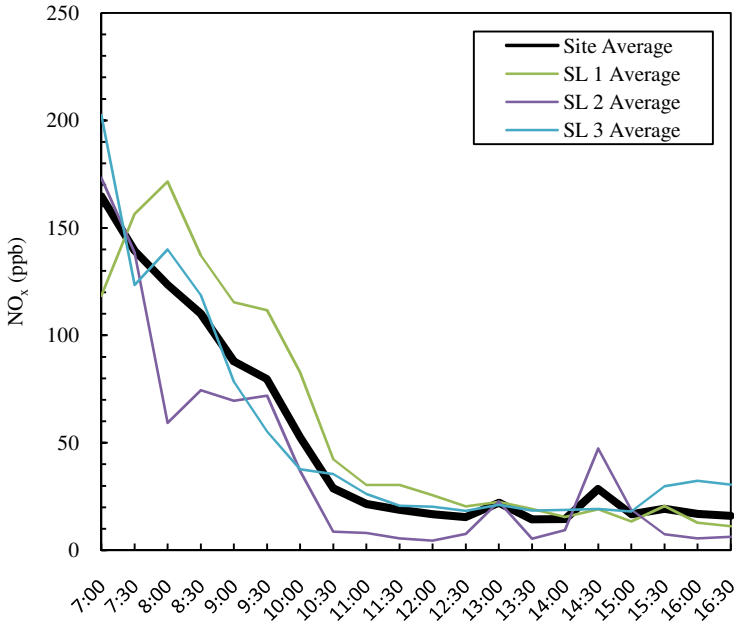

Figure 32. Diurnal profile of NO_x averaged over all sites (thick black line) and at individual sites.

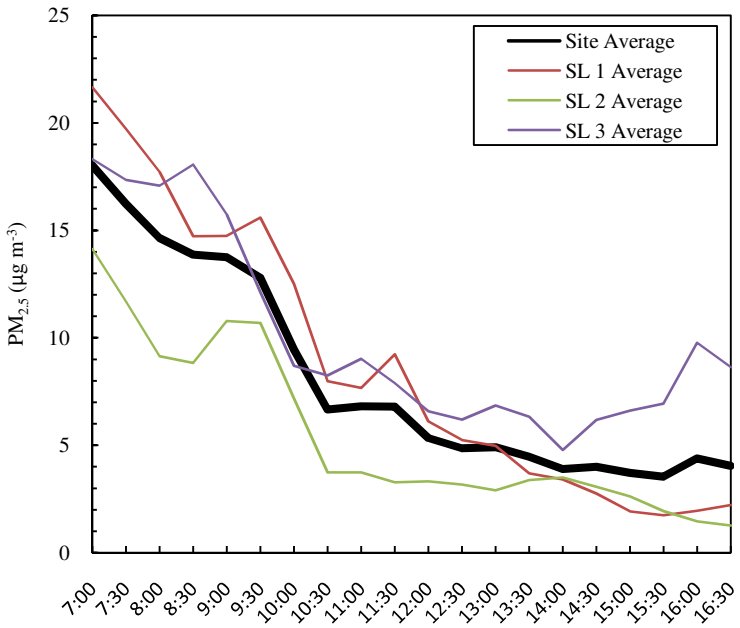

Figure 33. Diurnal profile of $PM_{2.5}$ averaged over all sites (thick black line) and at individual sites.

3.2 Fluxes

3.2.1 VOCs

Table 8 presents average VOC fluxes for 2,2,4-trimethylpentane, toluene, ethylbenzene, xylenes and styrene at each site. All VOC fluxes were positive. Figures 34, 35 and 36 show the fluxes of each species at each site. Since prevailing winds were northerly from a heavily forested neighborhood, fluxes at SL 1 were almost negligible on the first day; however, on the second and third, the fluxes were significantly higher. For example, toluene fluxes reached 5.1×10^{-3} and 3.6×10^{-3} mg m^{-2} s^{-1} on the second day and 1.6×10^{-3} and 2.4×10^{-3} mg m^{-2} s^{-1} on the third at 8:00 and 14:00, times of peak bus and personal vehicle traffic. Fluxes of 2,2,4-trimethylpentane also peaked at these times with fluxes measuring 3.7×10^{-3} and 2.0×10^{-3} on the second day and 1.2×10^{-3} and 1.5×10^{-3} mg m^{-2} s^{-1} on the third. At SL 2, VOC fluxes were highest on the afternoon of the second day and morning of the third. Possible sources nearby included maintenance work and painting, solvent use, and/or refueling at an auto repair shop. SL 3 was close to I-581 as well as a construction site at the high school. On the morning of the first day, when heavy construction-related traffic and commuter traffic on I-581 were observed, fluxes peaked at 5.0×10^{-3} mg m^{-2} s^{-1} for toluene and 3.3×10^{-3} mg m^{-2} s^{-1} for 2,2,4-trimethylpentane, some of the highest values recorded during the field campaign.

Fluxes were lower on the second day since the winds were high this day and northeasterly from the direction of a golf course. On the third day, fluxes were higher again; wind was northerly from the direction of construction.

Table 8. Average±standard deviation VOC fluxes measured at each site.

	2,2,4-trimethylpentane ($mg\ m^{-2}\ s^{-1}$)	Toluene ($mg\ m^{-2}\ s^{-1}$)	Ethylbenzene ($mg\ m^{-2}\ s^{-1}$)	Xylenes ($mg\ m^{-2}\ s^{-1}$)	Styrene ($mg\ m^{-2}\ s^{-1}$)
SL 1	$0.9\pm1.1\times10^{-3}$	$1.4\pm1.6\times10^{-3}$	$2.4\pm2.6\times10^{-4}$	$0.41\pm4.5\times10^{-3}$	$1.1\pm1.0\times10^{-4}$
SL 2	$6.5\pm7.4\times10^{-4}$	$1.3\pm1.3\times10^{-3}$	$2.2\pm1.9\times10^{-4}$	$0.4\pm3.3\times10^{-3}$	$9.9\pm8.7\times10^{-5}$
SL 3	$4.9\pm8.2\times10^{-4}$	$0.9\pm1.2\times10^{-3}$	$2.0\pm2.2\times10^{-4}$	$3.3\pm3.9\times10^{-4}$	$8.9\pm9.1\times10^{-5}$

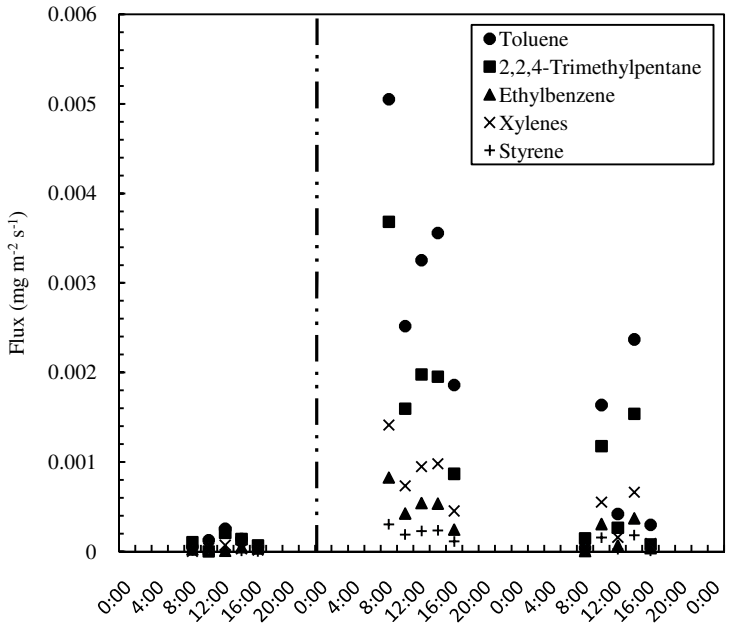

Figure 34. VOC fluxes at SL 1 on 20, 22 and 23 October (vertical line separates the 20th and 22nd).

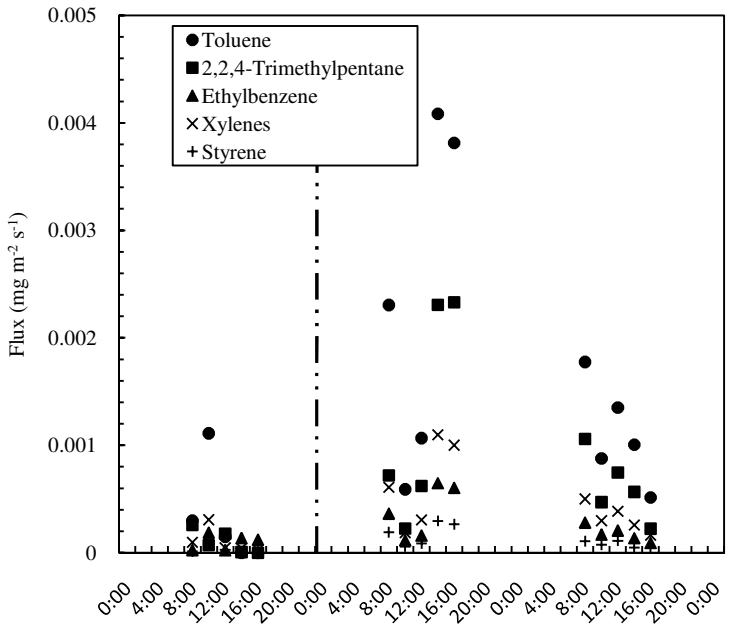

Figure 35. VOC fluxes at SL 2 on 27, 29 and 30 October (vertical line separates the 27th and 29nd).

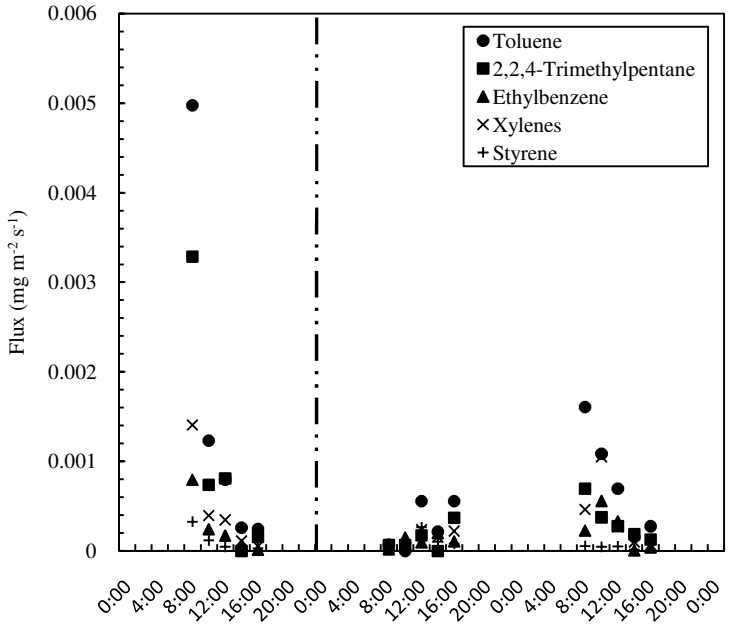

Figure 36. VOC fluxes at SL 3 on 3, 5 and 6 November (vertical line separates the 3rd and 5th).

3.2.2 CO_2, $PM_{2.5}$ and NO_x

Table 9 shows the average of all 30-min fluxes of CO_2, NO_x and $PM_{2.5}$ at each site. Positive-only fluxes are also shown because they more closely represent emissions. Negative fluxes are dominated by active uptake by plants in the case of CO_2 and dry deposition for NO_x and

$PM_{2.5}$. Figures 37, 38 and 39 show time series of fluxes throughout the entire campaign. All average fluxes are positive, which means that the areas around these sites are a net source of emissions.

Average positive CO_2 fluxes ranged between 1.0±1.4 and 1.4±1.8 mg m^{-2} s^{-1} which, at the high end of the range, was approximately two times lower than the overall 16 site average of positive CO_2 fluxes measured in Norfolk *(10)*. As seen in Figure 37, 30-min fluxes ranged between -3.0 and 4.0 mg m^{-2} s^{-1}. SL 3 experienced higher morning fluxes (>4 mg m^{-2} s^{-1}) likely due to the morning commuter traffic along I-581 and the morning bus traffic at the two schools adjacent to the site. Uptake, with fluxes <2 mg m^{-2} s^{-1}, was detected in the afternoons at SL 3, when winds were northeasterly, from the direction of a golf course. In contrast, fluxes at SL 1 and 2 were large and positive in the afternoon, 4.1 and 3.2 mg m^{-2} s^{-1}, respectively. SL 1 experienced increased traffic during the afternoon when buses and cars were picking up children from school. SL 2's positive spikes in fluxes were likely due to afternoon residential commuter traffic. Although concentrations were higher during the morning hours at SL 1 and SL 2 (>500 ppm), both sites were surrounded by some green space, which may be responsible for uptake during these hours.

Average positive NO_x fluxes ranged between $8.3\times10^{-4}\pm1.8\times10^{-3}$ and $1.8\times10^{-3}\pm2.0\times10^{-3}$ mg m^{-2} s^{-1}, approximately 1.5 to 7 times lower than the average positive fluxes at 16 sites in Norfolk *(10)*. Seventy-seven percent of 30-min NO_x fluxes were positive. Figure 38 shows that on average, NO_x fluxes measured during the campaign were positive with the exception of a large negative flux of -6.0×10^{-3} mg m^{-2} s^{-1} at 13:00 at SL 2. The city's major airport was near SL 2, and a plane was landing during this time. It flew directly over the FLAME, possibly contributing to the negative flux during this period. Fluxes at SL 1 and 3 were much higher and mostly positive throughout the day. For example, at SL 1, fluxes were greater than 6.0×10^{-3} mg m^{-2} s^{-1} at 14:00, most likely due to the afternoon bus traffic. Also, during the afternoon hours, winds were typically easterly, from the direction of the bus parking lot and the student commuter lot. Fluxes at SL 1 were negative during the early morning hours when winds were southerly from the direction of a large grass field which may have enhanced NO_x deposition (-7.8×10^{-4} mg m^{-2} s^{-1}). Also at SL 1, fluxes became positive

(>2.0×10^{-3} mg m^{-2} s^{-1}) around 8:00, most likely due to morning bus and vehicle traffic delivering students. Fluxes at SL 3 followed typical diurnal rush hour patterns, with spikes during the morning, noon and late afternoon. This diurnal pattern may have resulted from commuter traffic along I-581.

Average positive $PM_{2.5}$ fluxes ranged between $2.8\times10^{-5}\pm6.0\times10^{-5}$ and $1.0\times10^{-4}\pm1.5\times10^{-4}$ mg m^{-2} s^{-1}, and overall, 58% of 30-min $PM_{2.5}$ fluxes were positive. Average positive $PM_{2.5}$ fluxes measured at 16 sites in Norfolk were between 0.05 and 3.1×10^{-4} mg m^{-2} s^{-1} *(10)*, a much larger range than found in Roanoke, approximately five times lower on the low end of the range and three times higher on the high end of the range. Figure 39 shows that fluxes were occasionally very high (>4×10^{-4} mg m^{-2} s^{-1}). Fluxes were smaller at SL 2, likely a result of the site being adjacent to a park and lacking the influence of diesel traffic. At SL 1, the largest spike of the campaign occurred at 12:00 on the second day, when winds were northerly in the direction of local road and parking lot construction. Fluxes at SL 3 were mostly positive, and the largest fluxes occurred around 10:30 and 16:00. Spikes may have been caused by construction activity occurring at the high school approximately 200 m from the site. Diesel-powered traffic was prevalent on the school grounds, and heavy equipment was being used to move soil 100 m to the north. Diesel-powered traffic along I-581 may have been another source of $PM_{2.5}$, but spikes were correlated with wind direction out of the north, from the construction site.

Table 9. Average ± standard deviation of CO_2, NO_x and $PM_{2.5}$ all and positive-only (+) fluxes measured at SL 1, 2 and 3.

	All CO_2 (mg m^{-2} s^{-1})	+CO_2 (mg m^{-2} s^{-1})	All NO_x (mg m^{-2} s^{-1})	+NO_x (mg m^{-2} s^{-1})	All $PM_{2.5}$ (mg m^{-2} s^{-1})	+$PM_{2.5}$ (mg m^{-2} s^{-1})
SL 1	0.6±1.8	1.4±1.8	$1.4\pm2.0\times10^{-3}$	$1.8\pm2.0\times10^{-3}$	$0.46\pm1.5\times10^{-4}$	$1.0\pm1.5\times10^{-4}$
SL 2	0.5±1.4	1.0±1.4	$0.14\pm1.8\times10^{-3}$	$0.83\pm1.8\times10^{-3}$	$0.58\pm6.0\times10^{-5}$	$2.8\pm6.0\times10^{-5}$
SL 3	0.3±2.4	1.3±2.4	$1.3\pm1.7\times10^{-3}$	$1.5\pm1.7\times10^{-3}$	$0.66\pm1.2\times10^{-4}$	$0.82\pm1.2\times10^{-4}$

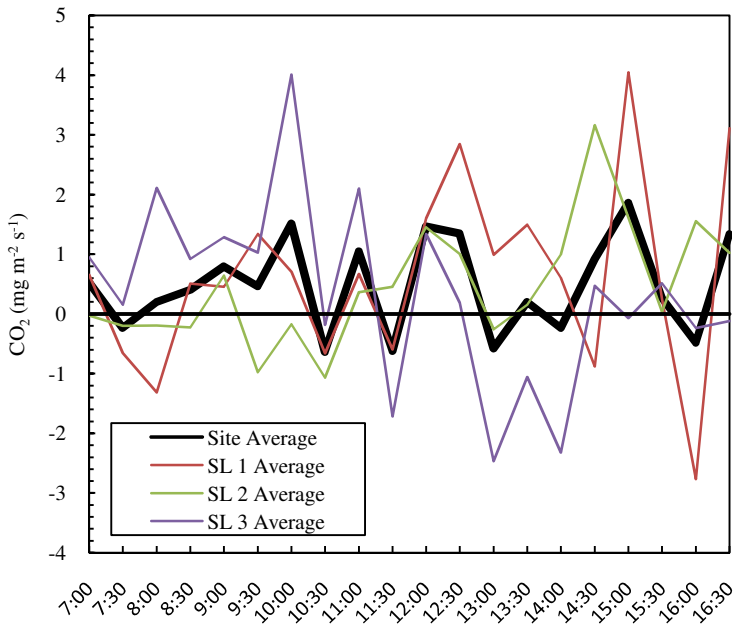

Figure 37. Diurnal profile of CO_2 fluxes averaged over all sites (thick black line) and at individual sites.

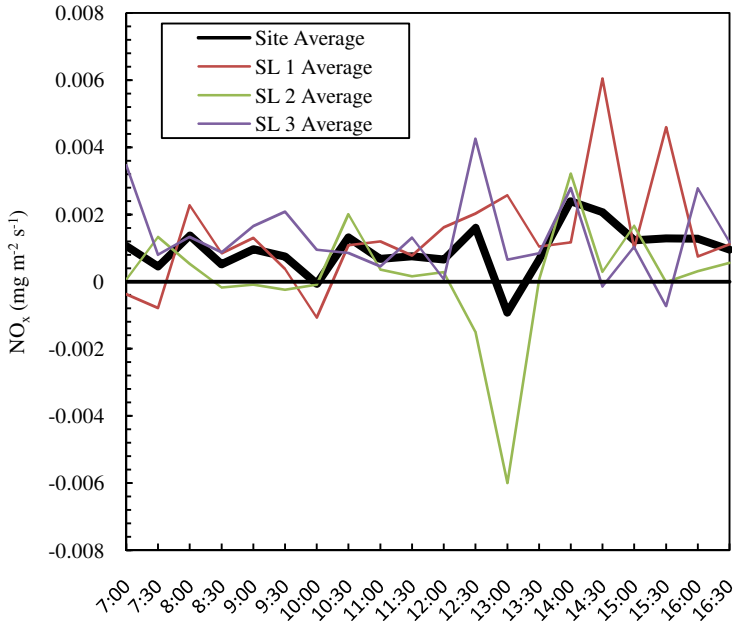

Figure 38. Diurnal profile of NO_x fluxes averaged over all sites (thick black line) and at individual sites.

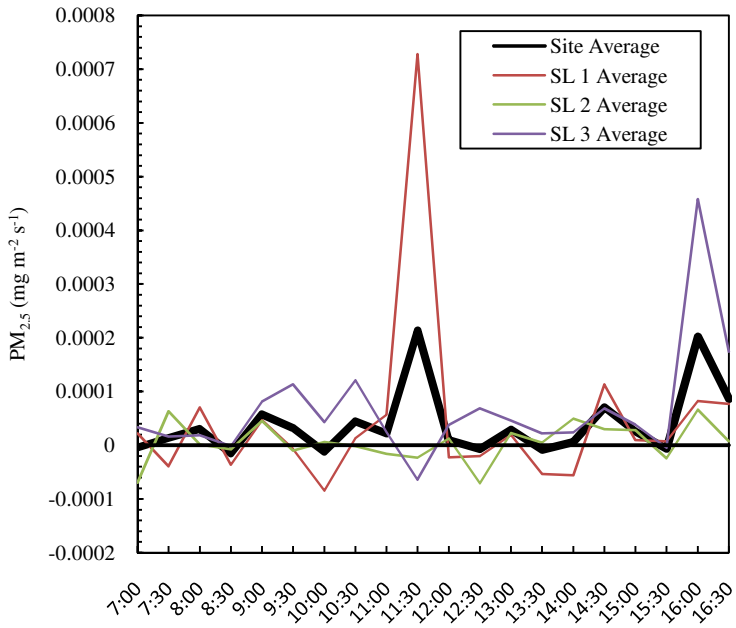

Figure 39. Diurnal profile of $PM_{2.5}$ fluxes averaged over all sites (thick black line) and at individual sites.

4.0 Discussion

4.1 Comparison to EPA Emission Inventory Data

4.1.1 VOCs

Very little data exist on a student's outdoor exposure level to VOCs at schools. Outdoor levels are important because elementary school students spend ~30 min at recess per day and because some pollutants found in classroom air may originate mainly from the penetration of ambient air. One of the few such studies measured children's personal exposures at multiple locations in Minneapolis and found concentrations of ethylbenzene, toluene, xylenes and styrene of 0.6, 2.7, 3.1 and 0.1 µg m^{-3}, respectively; however, these concentrations were integrated over an entire day spent at home, in vehicles and at school *(58)*. Compared to the integrated, full-day average concentrations, those outdoors at schools in this study were between 12 and 20 times higher for ethylbenzene, 4 and 17 times higher for toluene, 3 and 6 times higher for xylenes and 37 and 63 times higher for styrene. Clearly, concentrations at schools are much higher than other microenvironments in which children spend their day.

Only three studies are known to have measured speciated VOC fluxes in urban areas by eddy

covariance. Tower-based studies in Mexico City and Manchester, England measured average daily toluene fluxes of 0.23×10^{-3} mg m^{-2} s^{-1} *(22)* and 0.08×10^{-3} mg m^{-2} s^{-1} *(59)*, respectively. An aircraft measured toluene fluxes of 3.9×10^{-3} mg m^{-2} s^{-1} above Mexico City *(60)*. Thirty-min toluene fluxes in the present study ranged between 0.04 and 5.1×10^{-3} mg m^{-2} s^{-1}, similar to values found in other urban areas.

Official estimates of speciated VOC emissions and modeled ambient concentrations for Virginia are available through the 2002 EPA National-Scale Air Toxics Assessment (NATA). The purpose of the national-scale assessment is to identify and prioritize air toxics, emission source types and locations which are of greatest potential concern in terms of contributing to population risk. The national-scale assessment modeled 180 of the 187 Clean Air Act air toxics plus diesel particulate matter. The assessment includes a national emission inventory of air toxics from outdoor sources, modeled estimates of ambient concentrations of air toxics across the US, estimates of population exposures and public health risk assessment due to inhalation of air toxics *(61)*.

Exposure to air toxics of those attending and living near schools may not be adequately represented by NATA methods. Table 10 compares VOC concentrations averaged across all nine days of the field campaign (three sites) with NATA predictions for Roanoke. According to EPA's model, 2,2,4-trimethylpentane concentrations in 2002 were estimated to be 1.5±0.3 μg m^{-3}, 8 to 22 times lower than the values measured during this field campaign. As seen in Table 10, measured toluene concentrations were up to 70 times higher than NATA's estimates. Ethylbenzene concentrations were over 80 times higher at the upper end of the range with concentrations ranging between 4.7± 4.8 – 6.7±7.0 μg m^{-3} versus NATA concentrations of 0.08±0.01 μg m^{-3}. Xylenes and styrene concentrations ranged between 7.7±8.5 and 11.7±12.2 μg m^{-3} and between 2.4±2.6 and 3.0±2.9 μg m^{-3} respectively and compared well with NATA concentrations of 4.0±0.7 μg m^{-3} for xylenes and 2.5±0.4 μg m^{-3} for styrene. Measured xylene concentrations were three times higher and styrene concentrations only 1.2 times higher than predicted values at the upper end of the range. The large differences between the measurements and NATA estimates indicate that the sites may not have been representative of the wider city but were instead "hot spots" and that seasonal

influences may be at work. The field campaign took place in the fall, while the NATA estimates represent annual averages. If temperatures were warmer during the campaign, evaporative emissions of these compounds may have been higher than typical over the whole year. For perspective, concentrations of toluene in Manchester U.K. were as high as 2.7 µg m^{-3} *(59)*, which though lower than found at schools in Roanoke is still five times higher than predicted for Roanoke by the NATA.

Table 10. VOC concentrations measured in this study versus EPA NATA predictions for Roanoke.

	2,2,4-Trimethylpentane (µg m^{-3})	Toluene (µg m^{-3})	Ethylbenzene (µg m^{-3})	Xylenes (µg m^{-3})	Styrene (µg m^{-3})
This study	21.1±20.3	29.3±31.2	9.4±5.2	14.1±8.8	5.1±2.4
EPA NATA	1.5±0.3	0.6±0.1	0.08±0.01	4.0±0.7	2.5±0.4
Ratio of this study / NATA	14	49	117	4	2

Table 11 summarizes the estimated emissions (kg hr^{-1}) of VOCs, based on the average flux across all three sites and Roanoke's area of 111 km^2, EPA's estimates of emissions were 5-17 times lower. The large differences between VOC fluxes measured at schools in this study and emissions predicted in the NATA suggest again that schools are "hot spots" for air toxic emissions or that the official emissions for Roanoke may be underestimated. Seasonality may also play a role. Emissions from idling vehicles at schools are the most likley cause of elevated levels of air toxics. Results from this study should add to the urgency of implementing no-idling and other rules to reduce the exposure of children to such pollutants.

Table 11. VOC emissions estimated from this study versus EPA NATA inventory for Roanoke.

	2,2,4-Trimethylpentane (kg hr^{-1})	Toluene (kg hr^{-1})	Ethylbenzene (kg hr^{-1})	Xylenes (kg hr^{-1})	Styrene (kg hr^{-1})
This study	275	474	88	147	39
EPA NATA	16	47	9	30	5
Ratio of this study / NATA	17	10	10	5	8

4.1.2 CO_2, NO_x and $PM_{2.5}$

Concentrations of NO_2 and $PM_{2.5}$ have been previously recorded in studies of schoolchildren's exposure. For example, students in Los Angeles have been shown to be subjected to between 13 and 40 ppb NO_2 concentration levels while commuting to school *(13)*, while research in Taiyung, China shows outdoors levels of NO_2 to be between 10 and

17 ppb *(62)*. Concentrations of NO_x measured in Roanoke averaged between 39 and 59 ppb, which is consistent with the upper range of concentrations observed in Los Angeles but is 3.5 times higher than concentrations observed outdoors in China.

Table 12 shows emissions of CO_2, NO_x, and $PM_{2.5}$ in Roanoke according to EPA's National Emission Inventory *(63)* and FLAME-based measurements in both Roanoke and Norfolk. CO_2 emission results were reported on a per capita basis since the EPA provides information at the level of states but not cities and counties *(64)*. Because measurements took place only during the daytime, we expect our emissions estimates to be larger than those averaged over a full 24-hr day, assuming emissions activity is higher during the daytime than nighttime. The most extreme correction would assume that emissions are zero during the 14 hours overnight that we did not measure fluxes and would therefore multiply our emissions estimates by a factor of 10/24, or 0.4.

CO_2 emissions were within a factor of two, with a measurement-based value of 1.65 kg person^{-1} hr^{-1} versus the reported value of 0.94 kg person^{-1} hr^{-1}. CO_2 emissions in Norfolk, where the field campaign encompassed a much larger sample of 16 evenly spaced sites across the city, were 0.98 kg person^{-1} hr^{-1} *(10)*, closer to reported values. Measured versus reported NO_x emissions for Roanoke were 547 and 401 kg hr^{-1} respectively, amounting to a 36% difference, well within the uncertainties associated with the eddy covariance method. NO_x emissions in Norfolk were more than 3.5 times greater.

Comparisons between measurement-based and reported emissions of $PM_{2.5}$ revealed larger differences. For $PM_{2.5}$, emissions from 2001 were used since southwestern Virginia was experiencing severe drought and thus an excessive number of wildfires in 2002, resulting in severely elevated $PM_{2.5}$ emissions. Also, 2001 emissions more closely resembled estimates from previous years. The NEI's estimates of $PM_{2.5}$ emissions were 2.8 times, or 280% higher than, measurement-based values for Roanoke. Differences between emissions measured in this study and the inventory for Roanoke are expected because the sites in this study are likely not representative of Roanoke as a whole. Site selection focused on schools rather than a geographically broad sample.

Table 12. Measured versus reported emissions for Roanoke and Norfolk and EPA-reported emissions for Roanoke.

	CO_2 (kg person^{-1} hr^{-1})	NO_x (kg hr^{-1})	$PM_{2.5}$ (kg hr^{-1})
Measured in Roanoke	1.65	547	29
Measured in Norfolk	0.98	1,470	32
Reported for Roanoke	0.94[a]	401[b]	82[b]

[a] USEPA – Inventory of US Greenhouse Gas Emissions and Sinks: 1990 - 2007
[b] USEPA AirData. http://www.epa.gov/air/data/geosel.html

5.0 Acknowledgements

This research was supported by a National Science Foundation (NSF) CAREER award (CBET-0547107), NSF Research Experience for Undergraduates grant (CBET-0715162), and a Virginia Tech NSF Advance seed grant. Amanda Neighbors assisted with VOC analyses. We thank the Virginia Tech Transportation Institute for use of the van and the City of Roanoke for their support during the field campaign.

6.0 Notes and References

1. Daisey, J. M.; Angell, W. J.; Apte, M. G., Indoor air quality, ventilation and health symptoms in schools: an analysis of existing information. *Indoor Air* **2003,** *13*, 53-64.
2. Godwin, C.; Batterman, S., Indoor air quality in Michigan schools. *Indoor Air* **2007,** *17*, 109-121.
3. Norback, D., Subjective indoor air quality in schools - The influence of high room temperature, carpeting, fleecy wall materials and volatile organic compounds (VOC). *Indoor Air* **1995,** *5*, 237-246.
4. Norback, D.; Walinder, R.; Wieslander, G.; Smedje, G.; Erwall, C.; Venge, P., Indoor air pollutants in schools: nasal patency and biomarkers in nasal lavage. *Allergy* **2000,** *55*, 163-170.
5. Petronella, S. A.; Thomas, R.; Stone, J. A.; Goldblum, R. M.; Brooks, E. G., Clearing the air: A model for investigating indoor air quality in Texas schools. *J. Environ. Health* **2005,** *67*, 35-42.
6. Shendell, D. G.; Winer, A. M.; Stock, T. H.; Zhang, L.; Zhang, J. F.; Maberti, S.; Colome, S. D., Air concentrations of VOCs in portable and traditional classrooms: Results of a pilot study in Los Angeles County. *J. Expo. Anal. Env. Epid.* **2004,** *14*, 44-59.
7. Smedje, G.; Norback, D.; Edling, C., Subjective indoor air quality in schools in relation to exposure. *Indoor Air* **1997,** *7*, 143-150.
8. Valavanidis, A.; Vatista, M., Indoor air quality measurements in the chemistry department building of the University of Athens. *Indoor Built Environ.* **2006,** *15*, 595-605.
9. Pekey, H.; Arslanbas, D., The relationship between indoor, outdoor and personal VOC concentrations in homes, offices and schools in the metropolitan region of Kocaeli, Turkey. *Water Air Soil Poll.* **2008,** *191*, 113-129.
10. Moore, T. O.; Killar, M. B.; Marr, L. C., Validation of an Urban Area Emission Inventory by Eddy Covariance Flux Measurements. In Virginia Polytechnic Institute and State University: Blacksburg, Virginia, 2009.

11. Li, C. L.; Nguyen, Q.; Ryan, P. H.; LeMasters, G. K.; Spitz, H.; Lobaugh, M.; Glover, S.; Grinshpun, S. A., School bus pollution and changes in the air quality at schools: a case study. *J. Environ. Monitor.* **2009,** *11*, 1037-1042.
12. Marshall, J. D.; Behrentz, E., Vehicle self-pollution intake fraction: Children's exposure to school bus emissions. *Environ. Sci. Technol.* **2005,** *39*, 2559-2563.
13. Sabin, L. D.; Kozawa, K.; Behrentz, E.; Winer, A. M.; Fitz, D. R.; Pankratz, D. V.; Colome, S. D.; Fruin, S. A., Analysis of real-time variables affecting children's exposure to diesel-related pollutants during school bus commutes in Los Angeles. *Atmos. Environ.* **2005,** *39*, 5243-5254.
14. Fauser, P.; Illerup, J. B., Danish emission inventory for solvents used in industries and households. *Atmos. Environ.* **2008,** *42*, 7947-7953.
15. Woo, J. H.; He, S.; Tagaris, E.; Liao, K. J.; Manomaiphiboon, K.; Amar, P.; Russell, A. G., Development of North American Emission Inventories for Air Quality Modeling under Climate Change. *J. Air Waste Manage.* **2008,** *58*, 1483-1494.
16. Zhang, J.; Wang, T.; Chameides, W. L.; Cardelino, C.; Blake, D. R.; Streets, D. G., Source characteristics of volatile organic compounds during high ozone episodes in Hong Kong, Southern China. *Atmos. Chem. Phys.* **2008,** *8*, 4983-4996.
17. Song, J.; Vizuete, W.; Chang, S.; Allen, D.; Kimura, Y.; Kemball-Cook, S.; Yarwood, G.; Kiournourtzoglou, M. A.; Atlas, E.; Hansel, A.; Wisthaler, A.; McDonald-Buller, E., Comparisons of modeled and observed isoprene concentrations in southeast Texas. *Atmos. Environ.* **2008,** *42*, 1922-1940.
18. Kannari, A.; Streets, D. G.; Tonooka, Y.; Murano, K.; Baba, T., MICS-Asia II: An inter-comparison study of emission inventories for the Japan region. *Atmos. Environ.* **2008,** *42*, 3584-3591.
19. Vivanco, M. G.; Andrade, M. D., Validation of the emission inventory in the Sao Paulo Metropolitan Area of Brazil, based on ambient concentrations ratios of CO, NMOG and NOx and on a photochemical model. *Atmos. Environ.* **2006,** *40*, 1189-1198.
20. Wang, Q. G.; Han, Z. W.; Wang, T. J.; Zhang, R. J., Impacts of biogenic emissions of VOC and NOx on tropospheric ozone during summertime in eastern China. *Sci. Total Environ.* **2008,** *395*, 41-49.
21. Ryerson, T. B.; Trainer, M.; Angevine, W. M.; Brock, C. A.; Dissly, R. W.; Fehsenfeld, F. C.; Frost, G. J.; Goldan, P. D.; Holloway, J. S.; Hubler, G.; Jakoubek, R. O.; Kuster, W. C.; Neuman, J. A.; Nicks, D. K.; Parrish, D. D.; Roberts, J. M.; Sueper, D. T., Effect of petrochemical industrial emissions of reactive alkenes and NOx on tropospheric ozone formation in Houston, Texas. *J. Geophys. Res.-Atmos.* **2003,** *108*.
22. Velasco, E.; Lamb, B.; Pressley, S.; Allwine, E.; Westberg, H.; Jobson, B. T.; Alexander, M.; Prazeller, P.; Molina, L.; Molina, M., Flux measurements of volatile organic compounds from an urban landscape. *Geophys. Res. Lett.* **2005,** *32*.
23. Cai, H.; Xie, S. D., Estimation of vehicular emission inventories in China from 1980 to 2005. *Atmos. Environ.* **2007,** *41*, 8963-8979.
24. de Gouw, J.; Warneke, C., Measurements of volatile organic compounds in the earth's atmosphere using proton-transfer-reaction mass spectrometry. *Mass Spectrom. Rev.* **2007,** *26*, 223-257.
25. Karl, T.; Harren, F.; Warneke, C.; de Gouw, J.; Grayless, C.; Fall, R., Senescing grass crops as regional sources of reactive volatile organic compounds. *J. Geophys. Res.-Atmos.* **2005,** *110*.
26. Velasco, E.; Lamb, B.; Westberg, H.; Allwine, E.; Sosa, G.; Arriaga-Colina, J. L.; Jobson, B. T.; Alexander, M. L.; Prazeller, P.; Knighton, W. B.; Rogers, T. M.; Grutter, M.; Herndon, S. C.; Kolb, C. E.; Zavala, M.; de Foy, B.; Volkamer, R.; Molina, L. T.; Molina, M. J., Distribution, magnitudes, reactivities, ratios and diurnal patterns of volatile organic compounds in the Valley of Mexico during the MCMA 2002 & 2003 field campaigns. *Atmos. Chem. Phys.* **2007,** *7*, 329-353.
27. Velasco, E.; Marquez, C.; Bueno, E.; Bernabe, R. M.; Sanchez, A.; Fentanes, O.; Wohrnschimmel, H.; Cardenas, B.; Kamilla, A.; Wakamatsu, S.; Molina, L. T., Vertical distribution of ozone and VOCs in the low boundary layer of Mexico City. *Atmos. Chem. Phys.* **2008,** *8*, 3061-3079.
28. Moore, T. O.; Doughty, D. C.; Marr, L. C., Demonstration of a mobile Flux Laboratory for the Atmospheric Measurement of Emissions (FLAME) to assess emissions inventories. *J. Environ. Monitor.* **2009,** *11*, 259-268.

29. Desjardins, R. L., Description and evaluation of a sensible heat flux detector. *Bound.-Lay. Meteorol.* **1977,** *11*, 147-154.
30. Businger, J. A.; Oncley, S. P., Flux measurement with conditional sampling. *J. Atmos. Ocean Tech.* **1990,** *7*, 349-352.
31. Ciccioli, P.; Brancaleoni, E.; Frattoni, M.; Marta, S.; Brachetti, A.; Vitullo, M.; Tirone, G.; Valentini, R., Relaxed eddy accumulation, a new technique for measuring emission and deposition fluxes of volatile organic compounds by capillary gas chromatography and mass spectrometry. *J. Chromatagr. A* **2003,** *985*, 283-296.
32. Bowling, D. R.; Turnipseed, A. A.; Delany, A. C.; Baldocchi, D. D.; Greenberg, J. P.; Monson, R. K., The use of relaxed eddy accumulation to measure biosphere-atmosphere exchange of isoprene and of her biological trace gases. *Oecologia* **1998,** *116*, 306-315.
33. Baker, B.; Guenther, A.; Greenberg, J.; Fall, R., Canopy level fluxes of 2-methyl-3-buten-2-ol, acetone, and methanol by a portable relaxed eddy accumulation system. *Environ. Sci. Technol.* **2001,** *35*, 1701-1708.
34. Beverland, I. J.; Oneill, D. H.; Scott, S. L.; Moncrieff, J. B., Design, construction and operation of flux measurement systems using the conditional sampling technique. *Atmos. Environ.* **1996,** *30*, 3209-3220.
35. Christensen, C. S.; Hummelshoj, P.; Jensen, N. O.; Larsen, B.; Lohse, C.; Pilegaard, K.; Skov, H., Determination of the terpene flux from orange species and Norway spruce by relaxed eddy accumulation. *Atmos. Environ.* **2000,** *34*, 3057-3067.
36. Schade, G. W.; Goldstein, A. H., Fluxes of oxygenated volatile organic compounds from a ponderosa pine plantation. *J. Geophys. Res.-Atmos.* **2001,** *106*, 3111-3123.
37. Valverde-Canossa, J.; Ganzeveld, L.; Rappengluck, B.; Steinbrecher, R.; Klemm, O.; Schuster, G.; Moortgat, G. K., First measurements of H2O2 and organic peroxides surface fluxes by the relaxed eddy-accumulation technique. *Atmos. Environ.* **2006,** *40*, S55-S67.
38. Graus, M.; Hansel, A.; Wisthaler, A.; Lindinger, C.; Forkel, R.; Hauff, K.; Klauer, M.; Pfichner, A.; Rappengluck, B.; Steigner, D.; Steinbrecher, R., A relaxed-eddy-accumulation method for the measurement of isoprenoid canopy-fluxes using an online gas-chromatographic technique and PTR-MS simultaneously. *Atmos. Environ.* **2006,** *40*, S43-S54.
39. Kuhn, U.; Dindorf, T.; Ammann, C.; Rottenberger, S.; Guyon, P.; Holzinger, R.; Ausma, S.; Kenntner, T.; Helleis, F.; Kesselmeier, J., Design and field application of an automated cartridge sampler for VOC concentration and flux measurements. *J. Environ. Monitor.* **2005,** *7*, 568-576.
40. Nie, D.; Kleindienst, T. E.; Arnts, R. R.; Sickles, J. E., The design and testing of a relaxed eddy accumulation system (vol 100, pg 11415, 1995). *J. Geophys. Res.-Atmos.* **1996,** *101*, 4315-4315.
41. Olofsson, M.; Ek-Olausson, B.; Ljungstrom, E.; Langer, S., Flux of organic compounds from grass measured by relaxed eddy accumulation technique. *J. Environ. Monitor.* **2003,** *5*, 963-970.
42. Aubinet, M.; Grelle, A.; Ibrom, A.; Rannik, U.; Moncrieff, J.; Foken, T.; Kowalski, A. S.; Martin, P. H.; Berbigier, P.; Bernhofer, C.; Clement, R.; Elbers, J.; Granier, A.; Grunwald, T.; Morgenstern, K.; Pilegaard, K.; Rebmann, C.; Snijders, W.; Valentini, R.; Vesala, T., Estimates of the annual net carbon and water exchange of forests: The EUROFLUX methodology. In *Advances in Ecological Research, Vol 30*, 2000; Vol. 30, pp 113-175.
43. Grimmond, C. S. B.; King, T. S.; Cropley, F. D.; Nowak, D. J.; Souch, C., Local-scale fluxes of carbon dioxide in urban environments: Methodological challenges and results from Chicago. *Environ. Pollut.* **2002,** *116*, 243-254.
44. Velasco, E.; Pressley, S.; Allwine, E.; Westberg, H.; Lamb, B., Measurements of CO2 fluxes from the Mexico City urban landscape. *Atmos. Environ.* **2005,** *39*, 7433-7446.
45. Martensson, E. M.; Nilsson, E. D.; Buzorius, G.; Johansson, C., Eddy covariance measurements and parameterisation of traffic related particle emissions in an urban environment. *Atmos. Chem. Phys.* **2006,** *6*, 769-785.
46. Vickers, D.; Mahrt, L., Quality control and flux sampling problems for tower and aircraft data. *J. Atmos. Ocean Tech.* **1997,** *14*, 512-526.

47. Fotiadi, A. K.; Lohou, F.; Druilhet, A.; Serca, D.; Brunet, Y.; Delmas, R., Methodological development of the conditional sampling method. Part I: Sensitivity to statistical and technical characteristics. *Bound.-Lay. Meteorol.* **2005,** *114*, 615-640.
48. Fotiadi, A. K.; Lohou, F.; Druilhet, A.; Serca, D.; Said, F.; Laville, P.; Brut, A., Methodological development of the conditional sampling method. Part II: Quality Control Criteria of Relaxed Eddy Accumulation Flux Measurements. *Bound.-Lay. Meteorol.* **2005,** *117*, 577-603.
49. Baldocchi, D. D., Assessing the eddy covariance technique for evaluating carbon dioxide exchange rates of ecosystems: past, present and future. *Glob. Change Biol.* **2003,** *9*, 479-492.
50. Seinfeld, J. H.; Pandis, S. N., *Atmospheric Chemistry and Physics - From Air Pollution to Climate Change*. 2 ed.; John Wiley & Sons, Inc.: Hoboken, New Jersey, 2006 Vol. 2, p 1203.
51. Massman, W. J.; Lee, X., Eddy covariance flux corrections and uncertainties in long-term studies of carbon and energy exchanges. *Agr. Forest Meteorol.* **2002,** *113*, 121-144.
52. Loescher, H. W.; Law, B. E.; Mahrt, L.; Hollinger, D. Y.; Campbell, J.; Wofsy, S. C., Uncertainties in, and interpretation of, carbon flux estimates using the eddy covariance technique. *J. Geophys. Res.-Atmos.* **2006,** *111*.
53. Hollinger, D. Y.; Richardson, A. D., Uncertainty in eddy covariance measurements and its application to physiological models. *Tree Physiol.* **2005,** *25*, 873-885.
54. Kruijt, B.; Elbers, J. A.; von Randow, C.; Araujo, A. C.; Oliveira, P. J.; Culf, A.; Manzi, A. O.; Nobre, A. D.; Kabat, P.; Moors, E. J., The robustness of eddy correlation fluxes for Amazon rain forest conditions. *Ecol. Appl.* **2004,** *14*, S101-S113.
55. Foken, T.; Wichura, B., Tools for quality assessment of surface-based flux measurements. *Agr. Forest Meteorol.* **1996,** *78*, 83-105.
56. Lenschow, D. H.; Mann, J.; Kristensen, L., How long is long enough when measuring fluxes and other turbulence statistics. *J. Atmos. Ocean Tech.* **1994,** *11*, 661-673.
57. USEPA Air Quality System. <http://www.epa.gov/ttn/airs/airsaqs/>
58. Adgate, J. L.; Church, T. R.; Ryan, A. D.; Ramachandran, G.; Fredrickson, A. L.; Stock, T. H.; Morandi, M. T.; Sexton, K., Outdoor, indoor, and personal exposure to VOCs in children. *Environ. Health Perspect.* **2004,** *112*, 1386-1392.
59. Langford, B.; Davison, B.; Nemitz, E.; Hewitt, C. N., Mixing ratios and eddy covariance flux measurements of volatile organic compounds from an urban canopy (Manchester, UK). *Atmos. Chem. Phys.* **2009,** *9*, 1971-1987.
60. Karl, T.; Apel, E.; Hodzic, A.; Riemer, D. D.; Blake, D. R.; Wiedinmyer, C., Emissions of volatile organic compounds inferred from airborne flux measurements over a megacity. *Atmos. Chem. Phys.* **2009,** *9*, 271-285.
61. USEPA 2002 National-Scale Air Toxics Assessment. <http://www.epa.gov/ttn/atw/nata2002/tables.html>
62. Zhao, Z. H.; Sebastian, A.; Larsson, L.; Wang, Z. H.; Zhang, Z.; Norback, D., Asthmatic symptoms among pupils in relation to microbial dust exposure in schools in Taiyuan, China. *Pediatr. Allergy Immu.* **2008,** *19*, 455-465.
63. USEPA AirData. http://www.epa.gov/air/data/geosel.html
64. USEPA *Inventory of U.S. Greenhouse Gas Emissions and Sinks: 1990-2006* 2008; p 473.

Chapter 5: Conclusion

1.0 Introduction

We have designed a mobile eddy covariance system dubbed the Flux Laboratory for the Atmospheric Measurement of Emissions (FLAME) and deployed it in three field campaigns to gain new insight into anthropogenic emisssions of air pollutants. This research has contributed novel, independent, measurement-based verification of air pollution emission inventories, whose large uncertainties are the bane of policymakers and modelers trying to manage and understand air quality. Experiments focused on carbon dioxide (CO_2), nitrogen oxides (NO_x), carbon monoxide (CO), fine particulate matter ($PM_{2.5}$) and the volatile organic compunds (VOCs) 2,2,4-trimethylpentane, toluene, ethylbenzene, m-, o- and p- xylenes and styrene.

Thanks to its mobility, the FLAME is capable of providing some of the first direct measurements of neighborhood-scale anthropogenic emissions of CO_2, NO_x, CO, $PM_{2.5}$ and VOCs combined across a region. The results of each campaign, described in detail below, indicate that a mobile eddy covariance system can be used successfully to measure fluxes of multiple pollutants in a variety of rural or urban settings. Measured concentrations and emissions can also be used to estimate pollutant exposures of various target groups such as under-represented populations located in industrial emissions “hot zones” or primary school students and their exposure to daily diesel-powered school bus emissions. Ultimately, the results of this study can be used in combination with knowledge from existing emission inventories to improve the science and policies surrounding air pollution and to provide populations with more accurate knowledge of air pollution exposure levels within a neighborhood.

2.0 Emissions in a Coal Transport Town of Appalachia

To demonstrate and test the FLAME’s capabilities, we deployed it in the Huntington-Ashland region at the borders of Ohio, Kentucky and West Virginia. This area routinely

experiences high ozone and $PM_{2.5}$ concentrations and is home to a significant amount of industry as well as coal storage and transport. Experiments focused on CO_2, NO_x and $PM_{2.5}$. Spikes in CO_2 and NO_x concentrations were correlated with the passage of trains and barges through the FLAME's footprint. Barge emissions factors were calculated and ranged from 49 to 76 kg NO_x tonne $fuel^{-1}$, which correlated well with previously published values. Fluxes measured at three sites in the town of Worthington were mainly positive. They ranged between -6.2 to 30 mg m^{-2} s^{-1} for CO_2 and -2.2×10^{-4} to 1.2×10^{-4} mg m^{-2} s^{-1} for $PM_{2.5}$. Compared to the state's official inventory, the measured CO_2 flux was 1.5-60 times higher, and the $PM_{2.5}$ flux was 5-60 times higher. The results showed that a mobile eddy covariance system can be used successfully to measure fluxes of multiple pollutants in a variety of settings. This alternative method for estimating emissions was determined to be a useful approach for assessing uncertainties in emissions inventories and for improving their accuracy. A successful campaign in Worthington provided the framework for a more intensive study of VOCs near schools in a medium-sized urban area (Roanoke, Virginia) and a more geographically comprehensive study in a large urban area (Norfolk, Virginia).

3.0 Emissions Near Schools in a Medium Urban Area

This study focused on schools to better understand and describe quantitatively the air quality experienced by children. The campaign took place in a medium-sized urban area, Roanoke, Virginia, and the three sampling locations were near seven public schools. Daytime average VOC fluxes of 2,2,4-trimethylpentane, toluene, ethylbenzene, xylenes (m-, o- and p-), and styrene ranged between 8.9×10^{-5} and 1.4×10^{-3} mg m^{-2} s^{-1}. Among the species, toluene fluxes were highest and styrene fluxes lowest. The correlation in time between spikes in fluxes and school bus activity suggests that idling buses are a large source of emissions of air toxics. From the positive fluxes, we estimated daytime emission rates of 275, 474, 88, 147 and 39 kg hr^{-1} for 2,2,4-trimethylpentane, toluene, ethylbenzene, xylenes (m-, o- and p-), and styrene, respectively, which was between 5 and 17 times higher than EPA reported values. The large differences between the measurements and NATA estimates indicate that the sites may not have been representative of the wider city but were instead "hot spots," and/or that emissions may be underestimated by EPA, and/or that seasonal influences may be at work. Positive

(upward) fluxes, which define a lower bound on emissions, for CO_2, NO_x and $PM_{2.5}$ across the three sites ranged between 1.3-1.4, 1.5×10^{-3}-1.8×10^{-3} and 0.82×10^{-3}-1.0×10^{-3} mg m^{-2} s^{-1}, respectively. If the selected sites were representative of the broader area, then per capita CO_2 emissions were estimated to be 0.69 – 1.65 kg $person^{-1}$ hr^{-1}, a range which encompasses EPA-reported values for the state. Emissions from idling vehicles at schools are the most likely cause of elevated levels of air toxics. Results from this study should add to the urgency of implementing no-idling and other rules to reduce the exposure of children to such pollutants.

4.0 Comprehensive Urban Area Emissions

A field campaign in Norfolk, Virginia ran for one month over a broad geographic area in an effort to provide a more comprehensive picture of emissions in an urban area. Specifically, the goal was to test the limits of the FLAME's ability to accurately measure neighborhood-scale emissions and in turn compare those emissions with the National Emission Inventory (NEI) to provide independent, measurement-based validation of the inventory. Air pollutant concentrations showed significant spatial and temporal variability across the 144 km^2 area with CO_2, NO_x, CO, and $PM_{2.5}$ ranging between 464±65–606±80 ppm, 22±7–89±48 ppb, 300±80–650±300 ppm and 1±0.3–19±23 μg m^{-3}, respectively, at each of 16 sites. Average positive fluxes for CO_2, NO_x and $PM_{2.5}$ ranged between 0.7±0.8–3.1±5.5, $5.6\pm5.0\times10^{-4}$–$1.2\pm1.5\times10^{-2}$ and $5.4\pm6.7\times10^{-6}$–$3.0\pm6.1\times10^{-4}$ mg m^{-2} s^{-1}, respectively, across sites. Average positive daytime emissions measured during the Norfolk campaign, calculated by multiplying CO_2 fluxes (the average of positive ones only across all 16 sites) by the area of Norfolk (139 km^2), were 800,640 kg hr^{-1} for CO_2, 1,470 kg hr^{-1} for NO_x and 32 kg hr^{-1} for $PM_{2.5}$. Within the precision and limitations of the eddy covariance method, the measurements agree with official CO_2 and NO_x emission inventories but suggest that $PM_{2.5}$ emissions may be overstated. Because the NEI uses the same methods and often the same emission factors for the whole country, results from this study translate to other urban areas such as New York or San Francisco as well. Measured fluxes were also compared with the Visibility Improvement State and Tribal Association of the Southeast (VISTAS) inventory, developed using the Sparse Matrix Operator Kernel Emissions (SMOKE) modeling system. Hourly

SMOKE emissions of NO_x and $PM_{2.5}$ ranged between 393 – 1,330 and 15 – 54 kg hr^{-1}, respectively, which is was very similar to the measured hourly emissions results of 384 – 2,461 and 7 – 49 kg hr^{-1}.

5.0 Research Goal

The goals of this research were to design and utilize a uniquely mobile system capable of measuring local area emissions on a neighborhood scale, use the FLAME to characterize anthropogenic emissions in urban areas and assess the accuracy of official emission inventories by comparing them to measured fluxes. These goals were accomplished. Of particular significance in this research is the ability to pinpoint and quantify area emissions sources such as rail and barge traffic or school bus traffic, because to date, these sources have been poorly characterized. In the past, there has been no way to validate estimates of emissions from area sources. In this research, calculated fluxes are used to better quantify emissions from these such sources, which due to lack of measurement-based validation, are often under or over estimated in emission inventories. With the breakthroughs in emissions measurement provided by the mobile platform utilized in this research, flux measurements can now be compared with official emission inventories to help regulatory agencies identify areas in which to focus their efforts. Improved inventories will lead to more effective management of air quality and cleaner air for future generations.

5.0 Future Work

Future work with the FLAME will expand the relaxed eddy accumulation system to measure additional VOCs such as ethanols and aldehydes. The VOC campaign will take place within a larger urban area in the hopes of obtaining detailed anthropogenic VOC information in highly populated areas. The campaign will also involve the measurement of CO_2, $PM_{2.5}$, NO_x, and CO, which will then be combined with wind speed and direction to further explore the footprinting process and capabilities of the FLAME to provide insight into the air quality experienced by various populations within specific footprints. For example, using GIS, fluxes can be compared to land use characteristics as well as the socioeconomic characteristics of various areas in an effort to further utilize the FLAME's mobile

capabilities to understand exposure levels of underrepresented populations. The goal of this future campaign is threefold: 1) utilize a mobile relaxed eddy accumulation measurement system capable of measuring multiple VOCs to further investigate exposure levels of various populations in urban areas, 2) continue to introduce an education component into the FLAME research in an effort to promote an interest in the sciences among younger students, and 3) using GIS, analyze the air quality affecting underrepresented populations in urban areas and provide the necessary tools and information to regulatory agencies for proper air contaminant control.